UNIVERSITY OF SOUTHAMPTON

FACULTY OF ENGINEERING AND THE ENVIRONMENT

Institute of Sound and Vibration Research

Reverberation Enhancement for Small Rooms

by

Hugh Alexander Hopper

Thesis for the degree of Doctor of Philosophy

January 2012

UNIVERSITY OF SOUTHAMPTON

ABSTRACT

FACULTY OF ENGINEERING AND THE ENVIRONMENT

Institute of Sound and Vibration Research

Doctor of Philosophy

REVERBERATION ENHANCEMENT FOR SMALL ROOMS

by

Hugh Alexander Hopper

Reverberation enhancement is a technology which allows the reverberation time of a room to be increased through the use of an electronic system. These systems have traditionally been applied to improve the acoustics of large concert halls but the technology can also be used in smaller spaces with several possible applications. Previous uses of reverberation enhancement in small rooms have largely consisted of direct transplants of systems designed for large concert halls. This work investigates the complications which arise when using reverberation enhancement in a small room due to the differences in the acoustic properties of the space and also the restriction on the channel count of the system due to physical constraints.

The first part of this work deals with increasing the resultant reverberation time of the room without requiring additional system channels. This is achieved through the use of processing within the system. Two methods have been investigated. The first extends the resultant reverberation time without changing the feedback gain. The processing used for this purpose is either electronic reverberation or simple delay, both of which have been shown to allow significant increases in resultant reverberation time. These changes can be predicted accurately using diffuse field theory. The other method uses time-varying processing to increase the maximum stable feedback gain. This has been shown to allow increases in resultant reverberation time but also causes undesirable artefacts which limit the usability of this technique.

The second part of this work focuses on the differences in the acoustic properties of small rooms and especially the ways in which these rooms differ from a diffuse field. This includes the consideration of the modal properties of the room at low frequency which are insignificant in a large room. It has been shown that the spatial and frequency variations of the room at low frequency can be reduced through numerical optimisation of the processing within the reverberation enhancement system. Finally, the diffusion of the sound field and the early energy in the impulse response have been considered. It is shown that restrictions on the resultant reverberation time may be required in order to create a subjectively acceptable acoustic response. Overall, this work has shown that by accounting for the properties of the room, excellent performance of the system can be achieved.

List of Contents

1 Introduction 1

1.1 Theory of room acoustics 3

1.1.1 Modal response of a room 3

1.1.2 Diffuse field model of a room 9

1.1.3 Numerical methods 13

1.1.4 Measuring room acoustic parameters 14

1.2 Reverberation enhancement 17

1.2.1 The beginnings of reverberation enhancement 18

1.2.2 In-line reverberation enhancement 20

1.2.3 State of the art non-in-line reverberation enhancement 21

1.2.4 Active wall 23

1.2.5 Flat panel loudspeakers 24

1.3 Summary of this work 25

1.3.1 Research goals 25

1.3.2 Main original contributions 27

2 Increasing the resultant reverberation time 29

2.1 Including artificial reverberation 30

2.1.1 Algorithms for digital reverberation 30

2.1.2 Analysis of a system including electronic reverberation 31

2.1.3 Simulation of a system with electronic reverberation 34

2.1.4 Experiments with a system including electronic reverberation 37

2.2 Non-in-line system including delay 39
2.2.1 Analysis of a system including delay 40
2.2.2 Simulation of system including delay 42
2.2.3 Experiments with a system including delay 43
2.3 Summary 45
3 Increasing the maximum stable feedback gain 47
3.1 Stability of feedback systems in a diffuse field 47
3.1.1 Introduction to feedback control theory 48
3.1.2 Stability of a reverberation enhancement system 49
3.1.3 Methods for increasing the stable feedback gain 52
3.2 Time variant processing 54
3.2.1 Digital implementation of time variant signal processing 55
3.2.2 Simulations of frequency shifting 56
3.2.3 Experimental results including frequency shifting 59
3.2.4 Simulations of time-varying delay 62
3.2.5 Experimental results including time-varying delay 63
3.2.6 Summary of time variant reverberation enhancement 64
3.3 Distributed mode loudspeakers 65
3.3.1 Operation of distributed mode loudspeakers 65
3.3.2 Experiments with a DML 68
3.4 Summary 71
4 Reverberation enhancement in a modal sound field 73
4.1 Analysis of the system 73

4.1.1 Derivation of the system response 73
4.1.2 Stability of a modal feedback system 76
4.2 Optimising the system 76
4.2.1 Frequency variation 80
4.2.2 Spatial variations 82
4.2.3 Time domain response 85
4.3 Consideration of more complex performance metrics 87
4.3.1 Alternative individual performance metrics 88
4.3.2 Generic performance metric 91
4.4 Effect of source and receiver positions 92
4.4.1 Primary source position 93
4.4.2 Altering the number of microphone positions 95
4.4.3 Optimising to a practical number of source and receiver positions 96
4.4.4 Summary 98
4.5 Summary 98
5 Diffusion and early energy 103
5.1 Diffusion of the sound field 103
5.1.1 Diffusion analysis of the experimental data 105
5.1.2 Simulation of diffusion 109
5.1.3 Relationship of diffusion to subjective preference 111
5.1.4 Discussion of the utility of the measures of diffusion 115
5.2 Early energy in the impulse response 116
5.2.1 Preferred values for early decay time and clarity 117

5.2.2 Early decay time and reverberation enhancement 118

5.2.3 Clarity and reverberation enhancement 126

5.3 Summary 130

6 Conclusions 133

6.1 Summary of conclusions 134

6.2 Future work 139

A Additional simulations of frequency shifting 141

References 145

List of Figures

Figure 1.1: Standing wave resonances in a pipe with rigid ends. The pressure distributions of the first five normal modes are shown. 4

Figure 1.2: Histogram of natural frequencies of a rectangular enclosure with dimensions 10 × 5 × 3 m. Each bar covers a 10 Hz bandwidth. 6

Figure 1.3: Frequency response of individual modes of a 10 × 5 × 3 m rectangular enclosure. The peaks are labelled with the natural frequencies in Hz. 8

Figure 1.4: Example decay trace shown as a solid line and the line of best fit which is used to measure the reverberation time is shown as a dotted line. This was measured as part of the experiment detailed in section 2.1.3. 14

Figure 1.5: Example of a room impulse response. This was measured as part of the experiment detailed in section 2.1.3. 16

Figure 2.1: Signal flow diagram for an all-pass filter where M is the number of delay samples, u and y are time signals and g is the gain which must be less than unity. 31

Figure 2.2: Gain in reverberation time for various values of γ, the ratio between the reverberation times of the electronic reverberator and the unaltered room, for a single channel VRAS with feedback gain of −20 dB. The dotted line shows the gain made by the equivalent MCR system and the vertical dashed line shows the value of γ_{max}. 34

Figure 2.3: Diagram showing the basic layout of the simulation. The secondary sources and receivers make up the reverberation enhancement system whilst the primaries are used to measure the room. 35

Figure 2.4: Simulation results for a 4 channel system including electronic reverberation in the feedback loop. The solid line shows the results of the simulation whilst the dotted line shows the reverberation times predicted analytically using equation (2.1.8). The errorbars show one standard deviation above and below the mean. 36

Figure 2.5: Predicting the reverberation time from the two-term decay trace, as opposed to the single term used in Figure 2.4, allows much better agreement with the simulation results especially for values of γ greater than $\gamma_{\max}$. 37

Figure 2.6: Block diagram of the experimental setup. 38

Figure 2.7: Measured reverberation times of a single channel system including electronic reverberation. Two different prediction methods are used; the solid line shows the values predicted using a two term decay model whilst the dotted line shows the values from a single term model. The vertical dashed line shows the value of γ_{max} predicted from equation (2.1.11). 39

Figure 2.8: Reverberation time gain against delay as a percentage of unaltered reverberation time. The modelled system has a single channel and a feedback gain of −12dB. 42

Figure 2.9: Simulation of a system including time delay for several values of delay and unaltered reverberation time. The dotted line shows the times predicted analytically and the solid lines show the simulation results. The errorbars show one standard deviation above and below the mean. 42

Figure 2.10: Measured reverberation times for a system with time delay in the feedback loop. Various values of delay are shown. The errorbars show one standard deviation above and below the mean. 43

Figure 2.11: Comparison of the measured reverberation time against the value predicted analytically with unity indicated by the dotted line. Points are included, for reference, which represent the unaltered room reverberation time and that which would be possible with a system without delay. 44

Figure 3.1: Diagram of a simple feedback system. 48

Figure 3.2: Example of a Nyquist plot. This system would be stable if negative feedback was implemented but unstable with positive feedback unless the feedback gain was sufficiently low. 49

Figure 3.3: Probability of instability for a single channel system in the diffuse field against the feedback gain of various values of the product of reverberation time and system bandwidth. 51

Figure 3.4: Signal flow diagram of a digital frequency shifter where ω_Δ is the desired shift in frequency. 55

Figure 3.5: Simulated reverberation time gain for a single channel system including 7.5 Hz frequency shifting in the feedback loop. Predicted results are from the analysis in chapter 2 but exclude frequency shifting. Audible artefacts are present above feedback gains of −6 dB. The unaltered reverberation time was 0.53 s. 57

Figure 3.6: Example impulse responses and decay for a single channel system including 7.5 Hz frequency shifting. The dotted lines indicate the decay trace which would be expected from a linear decay with reverberation time equal to the predicted value. 58

Figure 3.7: Reverberation time for a system with time invariant feedback. The resultant reverberation time is that including the effect of the system. This should be equal to the predicted values which use the analysis from chapter 2. The unaltered reverberation time of the room is included for comparison..... 60

Figure 3.8: Results for a system including frequency shifting. Two gain levels are shown; the lower plot is closer to the stability limit. Legend labels as in Figure 3.7..... 61

Figure 3.9: Simulated mid-frequency reverberation time as a function of feedback gain in a system including time-varying delay. 62

Figure 3.10: Reverberation times of a room affected by a system including time-varying delay. The two plots have different feedback gains with the lower plot having a higher gain. Legend labels as in Figure 3.7. 64

Figure 3.11: Frequency responses of a cone loudspeaker and a distributed mode loudspeaker. The measurements were made on-axis in a hemi-anechoic chamber. Note that the values of power gain include the amplifier gain and so do not represent the sensitivity of the transducer. 66

Figure 3.12: Diffuse field sound power measurements made in a reverberation chamber. The measurement is purely for comparison and is neither a sensitivity measurement nor a measure of absolute sound power. 67

Figure 3.13: Measured transfer function in the listening room. The response at low frequency is misleading due to the presence of background noise in this room below 100 Hz. 68

Figure 3.14: Open loop feedback gain in octave bands. The values for the 63 Hz and 31.5 Hz bands are too high because of background noise. 69

Figure 3.15: Reverberation times (T_{20}) measured with a single channel reverberation enhancement system using two different transducers with similar values of feedback gain. 70

Figure 3.16: Measured reverberation time (T_{20}) of a system using a DML averaged over several positions of the system..... 71

Figure 4.1: Block diagram showing the steps for calculating the metrics used for assessing the frequency variation and spatial variation in the room. 78

Figure 4.2: Diagram showing the positions of the virtual 'transducers' which have been used for the simulations presented in this chapter. 79

Figure 4.3: Relative standard deviation over frequency averaged over 30 microphone positions. Values are given for the unaltered room, that including a system using an identity matrix or matrix of ones as well as an optimised system using either a constant coefficient matrix or an array of FIR filters. 80

Figure 4.4: Frequency response averaged over 30 microphone positions showing the difference between the response of the unaltered room (solid) and that including a system which uses an identity matrix (dashed) and a system which uses an array of FIR filters optimised to reduce frequency variations (dotted) 81

Figure 4.5: Standard deviation of SPL over 30 random microphone positions for the unaltered room and several systems. 82

Figure 4.6: Spatial standard deviation of SPL evaluated with 10 sets of 30 random microphone positions. 83

Figure 4.7: Average sound pressure level in dB from 14-132 Hz evaluated over a grid of positions at head height whilst standing for the unaltered room and that including a system using an optimised array of FIR filters. 84

Figure 4.8: Histogram of SPL at a grid of microphones at approximately standing head height. This is the same data as Figure 4.7. 84

Figure 4.9: Example impulse response using the time domain model introduced in chapter 1. This is the response between the primary source and one of the measurement microphones. 85

Figure 4.10: Simulated reverberation times for the unaltered room and that including a selection of reverberation enhancement systems. The errorbars shows one standard deviation, calculated across 30 microphone positions, above and below the mean. 86

Figure 4.11: Observed reverberation times for systems optimised to various values of desired reverberation times. The bar at 0.65 s relates to the unaltered enclosure and the dotted line

shows unity. The errorbars show the standard deviation of reverberation time over position. 88

Figure 4.12: Frequency response of a system optimised to reduce frequency variations and a system optimised to achieve a reverberation time of 1.5 s. 89

Figure 4.13: Values of standard deviation, range and kurtosis of SPL over position for three systems which are each optimised to reduce one of these parameters. The different optimisations are shown as three groups of bars and the bars within each group relate to the different measured parameters. 89

Figure 4.14: Spatial variation of reverberation time for several systems. The bars, from left to right, show the value for the unaltered room, for systems using the identity matrix and a matrix of ones and for systems with matrices optimised to the relative standard deviation over frequency, the standard deviation of SPL over position, the absolute difference of the mean reverberation time with 1.5 s and the spatial standard deviation of reverberation time. 90

Figure 4.15: Values of RSD over frequency and standard deviation over space for a system optimised to create a reverberation time of 1.5 s and two systems optimised using the generic performance metric including a term to set the reverberation time to 1.5 s. 92

Figure 4.16: Varying the primary source position significantly alters the observed performance of the systems which were optimised to a fixed primary source. The metrics have been evaluated over 30 microphone positions at each of 20 primary source positions. The bars in this plot show the mean and standard deviation of the metric over the primary source positions. 93

Figure 4.17: Values of frequency and spatial variations for a system optimised with multiple primary sources. The squares show the values of metrics evaluated over the 6 primary source positions which were used to optimise the system and the bars show those metrics evaluated over 20 primary source positions. 94

Figure 4.18: Evaluating the frequency and spatial variations over a changing number of microphone positions. 95

Figure 4.19: Simulated frequency deviations and spatial deviations for a system optimised to four source and 8 receiver positions which are positioned to allow simple practical application. The performance is measured over the 6 source and 30 microphone positions used in section 4.4.1 and Figure 4.17. 97

Figure 5.1: Decay traces measured at 12 independent positions using a single channel reverberation enhancement system with 138 ms of delay in the feedback loop. 105

Figure 5.2: Measured values of (a) NSDRT and (b) NSDL for various values of reverberation time caused by a reverberation enhancement system with electronic reverberation. A line of best fit is shown, solid line, with 95% confidence intervals, dotted. These values are taken from 4 octave bands, hence there are 4 points for the unaltered room. 106

Figure 5.3: Measured values of (a) NSDRT and (b) NSDL for various values of reverberation time caused by a reverberation enhancement system with delay. A line of best fit is shown, solid line, with 95% confidence intervals, dotted. These values are taken from 4 octave bands, hence there are 4 points for the unaltered room. The axes limits are set to match Figure 5.2. 107

Figure 5.4: Decay traces in the 1 kHz octave band for the systems with delay which have the lowest (a) and highest (b) values of NSDRT. The solid lines show the position which has the lowest measured reverberation time whilst the dotted line shows the position with the longest. 108

Figure 5.5: Decay traces in the 1 kHz octave band for the system with delay which have the lowest (a) and highest (b) values of NSDL. The solid lines show the position which has the lowest mean level whilst the dotted line shows the positions with the highest. 109

Figure 5.6: Simulated values of (a) NSDRT and (b) NSDL for a 4 channel system with delay in the feedback loop. The reverberation time is increased by increasing the delay time whilst the feedback gain is fixed. The line of best fit is shown as a solid line with 95% confidence intervals shown as dashed lines. The circular point with errorbars shows the mean value and confidence interval for the unaltered room. 110

Figure 5.7: Simulated values of (a) NSDRT and (b) NSDL for a 4 channel system with an electronic reverberator in the feedback loop. The meaning of the different line styles is identical to Figure 5.6. 111

Figure 5.8: Estimated difference between 2 positions of the reverberation time (a) and sound pressure level (b), dotted lines, compared against the just noticeable difference, solid line. Values of the estimated difference are shown for various values of NSDRT and NSDL which were observed experimentally in section 5.1.1. The dashed lines show the expected

difference between positions with values of NSDRT and NSDL which vary with the reverberation time according to the lines of best fit from Figure 5.3..... 112

Figure 5.9: Value of NSDRT (a) and NSDL (b) which causes an expected spatial variation of reverberation time or level, respectively, equal to the JND. 114

Figure 5.10: Values of clarity which would occur if the decay trace was linear for various values of reverberation time..... 117

Figure 5.11: Simulated values of EDT for a 4 channel system including electronic reverberation time. This system is simulated with various values of reverberation time of the processor. The unaltered EDT is 0.5 s. The predicted values, dotted line, are evaluated from the analytically predicted decay trace with two decaying exponentials. The value of γ_{max} is shown as a dashed vertical line. 119

Figure 5.12: Ratio of EDT to reverberation time from a simulated 4 channel system with electronic reverberation. The dotted line shows the minimum recommended value of EDT and the dashed line shows the value of γ_{max}, below which the decay trace should be linear. 120

Figure 5.13: Simulated early decay times for a 4 channel system including delay in the feedback loop for three different values of unaltered EDT. The dotted lines show values predicted assuming no delay by using equation (1.2.2). 121

Figure 5.14: Simulated values of the ratio of EDT to reverberation time for a 4 channel system including delay. Three different values of unaltered EDT were simulated. The horizontal dotted line shows the minimum recommended value of this quantity. Errorbars have been omitted from this figure for the sake of clarity. 122

Figure 5.15: Measured values of early decay time for a system with electronic reverberation. The unaltered EDT is shown as a horizontal solid line whilst the dotted line shows a predicted value using the two term decay model. 123

Figure 5.16: Measured early decay time using a single channel system including delay. The solid line shows the unaltered EDT and the dotted line shows a value predicted assuming no delay as in Figure 5.13. 123

Figure 5.17: Ratio of measured early decay time to reverberation time shown against γ. The solid line shows the value for the unaltered room and the dotted line shows the minimum recommended value. The vertical dashed line shows the value of γ_{max}. 124

Figure 5.18: Measured ratio of EDT to reverberation time for a single channel system with delay. The solid line shows the value measured for the unaltered and the dotted line shows the minimum recommended value. 125

Figure 5.19: Measured decay traces with values of delay in the system ranging from 85 to 133 ms. This shows the consistency of the early part of the decay trace and the change in increase in curvature as the reverberation time is elongated. 126

Figure 5.20: Simulated values of mid-frequency C_{80} for a 4 channel system using electronic reverberation. The solid line shows the value of clarity for the unaltered impulse response, which had a reverberation time of 0.53 s. The dotted line shows the value, calculated from the mean mid-frequency reverberation time, which would be expected if the decay trace was linear. The dash-dot line shows a value predicted from the two term energy decay model. The vertical dashed line shows the value of γ_{max}. 127

Figure 5.21: Simulated values of C_{80} for a 4 channel system using delay. Three different unaltered reverberation times are shown. The unaltered value of the clarity is shown as a solid line whilst that predicted from the resultant reverberation time assuming a linear decay is shown as a dotted line. 128

Figure 5.22: Measured values of the clarity with a single channel reverberation enhancement system with electronic reverberation. The solid line shows the unaltered value, the dotted line shows the value calculated from the measured reverberation time assuming a linear decay and the dash-dot line shows a prediction based on the two term decay model. The vertical dashed line shows the value of γ_{max}. 128

Figure 5.23: Measured values of clarity for a single channel system including delay. The unaltered value of clarity is shown as a solid line whilst that predicted from the measured reverberation time, assuming a linear decay, is shown as a dotted line. 129

Figure A.1: Simulated reverberation times for a single channel system with frequency shifting for various values of the normalised feedback gain. 141

Figure A.2: Simulated reverberation times of a single channel reverberation enhancment system including frequency shifting. This simulation used an image model to create impulse responses of a room with volume 75 m^3. 142

Figure A.3: Simulation of a single channel reverberation enhancement system with frequency shifting using a model of the room impulse response based on exponentially decaying white noise. The unaltered reverberation time of the room is 1.5 s. 143

Academic Thesis: Declaration of Authorship

I, Hugh Alexander Hopper declare that this thesis 'Reverberation Enhancement for Small Rooms' and the work presented in it are my own and has been generated by me as the result of my own original research.

I confirm that:

1. This work was done wholly or mainly while in candidature for a research degree at this University;

2. Where any part of this thesis has previously been submitted for a degree or any other qualification at this University or any other institution, this has been clearly stated;

3. Where I have consulted the published work of others, this is always clearly attributed;

4. Where I have quoted from the work of others, the source is always given. With the exception of such quotations, this thesis is entirely my own work;

5. I have acknowledged all main sources of help;

6. Where the thesis is based on work done by myself jointly with others, I have made clear exactly what was done by others and what I have contributed myself;

7. Parts of this work have been published as:
    a. Hopper, H., Thompson, D., and Holland, K. (**2011**). "Reverberation enhancement in the modal sound field," in *Proceedings of the 130th Convention of the AES*, London, UK. (Audio Eng. Soc.).
    b. Hopper, H., Thompson, D., and Holland, K. (**2011**). "Reverberation enhancement for music practice rooms," in *Proceedings of ACOUSTICS 2011*, Glasgow, UK. (Institute of Acoustics).
    c. Hopper, H., Thompson, D., and Holland, K. (**2011**). "The effect of reverberation enhancement on the diffusion of the sound field," Proceedings of Meetings on Acoustics, **14**, p. 15001. (Acoustical Soc. America)

Signed:

Date:

Acknowledgements

I would like to thank those who have been involved in supervising this project: Ken Frampton, Paolo Gardonio, Keith Holland and, in particular, David Thompson for their guidance and support. I would also like to thank Pierre Chobeau and James Patterson for their contributions to this work, Tim Brookes of the University of Surrey for the loan of equipment and Jordan Cheer for useful discussions and technical assistance.

Nomenclature

A	total absorbing area, the product of surface area and absorption coefficient, in Sabines
A_n	complex modal amplitude
$B_{½}$	Half power bandwidth measured in Hertz
C_{t_c}	clarity ratio, the ratio in dB between the energy in the first t_c seconds of the impulse response and the energy in the remainder of the impulse response
D_n	damping constant of the n^{th} mode
EDT	early decay time, reverberation time measured on the first 10 dB of the decay trace
G	gain in steady state energy density caused by a reverberation enhancement system
G_{VRAS}	the value of G specifically related to the Variable Room Acoustic System (VRAS) which has a full feedback matrix
N_f	number of modes in the frequency band $(0, f)$
L_n	length of the nth linear dimension of a rectangular room
P	sound power in Watts
S	internal surface area of a room
T	reverberation time, the time taken for the sound pressure level to decay by 60 dB after the abrupt cut-off of a noise source measured in seconds
T_{20}	reverberation time evaluated from a best fit line on the part of the decay trace -5 dB to -25 dB below the maximum amplitude (-5 dB to -35 dB is known as T_{30})
V	volume of a room in cubic metres
W	Lambert function
$\mathbf{X}$	feedback matrix of a multi-channel system
a	decay rate of an exponential in relation to the energy density in a room which is related to the reverberation time by $a = 13.8/T$
c_0	speed of sound in air in metres per second
f	frequency in Hertz
f_s	the Schroeder frequency, the lower frequency limit of the diffuse field, in Hertz

g feedback gain

i imaginary unit $i^2 = -1$

n integer mode number which lists the natural frequencies of a system in order of ascending frequency

$\mathbf{n}$ vector mode number where the three elements n_1, n_2 and n_3 correspond to the modal integer in each spatial dimension

p pressure in Pascals

r radius in metres, the distance from a point in spherical coordinates

r_{rev} reverberation radius, the distance from a sound source at which the direct sound has equal level to the diffuse field. Also known as the critical distance.

t time in seconds

w energy density in Joules per metre

w_0 steady state energy density of a room, unaffected by reverberation enhancement

$\mathbf{x}$ three element vector describing the position of a sound receiver in metres

$\mathbf{y}$ three element vector used to denote the position of sound sources

Z acoustic transfer impedance defined as the ratio of pressure to volume velocity

Δf_n average spacing in Hertz between natural frequencies

α absorption coefficient, equal to $1-\beta$

β reflection coefficient, the ratio of the one-sided intensities of the reflected and incident sound to a particular material

γ ratio of the reverberation time of the electronic reverberator and unaltered room in the context of the Variable Room Acoustic System (VRAS)

ε_{n_k} normalisation constant where $\varepsilon_{n_k} = 1$ if $n_k = 0$ and $\varepsilon_{n_k} = 2$ if $n_k > 0$

ζ_n modal damping ratio

μ normalised feedback gain which accounts for all transducer sensitivities and assumes unit power gain through the room transfer function

μ_{MCR} normalised feedback gain used in the analysis of the MCR system which is related to the absolute feedback gain by $\mu_{MCR} = g\sqrt{4/c_0 A}$

π constant ratio between the circumference and diameter of a circle

τ	delay time
ψ_n	mode shape function for the mode n
ω	angular frequency in radians per second
ω_n	natural frequency in radians per second of the mode n
∇^2	Laplacian operator denoting the sum of 2nd partial derivatives in each of the three spatial dimensions: $\partial^2/\partial x_1^2 + \partial^2/\partial x_2^2 + \partial^2/\partial x_3^2$

List of abbreviations

ACS	Acoustic Control System – a reverberation enhancement system based on the principles of wave field synthesis
AFC	Active Field Control – a commercial reverberation enhancement system developed by Yamaha
DML	Distributed Mode Loudspeaker – a transducer based around a flexible panel which is designed to maximise the density of the bending wave resonances in order to provide a sound radiation characteristic with flat frequency response and wide directivity
ERES	Early Reflected Energy System – a system designed specially to enhance the early energy in the impulse response of a concert hall
FIR	Finite Impulse Response – a digital filter which uses a set of coefficients to scale the incoming signal at corresponding delay times and has no internal feedback
LARES	Lexicon Acoustic Reinforcement and Enhancement System – reverberation enhancement system developed by Lexicon
MCR	Multi-Channel Reverberation – reverberation enhancement system developed by Philips
NSDL	Normalised Standard Deviation of Level – measure of spatial variation of sound pressure level normalised to expected variance based on the reverberation time
NSDRT	Normalised Standard Deviation of Reverberation Time – measure of spatial variation of reverberation time normalised to expected variance based on the average reverberation time
RODS	Reverberation-On-Demand Systems – reverberation enhancement system which used gating of the input and output signals to avoid instability
RSD	Relative Standard Deviation – the standard deviation divided by the mean
SIAP	System for Improved Acoustic Performance – reverberation enhancement system designed with consideration of the 'ideal' early reflection pattern
SPL	Sound Pressure Level – the time averaged square pressure measured in decibels
VRAS	Virtual Room Acoustic System – reverberation enhancement system developed by Mark Poletti and marketed commercially as the Constellation system by Meyer Sound Laboratories Inc.

1 Introduction

The perception of sound can be greatly affected by the medium of transmission; for example, speech communicated via a faulty telephone line can be extremely difficult to understand. When the speaker and listener are in the same room then the room itself effectively becomes a channel through which sound is conveyed. The difference between the resulting sound and that which would be observed in the open air is largely defined by the physical properties of the room. The basic requirements for sound quality, as noted by Wallace Sabine in his seminal paper on reverberation (Sabine, 1923), are for the sound to be appropriately loud, the relative amplitudes of the parts which make up a complex sound to be preserved and the sequence of sounds over time to be audible separately from each other and from external noise.

Although these conditions seem relatively simple, they can in fact work against each other and the required balance between them will change depending on the application. For instance, the separation of sounds over time is more important for music which is very percussive than for choral music. In fact it is desirable in choral music for the sounds to blend together over time to some extent.

This is brought about by the reverberation of the room which is the combination of the large number of reflections from the walls and the resonances of the volume. It has been suggested that the reverberant characteristics of a room in which music is destined to be performed have affected the stylistic changes observed in music through history (Beranek, 1996; Byrne, 2010). Therefore, the acoustic properties of a venue designed for a specific purpose must be considered in relation to that purpose.

If the acoustics of a venue do not suit the intended purpose it can be difficult and expensive to alter the physical properties of the room, especially if the reverberation is insufficient. It was for this reason that electronic reverberation enhancement was first implemented. The acoustics of the Royal Festival Hall in London were severely criticised after its construction in 1951 (Barron, 1988). In subsequent experiments it was found that the reverberation time was too short, especially at low frequency. The reverberation time is the time in seconds taken for the sound pressure level to decay by 60 dB after the abrupt cut-off of a noise source.

In order to extend the reverberation time, without altering the physical characteristics of the room, an electronic system referred to as “Assisted Resonance” was designed and implemented (Parkin and Morgan, 1965). This system used loudspeakers and microphones positioned away from the performers to amplify the reverberant sound of the room. The

system was well received (Parkin and Morgan, 1964) and was installed on a permanent basis in 1965 (Parkin and Morgan, 1970). In 1998 the system was removed prior to a total renovation of the building and the acoustics of the hall between 2005 and 2007 (Kirkegaard, 2011).

The "Assisted Resonance" system was designed with a very large number of channels (up to 172 loudspeaker and microphone pairs) each of which worked on a small frequency bandwidth. This meant that this method of lengthening the reverberation time was relatively complex and expensive. Further developments to the technology have allowed increases in performance and reductions in channel count; this will be discussed in detail later in this chapter. The improvements in the technology, along with the greater proliferation and falling cost of high quality electronics, allows reverberation enhancement to be applied more widely.

One application which has been facilitated by the improvements of the technology has been for multi-purpose halls. These venues are required to host multiple styles of music as well as speech and drama. The natural acoustic properties of the room cannot be ideal for all of these events. In order to address this problem, the room could be constructed so that its physical properties can be altered, for instance, by changing the volume of the space by opening or closing doors leading to external reverberation chambers. This technique is used in a concert hall in Lucerne, Switzerland for example (Beranek, 1996). Alternatively, the material properties of the surfaces can be changed by extending or retracting sound absorbing curtains or similar.

Instead of altering the physical properties of the room the changes in the acoustic response can be effected through the use of a reverberation enhancement system. The system can be specified so that a suitable acoustic response is available for different programmes. This is especially useful in smaller halls as generally a larger volume is required to achieve a longer reverberation time. A natural extension of this trend is to apply the technology to significantly smaller rooms, allowing a new set of applications.

Currently available commercial systems are designed to work in concert halls and theatres but it may be feasible for the technology to be applied in significantly smaller spaces such as recording studios, music practice rooms and interactive auralisation suites which have volumes below 100 m^3. Due to the different properties of the natural responses of these spaces, there are additional complications and difficulties which must be overcome to achieve the desired response. This problem forms the basis of the current work and will be expanded on near the end of this chapter.

The following section in this chapter will introduce the basic theory of room acoustics and control systems which will be used throughout this work. Following that, the history and development of reverberation enhancement will be reviewed leading on to a discussion of the motivation for this work. Finally, there is a summary of the original contributions of the thesis which are expanded upon in the following chapters.

1.1 Theory of room acoustics

A basic introduction to the general theory of acoustic disturbances will not be presented here due to the wide availability of this material e.g. (Kinsler *et al.*, 2000). It is sufficient to say that the problem of room acoustics can be considered to be linear and time invariant and can be analysed using the three dimensional Helmholtz equation. The room response can be represented in terms of the standing wave resonances which are set up between reflective surfaces; these are the modes of the room. Using a modal summation the overall response can be derived by summing over a large number of modes. This analysis will be considered first in section 1.1.1.

Due to the properties of the modal solution, the number of modes occurring within a particular frequency bandwidth increases with increasing frequency. At high frequency, the number of modes required to provide an accurate representation of the room response becomes very large. At this point it becomes superfluous to specify the details of each individual mode and a statistical approach can be used instead. This approach leads to an approximation of the response of the room known as the diffuse field model. This is the most commonly used tool for analysing the behaviour of reverberation enhancement systems and is discussed in section 1.1.2.

In the final part of this section the common numerical routines will be discussed which are used to model the response of the room. One commonly used method is the image model, which approximates each possible reflection path between source and receiver as a phantom image of the source. The impulse response of the room can be found by summing over a large number of image sources. Each image source contributes a simple impulse which is suitably delayed and scaled to take into account the distance from the receiver and the number of reflections corresponding to that image.

1.1.1 Modal response of a room

As has already been mentioned, the standing wave resonances set up between reflective surfaces in a room are known as the modes of that room. It is easiest to visualise this behaviour in a one dimensional system like an organ pipe. The standing wave is equivalent

to two plane waves travelling in opposite directions at the same frequency so that they interfere constructively. The two plane waves are actually caused by sound reflected from each end of the pipe.

The length of the pipe and the boundary conditions at either end determine the frequencies at which resonance will occur. If the ends are rigid, then the boundary conditions will force the particle velocity to be zero and as a consequence the pressure will have its maximum value at these points. Resonance will occur at several frequencies and, in a one dimensional system with rigid boundaries, all of these will be a multiple of that of the lowest mode. Figure 1.1 plots the variation in pressure over the length of the pipe for the first five modes.

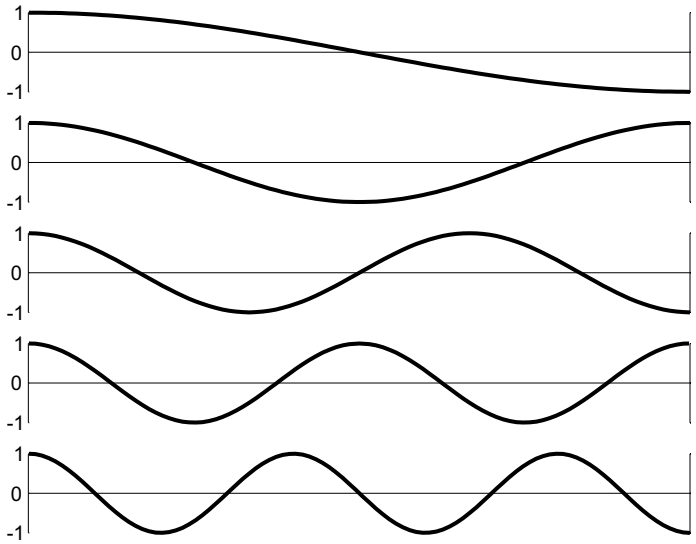

Figure 1.1: Standing wave resonances in a pipe with rigid ends. The pressure distributions of the first five normal modes are shown.

A mathematical analysis of this phenomenon can be derived by solving the Helmholtz equation. This assumes that the pressure varies harmonically with time; it is assumed that the time dependence is $e^{i\omega t}$. The Helmholtz equation is

$$\left(\nabla^2 + \frac{\omega^2}{c_0^2}\right) p(\mathbf{x}) = 0 \tag{1.1.1}$$

where ∇^2 denotes the Laplacian operator, i.e. $\nabla^2 = \partial^2/\partial x_1^2 + \partial^2/\partial x_2^2 + \partial^2/\partial x_3^2$, ω is the angular frequency, c_0 is the speed of sound in air, p is the complex pressure amplitude and $\mathbf{x}$ is the 3 element vector describing the position at which the pressure is evaluated. In a one dimensional system, the Laplacian operator can be replaced by the simple derivative $\mathrm{d}^2/\mathrm{d}x^2$.

Solving the Helmholtz equation in a three dimensional enclosure requires knowledge of the shape. A rigid walled rectangular box can be analysed easily and is representative of a typical room. It can be assumed that the pressure can be expressed as the multiple of three functions, each of which only varies over one spatial dimension (Nelson and Elliott, 1992). Taking into account the rigid walled boundary conditions, it can be shown that the solution is

$$p(\mathbf{x}) = \sum_{n=0}^{\infty} A_n \cos\frac{n_1 \pi x_1}{L_1} \cos\frac{n_2 \pi x_2}{L_2} \cos\frac{n_3 \pi x_3}{L_3} \tag{1.1.2}$$

where A_n is an arbitrary, complex modal amplitude, L_1, L_2 and L_3 are the dimensions of the room and n is an integer which linearly indexes all of the modes in order of ascending frequency and which maps to a vector index $\mathbf{n}$, whose elements n_1, n_2 and n_3 correspond to the modal integer in each dimension.

The spatial variation given by equation (1.1.2) can be isolated into a mode shape function given by

$$\psi_n(\mathbf{x}) = \sqrt{\varepsilon_{n_1}\varepsilon_{n_2}\varepsilon_{n_3}} \cos\frac{n_1 \pi x_1}{L_1} \cos\frac{n_2 \pi x_2}{L_2} \cos\frac{n_3 \pi x_3}{L_3} \tag{1.1.3}$$

where ε_{n_1}, ε_{n_2} and ε_{n_3} are normalization constants which ensure that

$$\int_V \psi_n^2(\mathbf{x}) \mathrm{d}V = V . \tag{1.1.4}$$

The value of the normalization constant is $\varepsilon_{n_k} = 1$ if $n_k = 0$ and $\varepsilon_{n_k} = 2$ if $n_k > 0$. For other geometries, the modeshape function will be different. In some simple cases, such as for a cylindrical enclosure, it will be possible to find an analytical expression for the modeshape function. However, this may not be possible for more complex geometries and in general the separation into functions of the three coordinate directions will not usually be possible.

The frequency at which the resonant behaviour of a mode occurs is known as a natural frequency of the enclosure. For a rectangular room these can be calculated from the dimensions of the room and the modal indices

$$\omega_n = c_0 \sqrt{\left(\frac{n_1 \pi}{L_1}\right)^2 + \left(\frac{n_2 \pi}{L_2}\right)^2 + \left(\frac{n_3 \pi}{L_3}\right)^2} \tag{1.1.5}$$

where ω_n is the natural frequency of the mode n and c_0 is the speed of sound in air. An example of the modal frequencies of a rectangular enclosure calculated using equation (1.1.5)

is shown in Figure 1.2 indicating the increasing number of modes in a fixed frequency bandwidth at higher frequency.

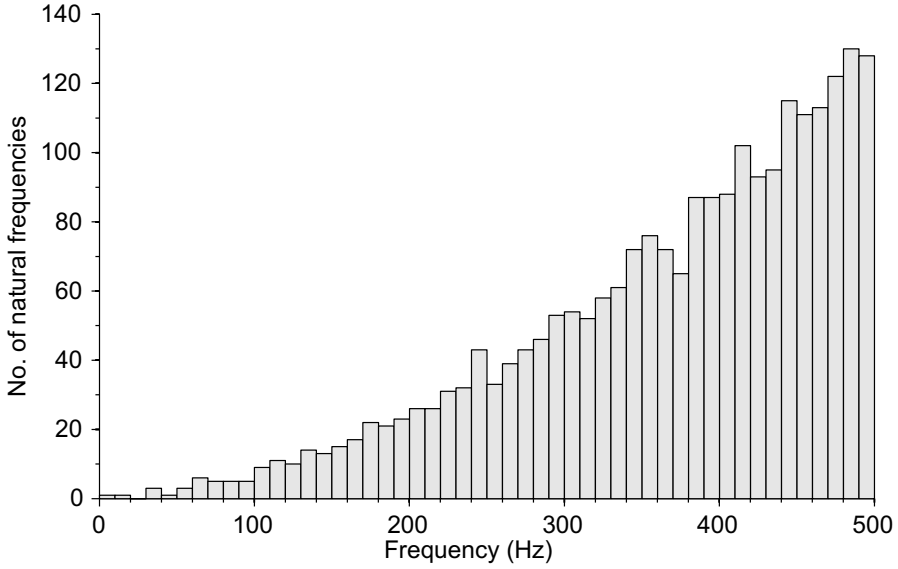

Figure 1.2: Histogram of natural frequencies of a rectangular enclosure with dimensions 10 × 5 × 3 m. Each bar covers a 10 Hz bandwidth.

Equation (1.1.1) does not include any terms for a noise source. This is included in the inhomogeneous Helmholtz equation which can be solved using a Green's function. The boundary conditions can be included by assuming that the enclosure is lightly damped and that the surfaces are locally reacting. This means that the enclosure walls are nearly rigid and no wave motion can occur within the walls. Given a small value of damping, the mode shape functions given above can be used.

Under these assumptions, a model of the behaviour of the sound field can be derived. The value of the modal amplitude A_n can be found in terms of the properties of the room so that the pressure becomes (Nelson and Elliott, 1992)

$$p(\mathbf{x}) = \sum_{n=0}^{\infty} \frac{\omega \rho_0 c_0^2 \psi_n(\mathbf{x})}{V\left[\omega c_0 D_n + i\left(\omega^2 - \omega_n^2\right)\right]} \int_V \psi_n(\mathbf{y}) q_{vol}(\mathbf{y}) \mathrm{d}V \tag{1.1.6}$$

where V is the volume of the enclosure, ρ_0 is the density of air, q_{vol} is the distributed volume velocity of the noise source, $\mathbf{y}$ is the source position vector, i is the imaginary unit and D_n is a damping constant related to the n^{th} mode. A simple model of damping is to assume that the damping term D_n is related to the natural frequency of each mode and the frequency of excitation. In this model the damping term can be expressed as

$$\omega c_0 D_n = 2\zeta_n \omega_n \omega \tag{1.1.7}$$

where ζ_n is the damping ratio which can also be expressed as a percentage. Typically the values of this ratio will be less than 10%.

For simple noise sources, it can be assumed that the source is a monopole described by the Dirac delta function in space. The sifting property of this function removes the integral so the source term becomes

$$\int_V \psi_n(\mathbf{y})\delta(\mathbf{y}-\mathbf{y}_p)q_0 \mathrm{d}V = \psi_n(\mathbf{y}_p)q_0 \tag{1.1.8}$$

where $\mathbf{y}_p$ is the position of this primary source and q_0 is the volume velocity of that source.

The simple damping model and point source assumption can be included by substituting equations (1.1.7) and (1.1.8) into (1.1.6) resulting in the pressure response

$$p(\mathbf{x}) = \sum_{n=0}^{\infty} \frac{\omega \rho_0 c_0^2 \psi_n(\mathbf{x})\psi_n(\mathbf{y}_p)q_0}{V\left[2\zeta_n\omega_n\omega + i(\omega^2 - \omega_n^2)\right]}. \tag{1.1.9}$$

This equation is similar to the Fourier transform of the differential equation modelling a single degree of freedom system and therefore an approximate model of the impulse response can be derived directly (Fahy and Walker, 1998) for a lightly damped system as

$$p(t,\mathbf{x}) = \sum_{n=0}^{\infty} \frac{\rho_0 c_0^2}{V\omega_n} e^{-\zeta_n\omega_n t} \sin(\omega_n t)\psi_n(\mathbf{y}_p)\psi_n(\mathbf{x})q_0 \tag{1.1.10}$$

where t is the time and the expression is only defined for positive times: $t \geq 0$. Each mode can be seen to decay in amplitude exponentially. The reverberation time for a mode can be approximated as the time taken for the exponential term to decay by 60 dB:

$$T \approx 6.9/\zeta_n\omega_n \,. \tag{1.1.11}$$

The reverberation of the room can be thought of as the sum of the decaying modes.

The impulse response given by equation (1.1.10) and the equivalent frequency domain response (1.1.9) require an infinite summation of modes. For practical application this summation must be truncated. Due to the shape of the frequency response function of each individual mode, the response within a fixed bandwidth will have negligible contributions from modes whose natural frequencies fall significantly outside that band.

The individual responses of the first ten modes of an enclosure, with a damping ratio of 5 % where the primary source located in a corner has a volume velocity of $1 \times 10^{-4}\ m^3 s^{-1}$, are

plotted in Figure 1.3 showing that the contribution of each mode below its corresponding natural frequency reduces significantly. If the bandwidth of interest was 0-20 Hz then the response would be dominated by the compliant mode **n** = (0,0,0) and the first longitudinal mode **n** = (1,0,0). All other modes are 15-20 dB lower than these two modes within this bandwidth and so the overall response could be calculated to a good approximation with just these two modes.

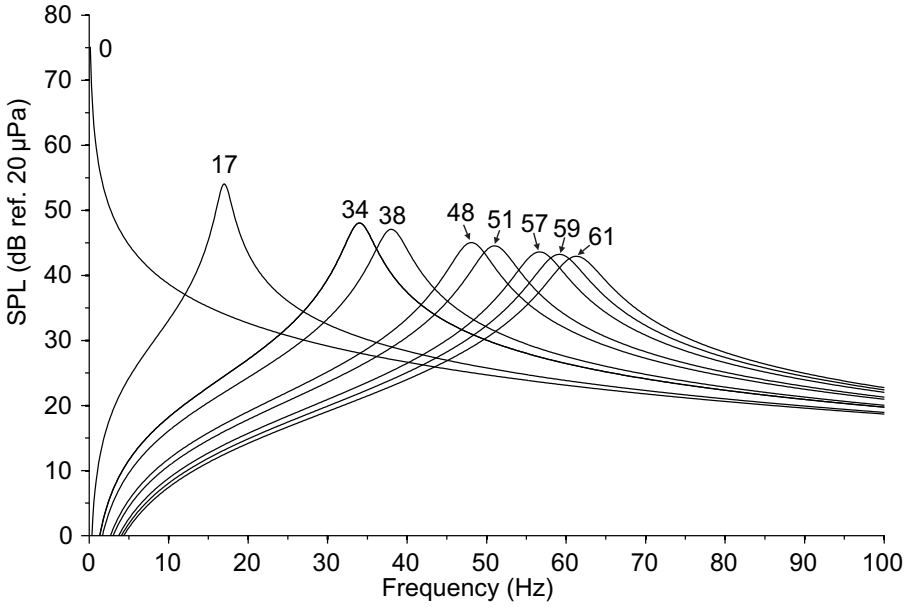

Figure 1.3: Frequency response of individual modes of a 10 × 5 × 3 m rectangular enclosure. The peaks are labelled with the natural frequencies in Hz.

On the other hand, if the bandwidth of interest was extended to 0-30 Hz then the next two modes have comparable amplitude to the contribution from the two lowest modes, despite having natural frequencies outside the band. The overall response would be significantly altered through the inclusion of these modes and therefore they must be included in the summation in order to achieve an accurate representation of the response. It may be necessary to include modes with natural frequencies 1.5 to 2 times that of the highest frequency of the bandwidth of interest.

Similarly, if the bandwidth under examination does not include 0 Hz, modes with natural frequencies below the lowest frequency of interest could conceivably be excluded from the summation if they have insignificant amplitude. Nevertheless, if the band of interest is at higher frequencies, the number of modes which must be included becomes very large (see Figure 1.2) making computation difficult. Also the assumptions which have been made during the derivation are less realistic at high frequency. For frequency bands with high

modal density a different model of the acoustic response of a room is required. The model usually employed is known as the diffuse field model and will be discussed in the next section.

1.1.2 Diffuse field model of a room

As was shown in Figure 1.2, the number of modes with natural frequencies within a fixed frequency bandwidth increases with increasing frequency. This means that at higher frequency the responses of each mode will overlap significantly. When the modal overlap is high, the spatial variations caused by individual modes will become less significant and the sound field will be more homogeneous. The value at which this behaviour occurs is usually considered to be the point at which at least three modes have natural frequencies which fall within the half power bandwidth of any particular mode. This point is known as the Schroeder frequency and above this limit the sound field can be considered to be diffuse.

The Schroeder frequency can be calculated from the physical properties of the room and is derived as follows (Schroeder, 1996). The number of natural frequencies between 0 Hz and a given frequency f can be calculated for a rectangular enclosure as

$$N_f(f) = \frac{4\pi V f^3}{3c_0^3} + \frac{\pi S f^2}{4c_0^2} + \frac{Lf}{8c_0} \tag{1.1.12}$$

where V is the volume, S is the total surface area and L is the total length of the edges (Kuttruff, 2000). The modal density, the average number of modes within a 1 Hz bandwidth, is then calculated as the derivative of (1.1.12) with respect to frequency. A good approximation for the modal density can be found by discarding all but the leading term such that

$$\frac{\mathrm{d}N_f(f)}{\mathrm{d}f} \approx \frac{4\pi V f^2}{c_0^3}. \tag{1.1.13}$$

The half power bandwidth measures the width in Hertz of the resonant peaks of each mode and it can be calculated from the reverberation time using (1.1.11)

$$B_{\frac{1}{2}} = \frac{\zeta_n \omega_n}{\pi} \approx \frac{2.2}{T}. \tag{1.1.14}$$

The point at which the width is measured is 3 dB below the highest point. The modal overlap is simply the product of the modal density and the half power bandwidth.

By setting the modal overlap equal to 3 and simplifying the expression, it can be shown that the Schroeder frequency is approximately (Schroeder, 1996)

$$f_s = \sqrt{\frac{3c_0^3 T}{4\pi V \cdot 2.2}} \approx 2000\sqrt{\frac{T}{V}} \tag{1.1.15}$$

where the constant value of 2000 is valid only for SI units. This shows that a room with lower damping, and correspondingly narrower resonances and higher reverberation time, will have a higher Schroeder frequency whilst a room with larger volume will have a lower Schroeder frequency. However, since the volume can take a much larger range of values (10 – 100,000 m^3) than the reverberation time (0.1 – 10 s), the volume of the room will be the most important factor in determining the Schroeder frequency. Moreover, it will be shown that the reverberation time depends strongly on the room volume.

The reverberation time can be derived as a function of the physical properties of the room by considering the energy balance equation. This uses as its independent variable the diffuse field energy density which is the total acoustic energy present in a unit volume. In a room, the change in energy density over time will be equal to the power input by any source of sound minus the power which is absorbed by materials on the surfaces. Assuming that the energy density is constant throughout the room, the dynamic energy density can be modelled as (Kuttruff, 2000)

$$P(t) = V\frac{\mathrm{d}w(t)}{\mathrm{d}t} + \frac{c_0 A}{4}w(t) \tag{1.1.16}$$

where P is the sound power of the source, w is the energy density and A is the total absorbing area which is the product of the total surface area of the walls and the absorption coefficient of the materials on the walls $A = S\alpha$. If different materials are used for different walls then the total absorbing area becomes the sum of the absorbing areas of each surface calculated using their corresponding absorption coefficient. The absorption coefficient is related to the reflection coefficient β as

$$\alpha = 1 - \beta \tag{1.1.17}$$

where the reflection coefficient is the ratio of reflected to incident one-sided intensities.

After the sound source is turned on, the energy density will increase until it reaches a constant value; this is known as the steady state. At this point, the differential term will equal zero. Therefore the steady state energy density can be calculated as

$$w_0 = \frac{4P}{c_0 A}. \tag{1.1.18}$$

If the sound source is switched off at $t = 0$ equation (1.1.16) becomes homogeneous and can be solved simply with an exponential solution

$$w(t) = w_0 \exp\left(-\frac{c_0 A t}{4V}\right) \tag{1.1.19}$$

from which the reverberation time follows as

$$T \approx 0.163 \frac{V}{A} \tag{1.1.20}$$

which is known as the Sabine formula and where the constant value of 0.163 is valid only in SI units. This equation was originally derived by Wallace Sabine empirically and then confirmed with a similar analysis to that presented here (Kuttruff, 2000). This formula is only accurate when the surfaces have relatively low absorption coefficients. By taking into account air absorption, the accuracy of the formula can be improved, but this is not required in this work.

The diffuse field assumptions which allow the use of the Sabine formula and other useful analytical tools will only hold above the Schroeder frequency. Additionally, the sound close to the source will be dominated by the direct field and the diffuse field analysis cannot be used. The energy density of an omnidirectional sound source in the free field due to spherical spreading is given by

$$w_{dir} = \frac{P}{4\pi c_0 r^2} \tag{1.1.21}$$

where r is the distance from the source. The point at which the direct field energy density is equal to the diffuse field is known as the reverberation radius or critical distance

$$r_{rev} = \frac{1}{4}\sqrt{\frac{A}{\pi}} \approx 0.1\sqrt{\frac{V}{\pi T}}. \tag{1.1.22}$$

At distances from the source greater than the reverberation radius, the diffuse field will dominate the measured signal. Under this condition and above the Schroeder frequency, the diffuse field will be a good approximation of the room response.

The absorption coefficients of materials are generally frequency dependent. Therefore the reverberation time will vary with frequency. As the diffuse field model is based on the assumption of a large number of overlapping modes, it is not useful to analyse the frequency

variations with narrowband measurements. In this case the detail of the measured transfer functions, reverberation times and absorption coefficients will vary significantly with position. For this reason the diffuse field is analysed in 1/3-octave or octave bands which will encompass a very large number of modes.

Although the narrowband transfer function is not a reliable measure in the diffuse field, its statistical properties are definable. It can be shown that, due to the central limit theorem, the real and imaginary parts of a diffuse field transfer function are both Gaussian distributed with equal variance and zero mean (Kuttruff, 2000). The magnitude of the transfer function is then Rayleigh distributed. This model of the transfer function can be used, for example, to calculate the probability of instability of a feedback system in the diffuse field (Poletti, 2000).

The diffuse field is a powerful tool for modelling room acoustics. However, this model cannot account for some observed behaviour. One aspect which is not present in the diffuse field model is the early energy. The energy balance equation (1.1.16) predicts an exponential decay, but often the early part of the impulse response does not fit this decay trace. The early part of the impulse response is perceptually important; the early decay time and clarity ratio are standardised measures which can be used to quantify this aspect of the room response (ISO3382-1, 2009).

The early decay time (*EDT*) is the time taken for the sound pressure level (SPL) to decay by 10 dB from its maximum level, multiplied by 6 to allow comparison with the reverberation time. The clarity ratio (*C*) is the ratio between the energy in the early and late part of the impulse responses expressed in decibels. The division of the impulse response is made at 50 ms or 80 ms depending on whether the measured room is intended for speech or music respectively. A similar quantity, the definition (*D*), is the ratio between the early energy and the energy in the entire impulse response although this is expressed in natural units.

In addition to the linearity of its decay, another simplification present in an ideal diffuse field model is that it is spatially homogeneous. However, it is known that, for instance, the sound pressure level decreases with increasing distance from the stage in concert halls (Barron and Lee, 1988). Some attempts have been made to extend the diffuse field analysis to account for these effects (Martellotta, 2009). Another common method for calculating the response of a specific room is to use numerical methods, some examples of which will be introduced in the following section.

1.1.3 Numerical methods

Although the analytical methods presented above provide a good general understanding of the acoustic response of a room, they ignore complexities inherent in the response of real rooms and therefore do not correctly predict many observed characteristics. Numerical models sacrifice generality for detail by recreating much more detail of a single room. There are many methods which are used for modelling rooms numerically which can be split into two main categories.

Deterministic methods directly model the pressure in the medium by splitting a given geometry into small elements. Common examples of this method are finite element modelling, boundary element modelling (Pietrzyk, 1998) and finite difference time domain (Botteldooren, 1995). In order to model wave propagation accurately, several elements are necessary within a wavelength. Therefore a model of a large enclosure will require a very large number of elements and this can be computationally taxing especially at higher frequencies. For this reason, deterministic methods for room acoustics applications are restricted to low frequencies. These methods are sometimes termed "wave based" in room acoustics literature although the terminology is used differently elsewhere e.g. (Hepberger *et al.*, 2002).

At higher frequencies, where the wavelength is small compared to the dimensions of the room, the propagation of sound can be modelled as a ray instead of a wave. This leads to modelling techniques known as geometric methods. Ray tracing (Krokstad *et al.*, 1967) and image source modelling (Allen and Berkley, 1979) are commonly used, often in conjunction (Naylor, 1993). Image source modelling is best suited to the early reflections and becomes computationally inefficient for the late reverberant tail. This part of the impulse response is better modelled with ray tracing which is less precise but more efficient.

More recently a method known as acoustic radiance transfer has been proposed (Siltanen *et al.*, 2007). This is also a geometric method but unlike the image source model and ray tracing, which only account for specular reflections or random scattering, this method can include measured reflectance distribution functions which map the reflections from a material spatially. This method works best at high frequencies for the late part of the reverberation. Hybrid models have been implemented using image source modelling for the early reflections, acoustic radiance transfer for the rest of impulse response and deterministic methods for low frequency (Southern *et al.*, 2011).

The numerical methods discussed here allow a precise model of a particular room to be constructed which is restricted only by the available computational power. The accuracy of

the models will also be reduced by the level of detail present and by the boundary conditions included which, depending on the specific technique used, have varying degrees of correlation with real world behaviour. Whilst the analytical approaches presented in previous sections allow general statements to be made about the acoustic responses of rooms, recreating the impulse response or frequency response of a given room using a numerical method allows investigation into some of the additional complexities which are neglected due to the assumptions made by the analytical models.

1.1.4 Measuring room acoustic parameters

The methodology for measuring quantities which are used to characterise the response of a room is defined in a number of international standards (ISO3382-2, 2008; ISO3382-1, 2009). These methods will be introduced briefly in this section as they will be used throughout this work. Both the frequency domain and time domain responses of a room are important and measurement techniques will be discussed for both.

The time domain response of a room can be totally characterised through its impulse response, i.e. the resulting pressure when excited by a perfect impulse. This varies significantly with position, especially over small time scales and does not easily provide information about the room by inspection. The quantities mentioned above such as reverberation time, early decay time etc. allow information to be gained about the general room properties from the time domain response.

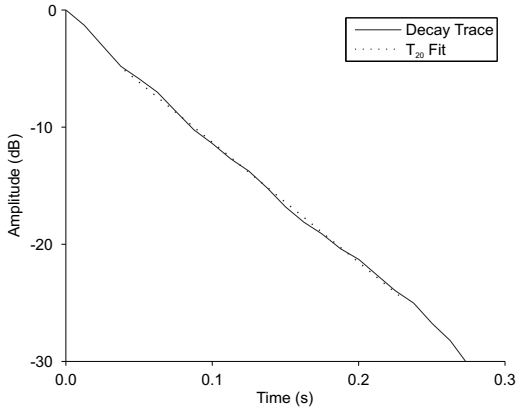

Figure 1.4: Example decay trace shown as a solid line and the line of best fit which is used to measure the reverberation time is shown as a dotted line. This was measured as part of the experiment detailed in section 2.1.3.

Measuring these quantities is achieved through analysis of the decay trace of the room. This is the resulting energy density, usually estimated as the squared pressure, which occurs when

a continuous sound source is abruptly cut off. Note that this is normally referred to as the decay curve; decay trace is the terminology used here for the purposes of clarity in the later chapters. As seen in equation (1.1.19), the energy density should decay exponentially. The decay trace is always viewed on a decibel scale and therefore it will be a straight line with negative gradient. An example decay trace is shown in Figure 1.4 showing that it is nearly a straight line.

The reverberation time is defined as the time taken for the energy density to decay by 60 dB. If the decay trace of the room is known and it was a perfectly straight line, the reverberation time could be found simply as the point where the amplitude is 60 dB lower than the initial amplitude. However, measured decay traces will always have some fluctuations from a straight line. The early part of the decay trace is often affected by strong early reflections and the end can be buried in background noise. These factors mean that a measurement of reverberation time based on the initial amplitude and the −60 dB point would be misleading.

In order to avoid these problems, the measured reverberation time is taken over a smaller section of the decay trace. The initial 5 dB of decay are ignored in order to avoid the effects of early reflections and the reverberation time is then measured over a smaller decay to avoid background noise. This leads to the quantities T_{20} and T_{30} which specify the length of decay over which the reverberation time is evaluated as 20 and 30 dB respectively. Note that these values only relate to the part of the decay trace over which the reverberation time is measured, the actual value is calculated so that it always corresponds to the time taken for a 60 dB decay.

In addition to inaccuracy caused by early reflections and background noise, the decay trace will often display short term fluctuations or even slight curvature in the centre of the range where the reverberation time is measured. In order to take these into account, the reverberation time is not evaluated from the simple −5 and −25 dB points, for T_{20}, but a regression line is fitted to this part of the decay trace and the gradient of the fitted line is used to calculate the reverberation time. The early decay time is measured from the gradient of a regression line fitted to the first 10 dB decay.

The decay trace can be measured by simply exciting the room with a noise source and then measuring the resulting pressure response when the noise source is switched off. This is known as the interrupted noise method. To ensure that the room is in the steady state before measuring the decay, the noise source must be active for at least a few seconds and not less than half of the estimated reverberation time. The use of random noise means that there will

be inherent variation of the measured reverberation time due to properties of the excitation signal. Therefore several decays are measured at each position.

Due to the spatial variations of reverberation time, several measurement positions must be used. The accuracy of the measurement depends on the number of positions used. For survey purposes, as few as two independent positions can be used, but 6 or 12 positions are recommended for 'engineering' and 'precision' measurements respectively with at least 2 source positions in either case (ISO3382-2, 2008). The number of decays measured at each position should be 1, 2 or 3 depending on whether survey, engineering or precision measurements are required.

In order to avoid the variability caused by the use of random noise, the decay trace can be calculated through reverse integration of the impulse response (Schroeder, 1965). Although this method theoretically gives the same precision as an infinite number of interrupted noise decay measurements, the true precision is thought to be approximately equivalent to 10 interrupted noise decay measurements (ISO3382-1, 2009). An example impulse response is shown in Figure 1.5.

In order to use the integrated impulse response method, the impulse response must be measured. This can be done simply by using an impulsive signal which approximates a true impulse such as a gunshot or balloon burst. However, this cannot always provide adequate signal level above the background noise. In order to improve the signal-to-noise ratio, the impulse response is often measured by deconvolution using special excitation signals. The most commonly used signals are swept sine and maximum length sequence. Using these signals allows significant improvements to the signal-to-noise ratio without increasing the sound power of the source.

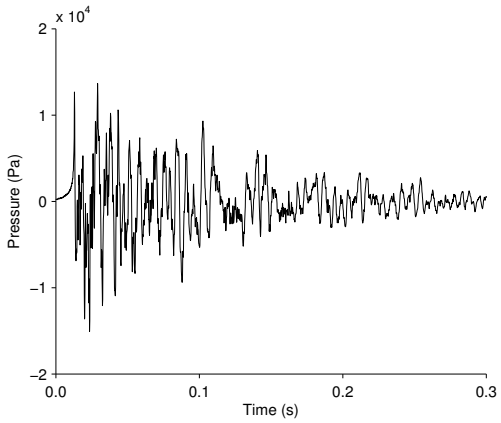

Figure 1.5: Example of a room impulse response. This was measured as part of the experiment detailed in section 2.1.3.

To measure the impulse response using a swept sine or maximum length sequence, the response of the room excited by the signal is measured. This is then deconvolved from the original unaltered signal which can be achieved using a simple cross correlation or a frequency domain method. The gain in signal-to-noise is related to the length of the swept sine signal or the number of repetitions of the maximum length sequence. These methods are robust to background noise and even non-linear distortions but cannot be used if there are any time varying elements in the room (ISO18233, 2006).

The reverberation time is usually analysed in octave or one-third octave bands. This is achieved by filtering the impulse response or interrupted noise signal prior to generating the decay trace using standard analogue or digital filters (ISO61260, 1996). The filtered signals can then be processed normally to create separate decay traces for each band which can then be used to find the banded reverberation times. When a single value is desired, a 'mid-frequency' value is often used which is the arithmetic mean of the values in the 500 Hz and 1 kHz bands.

The transducers used for the measurement should be omnidirectional and should have a flat frequency response within the bandwidth of interest. The positions of the transducers must be chosen to avoid the influence of the direct sound radiation or boundaries. This means that transducer positions must be further apart than the reverberation radius and should not be placed too close to the walls or floor of the room.

Using these guidelines, accurate measurement of the reverberation time and other parameters of the time domain response of the room can be achieved. The particular method used will depend on the available equipment and the characteristics of the room which is to be evaluated. This should have negligible effect on the measured result as long as sensible choices are made.

1.2 Reverberation enhancement

Since the invention of reverberation enhancement, the technology has developed significantly. There have been several commercial implementations each of which offered a slightly different strategy for improving the acoustic response of a room. This section will examine the development of reverberation enhancement and summarise the different commercial and academic perspectives.

1.2.1 The beginnings of reverberation enhancement

As was mentioned at the start of this chapter, the first electronic reverberation enhancement system was the Assisted Resonance which was implemented in the 1950s in the Royal Festival Hall in London in order to remedy the short reverberation time at low frequency (Parkin and Morgan, 1970). The system consisted of a large number of channels each of which was tuned, using a Helmholtz resonator, to a particular frequency. This system is part of a class of reverberation enhancement systems known as non-in-line which means that the microphones are placed such that the direct sound level from the primary source is negligible compared with that of the reverberant sound.

The other class of system, known as in-line, places the microphones, which are in this case often highly directional, close to the performers so that the direct sound dominates. The loudspeakers are then placed so that very little signal can feed back to microphones and the majority of their output is heard only by the audience. The first system of this kind was developed by Philips and was known as "Ambiphony" (Vermeulen, 1956). The original publication related to this system referred to it as "stereo reverberation" but this name was dropped in order to differentiate it from the newly introduced technology of stereophonic records (Dutton, 1966).

The Ambiphony system used directional microphones hung above the stage pointed at the performers. The signals from these microphones were recorded onto an analogue tape reel which had multiple playback heads. The resulting signals, delayed by various different times, were replayed into the auditorium via loudspeakers spaced around the audience. The system was used in several concert halls (Vermeulen, 1956) and also implemented in a recording studio (Dutton, 1966). The application in a recording studio is interesting as the performers are also the intended audience of the resulting reverberant sound.

Ambiphony and other in-line systems are quite similar to a standard public address system due to the avoidance of feedback and, for the most part, the separation between audience and performer. The main difference between in-line reverberation enhancement systems and public address systems is the fact that the in-line systems are concealed from the audience. This thesis will concentrate on the non-in-line systems, but the Ambiphony system is important in the development of reverberation enhancement because of the inclusion of electronic processing, the tape delay, to improve the performance of the system.

The next stage in the development of non-in-line reverberation enhancement systems was known as multi-channel amplification of reverberation (MCR). Unlike the Assisted Resonance system, MCR has broadband channels and can increase the reverberation time

over the entire audio bandwidth. Although the commonly used name of this type of system originates from the implementations made by Philips (de Koning, 1983/84), a mathematical analysis of this type of system was actually published earlier (Franssen, 1968) and first implemented in the Stockholm concert hall separately from that company (Dahlstedt, 1974).

The broadband nature of the MCR system means that the entire audio bandwidth is affected by every channel. The reverberation time cannot be increased arbitrarily due to the problem of instability. This phenomenon is known as 'howling' or sometimes as the Larsen effect and will occur if the amplifier gain of the system is set too high. As the gain of each channel is limited, the MCR system requires a large number of channels in order to create useful increases in the reverberation time. Due to the broadband nature of this system, fewer channels are required than for the Assisted Resonance system. In the system installed in the Stockholm concert hall, mentioned in the previous paragraph, 55 channels were used causing significant gains in the reverberation time (Dahlstedt, 1974).

The change in reverberation time caused by the introduction of the MCR system can be calculated using the energy balance equation (1.1.16) by adding a term for each feedback channel which is proportional to the energy density. By assuming that every channel has equal feedback gain, the resulting differential equation can be written as

$$P(t) + Ng^2 w(t) = V\frac{\mathrm{d}w(t)}{\mathrm{d}t} + \frac{c_0 A}{4}w(t) \tag{1.2.1}$$

where N is the number of channels and g is the feedback gain (Krokstad, 1988). Solving this equation shows that the reverberation time gain is given by

$$\frac{T_1}{T_0} = \frac{1}{1 - N\mu_{MCR}^2} \tag{1.2.2}$$

where T_0 is the unaltered reverberation time of the room, T_1 is the reverberation time including the effect of the system and μ_{MCR} is the normalised feedback gain given by $\mu_{MCR} = g\sqrt{4/c_0 A}$.

It can be shown that the feedback gain μ_{MCR} cannot exceed 0.25 without risk of instability and that this value must be lower for multi-channel systems (Poletti, 2000). In order to achieve large gains in reverberation time, a large number of channels must be used. However, since the steady state energy density will also increase by the same factor as the gain in reverberation time, a large MCR system can increase the sound pressure level significantly. This is not always desirable and can restrict the usable reverberation time gain.

1.2.2 In-line reverberation enhancement

In order to achieve higher gains in reverberation than are possible with an MCR system whilst reducing the required number of channels and reducing the risk of instability, many commercial systems were developed employing an in-line principle. Additionally several commercial systems were developed specifically to improve the early reflections. These systems will now be summarised.

The Electronic Reflected Energy System (ERES) was developed by Jaffe Acoustics in 1977 and comprised multiple microphones placed around the stage the signals from which were suitably delayed and replayed to an array of loudspeakers spaced around the auditorium (Jaffe, 1977). The length of the time delay was adjusted in accordance with the position of the loudspeakers. The loudspeakers placed near the stage had the shortest time delay and these were designed to enhance the early reflections.

In order to avoid the problem of instability due to feedback, the Reverberation-on-Demand Systems (RODS) implemented electronic gates which only allowed sound to be picked up by the microphones or output by the loudspeakers (Barnett, 1987). The system used electronic reverberators to which the microphone signals were fed when it was detected that the overall signal level was rising. Once it was detected that the signal level was falling, the connection between the microphones and reverberators was severed and the output of the reverberators was connected to the loudspeakers. Due to this method of operation, the RODS system could only enhance the late reverberation. For this reason the RODS system was also combined with ERES for some applications (Barnett, 1988).

One system which attempted to recreate a specific acoustic response, rather than simply increasing the reverberation time, was the Acoustic Control System (ACS). This was developed using the principles of wave field synthesis (Berkhout, 1988). Under this regime, signals from directional microphones placed close to the source were replayed with suitable delay in order to synthesise specific image sources related to the desired acoustic. This theoretically allows the acoustic design to be totally separate from the architectural design (Berkhout, 1992).

The proliferation of digital signal processing allowed further improvements to these systems. One particular example is the Lexicon Acoustic Reinforcement and Enhancement Systems (LARES) which took advantage of the high quality of the digital reverberation algorithms developed by Lexicon for use in recording studios (Griesinger, 1991). The first LARES system, deployed in the Elgin Theatre in Toronto, used two microphones hung above the stage connected to 120 loudspeakers via a bank of 16 time variant, digital reverberators.

LARES allows the reverberation time to be increased without increasing the steady state level and the use of time variant reverberation algorithms reduced the risk of instability (Griesinger, 1992). This allows the microphones to be placed more freely than in other in-line systems. Although the use of time variance to improve stability limits had been used in public address system previously (Schroeder, 1964), this is probably the first example of time variance being used to improve the performance of reverberation enhancement.

The LARES technology has also been adapted for use in music practice rooms. Despite the use of directional microphones pointed away from the loudspeakers, the feedback path cannot be eliminated as easily as for a system installed in a concert hall. In order to address this problem, the system is installed in specially constructed room with very low reverberation times which minimise the level of the reflected sounds as well as reducing transmission of sound to the outside environment (Freiheit, 1996).

Another in-line system which incorporates time varying processing is the System for Improved Acoustic Performance (SIAP). Whilst the construction and operation of SIAP is similar to the other in-line systems, the main difference is claimed to be the consideration of the existing acoustics of the hall and the creation of complementary early reflections (Prinssen, 1994). The system also includes at least one microphone positioned to pick up reflected sound from the source and one loudspeaker whose output is designed to reach the audience via a reflection (Prinssen, 1992). Therefore this could be considered to be the first hybrid in-line/non-in-line system, although it is heavily prejudiced to the former mode of operation.

These in-line systems can provide large increases in the reverberation time perceived by the audience and can also provide control over early reflections. The advantages of this design strategy in large halls are many, especially if separate control over the acoustic response on stage and in the audience is necessary. However, in smaller spaces, where it is impractical or undesirable to differentiate acoustically between the audience and the stage, this type of system is not appropriate. Non-in-line systems allow the acoustic response of the entire enclosure to be altered homogeneously and are therefore better suited to smaller spaces.

1.2.3 State of the art non-in-line reverberation enhancement

Non-in-line systems, based on similar principles to the MCR system, have continued to evolve. In a similar fashion to the development of in-line systems, modern non-in-line systems take advantage of digital signal processing to improve their performance. One example of this is the Active Field Control (AFC) system developed by Yamaha (Miyazaki *et al.*, 2003). This is a hybrid system including an in-line part to enhance the early reflections.

However, the reverberation time is altered using a non-in-line part which purposefully includes feedback from the loudspeakers to the microphones as part of the operation (Shimizu and Kawakami, 1991).

The non-in-line part consists of omni-directional microphones placed away from the stage, significantly outside the reverberation radius of the sound sources. The signals from these microphones are processed with an electronic microphone rotator, which periodically switches the loudspeaker to which each microphone is connected. Time variant FIR filters are also used to enhance the resulting reverberation time. The time variation caused by these two elements allows increases in feedback gain. The loudspeakers that make up the non-in-line part of the system are directed so that their output reaches the audience via a reflection (Kawakami and Shimizu, 1990). The system has been installed in smaller spaces including a music rehearsal room with a volume of 350 m^3 (Yamaha, 2009).

The Variable Room Acoustic System (VRAS) works on a similar principle. Omni-directional microphones are placed around the auditorium and their signals are affected by electronic reverberators. The feedback matrix is full, meaning that every microphone is connected to every loudspeaker (Poletti, 1999). This gives an increase in feedback gain proportional to the square root of the number of channels (Poletti, 1994b).

No time variant processing is used in this system, instead the reverberator has been designed to have a unitary frequency response, i.e. allpass (Poletti, 1998b). It has been shown that the benefits of including frequency shifting, a commonly used form of time variant processing, decrease with increasing number of channels (Poletti, 2004). Additionally the benefits of frequency shifting are even lower when the feedback path has a unitary frequency response. The unitary reverberator has additional advantages in that it decreases the “colouration” caused by the system (Poletti, 1994a). Colouration is defined as changes in the statistical distribution of the frequency response.

The use of electronic reverberators allows increases in reverberation time above the increases in diffuse field energy density. This has been likened to an increase in the volume of the room without alteration of the average absorption coefficient of the surfaces (Poletti, 1993). The VRAS system also includes an in-line part designed to increase the early energy (Poletti, 1998a; Poletti, 2006). Similarly to the non-in-line part of the system, the in-line part includes specifically designed multi-tapped delay lines which have unitary frequency responses in order to reduce colouration and the risk of instability (Poletti, 2007). The VRAS system is sold commercially by Meyer Sound under the brand name Constellation (Poletti, 2010).

Both AFC and VRAS are successful, commercial applications of non-in-line reverberation enhancement. They both take advantage of digital signal processing in order to increase the performance of a given number of channels. Measures are taken in both systems to avoid instability, although a different approach is taken for each system. AFC uses time variant FIR filters whilst VRAS uses unitary electronic reverberators. These systems can be considered to be the most advanced of their kind which are currently available.

1.2.4 Active wall

An alternative method for altering the reverberation time, known as an active wall, is achieved by placing the microphones in close proximity to the loudspeakers which are designed to alter the reflection coefficient of the wall surface (Guicking *et al.*, 1985). The feedback signal is reduced by either acoustic or electronic means. This has been done using bi-directional microphones with the null of the directivity pointed towards the loudspeaker (Vuichard and Meynial, 2000). It can also be achieved with feedback cancellation algorithms.

A commercially available version of this technology is the CARMEN system marketed by CSTB (Schmich *et al.*, 2011). This system consists of a large number of "cells" positioned on the walls and ceiling of the auditorium each of which consists of a microphone and associated loudspeakers. The main advantage of this system is claimed to be the conservation of the space and time coherence of the sound field (Vian and Meynial, 1998). This is assumed to improve the "naturalness" of the resultant sound and improve the audience's ability localise sound in comparison with other reverberation enhancement systems. It is also claimed that this system is easier to install and tune compared with other systems.

A similar system has been developed which also includes electronic reverberation to improve the performance. This system is designed for small rooms with low unaltered reverberation time (Nagatomo *et al.*, 2007). The system also places polyurethane balls in front of the loudspeaker which are designed to scatter sound. This reduces the directivity of the loudspeaker and creates a more diffuse radiation.

The inclusion of some mechanism by which the direct sound from the loudspeaker is reduced allows much shorter distances between loudspeaker and microphone. The overall behaviour is similar to a standard non-in-line reverberation enhancement system, namely a change in the effective absorption of the surfaces. Changes in the effective volume may also be realised through the use of time delay or electronic reverberation. The close placement of loudspeaker and microphone is convenient and may improve the coherence of the sound field.

1.2.5 Flat panel loudspeakers

All of the systems discussed above, use traditional cone loudspeakers. One unusual system has been created using a different kind of transducer. These consisted of wooden plates which were excited by a standard loudspeaker motor (Berndtsson, 1995). The design of the loudspeakers was inspired by the resonating soundboard of a guitar. The original purpose of these loudspeakers was to amplify instruments with a more "natural" sound in comparison to standard loudspeakers. A reverberation enhancement system, using these wooden loudspeakers, was constructed using an in-line principle (Berndtsson and Krokstad, 1994).

The reverberation enhancement system including these loudspeakers was found to give significant increases in measured reverberation time. However, it was noticed that the loudspeakers introduced large peaks in the frequency response which were due to resonances of the wooden panel. At the frequencies of these peaks, the risk of instability was much higher and ringing tones were problematic.

It was noted that the problem of these particular resonances could be reduced by altering the physical properties of the panel so that the modal density was much higher. This was effectively implemented independently in the form of the distributed mode loudspeaker (DML) marketed by NXT (Harris and Hawksford, 1997). These transducers retain a flat panel form, but the material properties and motor placement are specifically chosen to provide relatively flat broadband response.

The benefits of this type of transducer, in comparison to traditional cone loudspeakers, are the wide directivity at high frequency and the incoherence of the radiated sound (Gontcharov and Hill, 2000). The characteristics of the direct sound radiation have been likened to the diffuse sound field (Azima and Mapp, 1998). It has been shown that the incoherence of radiation reduces the effect of boundary interactions and room modes (Azima and Harris, 1997; Fazenda *et al.*, 2002). Diffuse radiation of sound for reverberation enhancement has been implemented using omnidirectional loudspeakers based on a dodecahedral arrangement of drivers (Woszczyk, 2011), but DMLs may achieve this more conveniently. Additionally, it has been found that DMLs can provide additional feedback gain before instability in certain situations (Mapp and Ellis, 1999).

Flat panel loudspeakers have been used within the context of reverberation enhancement. Since this implementation, significant improvements have been made to the performance of this class of transducer. These newer loudspeakers may provide performance improvements to reverberation enhancement systems due to the incoherent radiation of sound.

1.3 Summary of this work

The technology of reverberation enhancement is highly developed and is commercially successful, with several products currently available. Modern systems take advantage of digital signal processing to increase the performance of the systems significantly whilst reducing the required number of channels. This is achieved through the use of electronic reverberation, FIR filters and multi-tap delays. The colouration and risk of instability introduced by the systems has been reduced through the use of time-variant processing.

The basic motivation for this work is to improve understanding of the mechanisms by which reverberation enhancement operates and through this knowledge improve the performance of future systems. In this section the specific research topics which have been investigated will be introduced. Furthermore, the original contributions presented will be summarised.

1.3.1 Research goals

Although reverberation enhancement is a highly developed technology, it has almost exclusively been designed for concert halls intended for the performance of classical music. Whilst there have been applications of the technology to smaller spaces, such as music rehearsal rooms, these have mostly consisted of direct transplants of technology designed for large halls and the differences in the acoustic response of the room have been assumed to be negligible. The motivation for this work is to investigate this assumption and to suggest possible improvements to the specification of reverberation enhancement systems in small rooms.

In this work small rooms are assumed to be spaces with volumes less that 100 m^3. There are two main differences in the acoustic response of small and large rooms. The first of these is the extent to which the room approximates a diffuse field above the Schroeder frequency. The term “diffusion” can be used to describe this concept. The analysis of the behaviour of reverberation enhancement systems (Krokstad, 1988; Poletti, 1994b) is based on the theory of the diffuse field so the accuracy of this analysis will depend on the diffusion of the sound field. It is beyond the scope of this work to consider highly non-diffuse spaces such as long or flat rooms or rooms where there is a particularly uneven placement of absorptive material. Instead, the goal of this work is to test the accuracy of diffuse field analysis in relation to small rooms which, in theory at least, should be reasonably well estimated as a diffuse field.

Another difference between small and large rooms is the Schroeder frequency itself. In large rooms, the Schroeder frequency will be low enough that the frequency band below it will be small and not important for auditory perception. This is not the case in small rooms where

the modal frequency region will be a significant part of the audible frequency range. Therefore this work will investigate the effect of reverberation enhancement systems on the modal sound field at low frequencies in small rooms.

Another important consideration for reverberation enhancement in small rooms is the availability of space. By definition, there will not be a large amount of space for a large number of channels. Also it is preferable for the reverberation time to increase without increasing the overall sound level, which is already relatively high in small rooms. For this reason, the use of techniques which allow increased feedback gain before instability will be investigated as well as methods which allow increases in reverberation time without increasing the feedback gain.

Whilst these techniques have already been applied in reverberation enhancement systems in small and large rooms, their effectiveness in small rooms has not been well documented. This is especially important in relation to the diffusion of the room as much of the theory behind these techniques is dependent on the presence of a diffuse field. Additionally, there are some unexplored ideas, such as the use of DMLs, which will be investigated in this work.

The final consideration of this work will be the investigation of the effect on additional quantitative measures of the resultant room response. Whilst the reverberation time gives a good general impression of the room response there are several other variables which are commonly used to characterise a room. These include the early decay time and clarity ratio, both of which relate to the early part of the impulse response. Although there has been some work on the control of these parameters through the use of in-line reverberation enhancement systems, the effect of non-in-line systems in small rooms has not been investigated.

There are also several quantities relating to the diffusion of the sound field. One of these is the colouration which measures the degree to which the frequency response in the room matches that expected in an ideal diffuse field. There are also spatial measures such as the normalised standard deviation of level and the normalised standard deviation of reverberation time (Green, 2011). These quantities can be used to assess the performance of a reverberation enhancement system more comprehensively than can be done simply with the reverberation time. Also, this could allow a better estimate of the subjective quality of a given system.

The research goals given in this section have formed the basis of the work presented in this thesis. In the following section the original contributions from this work will be summarised.

1.3.2 Main original contributions

The major original contributions from this work are:

- Analysis, simulation and experimental verification of a reverberation enhancement system in the diffuse field which includes a pure time delay in the feedback loop. Although time delay has been used for in-line systems, the application and analysis of its effect on a non-in-line system is novel.
- Contrary to expectations based on the literature, it has been found that DMLs have a negative effect on the performance of reverberation enhancement. This main difference when using this type of transducer is a reduction in the stable feedback gain.
- Numerical optimisation of the feedback matrix of a reverberation enhancement system to improve its performance in a modal sound field. The results are heavily dependent on the specific room, system and desired performance but optimisation is considered to be more important for a modal sound field than a diffuse field.
- Showing that the degree to which a room approximates and diffuse field is affected by the reverberation enhancement system. This may cause spatial variations in reverberation time and level to be noticeable.
- Considering the effect of reverberation enhancement on the secondary parameters of the room response, such as early decay time, with respect to known subjective preferences. More stringent requirements are necessary for the systems to achieve desirable acoustic properties in a small room.

The work is presented in detail in the following four chapters. Chapters 2 and 3 deal with the possibility of increasing the resultant reverberation time of the room without increasing the number of channels that make up the system. This is done by using various signal processing methods. In chapter 2, delay and electronic reverberation effects are used within the system whereas chapter 3 investigates the use of time varying processing to increase the maximum stable feedback gain. These two chapters consider the methods which can be used to improve the performance of the system in this context whilst assuming a diffuse field.

The diffuse field model does not provide a complete picture of the response of a room. The performance of a reverberation enhancement system in non-diffuse conditions is investigated in chapters 4 and 5. As small rooms are the focus of this work, the response of the room at low frequencies will be dominated by isolated modal resonances. The performance of the system in this frequency region is considered in chapter 4. This frequency band is below the Schroeder frequency. Above this point the room may be a poor approximation of a diffuse

field. The degree to which the sound field approximates a diffuse field will be considered in chapter 5. Additionally, the properties of the room impulse response which are not predicted by the diffuse field model are explored. These quantities are used to assess the performance of a reverberation enhancement system.

The work presented here shows that it is possible to include a reverberation enhancement system in a small room and create a significantly different room response. However, the properties of the sound field place additional restrictions on the performance of the system in comparison with that placed in a larger space. By taking this into account, significant increases in reverberation time are possible, for example, in this work an increase in reverberation time from 0.5 to 0.7 s has been produced by a system with only a single channel.

2 Increasing the resultant reverberation time

The performance of a reverberation enhancement system can be assessed by the gain in reverberation time which is imparted on the room in which the system is installed. As shown in section 1.2.1, the possible gain in reverberation time is dependent on the number of channels present in the system. This means that a large number of channels are required in order to create large changes in the resulting reverberation time. This can lead to very expensive and complex systems with hundreds of channels. This kind of system would not be suitable for application to small rooms due simply to the lack of space.

Several methods have been developed which allow the performance of the system to be increased without increasing the channel count. One method is to increase the stable feedback gain and this will be analysed in detail in the following chapter. An alternative approach is to use signal processing in the system which causes an increase in the resulting reverberation without having to increase the feedback gain. These methods will be the focus of this chapter.

Several methods have already been introduced in section 1.2. One of the earliest processing schemes used within a reverberation enhancement system was a tape based delay in the in-line Ambiphony system (Vermeulen, 1956). Other systems, of both in-line and non-in-line configurations, have used reverberation created either by electro-acoustic coupling into a separate physical room or using an artificial, electronic reverberator. These techniques allow an increase in resultant reverberation time without increasing the feedback gain.

The focus of this work is on non-in-line reverberation enhancement deployed in rooms with a relatively small volume. The first part of this chapter will investigate the use of artificial reverberation within the processing of a system. The purpose of this is to confirm that previous results translate to smaller spaces which may not be well approximated by a diffuse field, although cases with highly disparate placement of absorptive material or large differences between linear dimensions will not be considered.

The second part of this chapter will introduce a new type of reverberation enhancement system which uses a simple delay. Although this processing has been used for in-line systems in the past, it has not been applied to non-in-line systems. More importantly, a novel analysis of the behaviour of this system will be derived. Simulation and experimental results will be presented which verify the analysis.

2.1 Including artificial reverberation

A wide variety of methods have been employed to create the effect of reverberation on a signal. Many of these were developed for use in recording studios in order to add ambience and reverberation to pre-recorded signals. One early method which was commonly used in recording studios was to construct an echo chamber into which a sound could be played via a loudspeaker with the resulting sound being picked up by a microphone (Rettinger, 1957). Mechanical means have also been used including reverberation effects based on springs (Hammond, 1941) and plates (Kuhl, 1960).

The method most commonly used within reverberation enhancement is digital reverberation. In this section some algorithms used for creating digital reverberation effects will be introduced. An analysis of the behaviour of a reverberation enhancement system including artificial reverberation will then be discussed. Finally, simulation and experimental results will be presented.

2.1.1 Algorithms for digital reverberation

There are two main strategies used for digital reverberation. One is to use real time convolution of the input signal and the desired impulse response. The impulse response can be measured from a real room or created artificially by a numerical method such as those described in section 1.1.3. If the source material is nearly anechoic, the use of convolution can create very accurate simulations of reverberation.

However, due to the length of many room impulse responses and the computational complexity of convolution, this technique has only been made possible recently with the advent of high power, affordable computation. Even these modern computers require complex algorithms to allow real time convolution (Gardner, 1995). This has meant that many alternative methods for creating digital reverberation have been invented.

The Schroeder reverberator is one of the earliest examples of digital reverberation and is based around a set of all-pass filters (Schroeder and Logan, 1961). These filters use a delay line and complementary feed-forward and feedback paths to create a unity amplitude response whilst having an extended impulse response. The signal flow of an all-pass filter is illustrated in Figure 2.1 showing the feedback and feed-forward paths. A Schroeder reverberator consists of several all-pass filters normally with different length delay lines which are chosen to be mutually prime in order to create a higher density of echoes.

This type of algorithm does not attempt to model the physical processes involved in reverberation but instead recreates the important characteristics of a room response. The advantage of this technique is that a good approximation of reverberation can be made at much lower computational cost. Additionally, the parameters of the impulse response can be altered more easily than would be possible in convolution based processing.

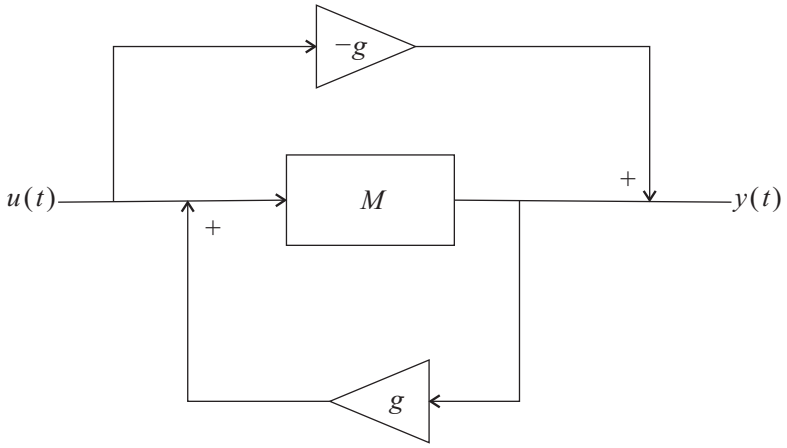

Figure 2.1: Signal flow diagram for an all-pass filter where *M* is the number of delay samples, *u* and *y* are time signals and *g* is the gain which must be less than unity.

Another algorithm, similar to the Schroeder reverberator, is the feedback delay network (FDN). This uses several delay elements the outputs of which are fed back to the inputs via a feedback matrix (Jot, 1992). The length of the delay lines is chosen to be mutually prime to maximise the echo density. In order to create an impulse response which resembles exponentially decaying white noise, which is similar to a generic room impulse response, a unitary matrix is used to route the feedback signals. This is augmented by a constant feedback gain, across all channels, which is used to set the decay time. Additional filters can be added to the output of the FDN in order to create frequency dependent reverberation times.

All of the algorithms described in this section will provide similar performance within the context of reverberation enhancement. However, the use of a Schroeder reverberator, FDN or similar algorithm rather than convolution may simplify the tuning of a system. These algorithms allow parameters such as the frequency dependence of reverberation time to be altered easily which will allow fine-tuning of the system performance to be implemented more quickly.

2.1.2 Analysis of a system including electronic reverberation

The use of electronic reverberation within reverberation enhancement has been analysed extensively by Poletti; see (Poletti, 1993; 1994b; 1998a). Some selected results will be

presented here. The analysis is based around the patented VRA system (Poletti, 1999; Poletti, 2007) and therefore is based on some of the particular peculiarities of this system. This includes the full feedback matrix which means that every microphone is connected to every loudspeaker which results in an effective increase in the feedback gain.

The diffuse field energy density within the room is increased by the VRA system by the same mechanism as the MCR system discussed in section 1.2.1 but with the increase in feedback gain due to the feedback matrix. It can be shown that the resultant steady state energy density is

$$w = \frac{w_0}{1 - N^2 \mu^2} \tag{2.1.1}$$

where μ is the normalised feedback gain including the effect of all transducer sensitivities, amplifier gains and assuming a mean power gain of unity for the room transfer functions (Poletti, 1994b). Unlike the MCR system, the VRA system can alter the reverberation time separately from the changes in energy density.

The resultant reverberation time of a room including the effect of the VRA system is obtained using an electrical analogy for the dynamics of the room and the electronic reverberator (Poletti, 1993). The full derivation will not be given here. The main result is that the decay curve becomes a sum of two decaying exponentials

$$w(t) = w_1(t) + w_2(t) = P_1 e^{-a_1 t} + P_2 e^{-a_2 t};\ t \geq 0. \tag{2.1.2}$$

The values of the constants for the relative power of the terms, P, and the decay rates of each term, a, can be calculated from the number of channels of the system N, the feedback gain μ, and the reverberation times of the unaltered room T_0 and the electronic reverberator T_1. Note that Poletti's analysis and that given here considers a system where all feedback channels are cross coupled, i.e. the feedback matrix is full. Only a single primary source and receiver will be considered.

By defining the ratio of reverberation times as $\gamma = T_1/T_0$ the amplitudes of the two decays can be calculated as a function of the input power P_{in}

$$P_1 = P_{in} \frac{1 - \frac{I}{J}}{K - J} \gamma \tag{2.1.3}$$

and $$P_2 = P_{in}\frac{1+\frac{I}{J}}{K+J}\gamma \tag{2.1.4}$$

where $$I = \gamma - 1, \tag{2.1.5}$$

$$J = \sqrt{(\gamma-1)^2 + 4\gamma N^2\mu^2} \tag{2.1.6}$$

and $$K = \gamma + 1. \tag{2.1.7}$$

The reverberation times of the two decay terms, which are equivalent to the decay rates by $T_{a1} = -13.8/a_1$ and $T_{a2} = -13.8/a_2$, can be calculated as

$$T_{a1} = \frac{\gamma T_0}{\left(\frac{\gamma+1}{2}\right) - \sqrt{\left(\frac{\gamma-1}{2}\right)^2 + \gamma N^2\mu^2}} \tag{2.1.8}$$

and $$T_{a2} = \frac{\gamma T_0}{\left(\frac{\gamma+1}{2}\right) + \sqrt{\left(\frac{\gamma-1}{2}\right)^2 + \gamma N^2\mu^2}}. \tag{2.1.9}$$

As long as the initial amplitudes are comparable, the term with the longer reverberation time will dominate and the resultant reverberation time of the room should approximately equal T_{a1} (Poletti, 1994b).

This analysis shows that the resultant reverberation time of a room can be altered by simply changing the reverberation time of the electronic reverberator, without changing the feedback gain. An example of this behaviour is shown in Figure 2.2 which plots the gain in reverberation time T_{a1}/T_0 against γ. Note that this curve is independent of T_0. The dotted line in this figure shows the gain in reverberation time caused by an MCR system with the same feedback gain, clearly showing the possible increase in performance facilitated through the use of electronic reverberation.

This result implies that very large gains in reverberation time are possible even with a single channel system. However, these gains are restricted further by the condition of linear decays. If the initial amplitudes are significantly different then the resultant decay trace will be curved. This should not occur in a diffuse field and is undesirable in terms of the subjective quality of the room response.

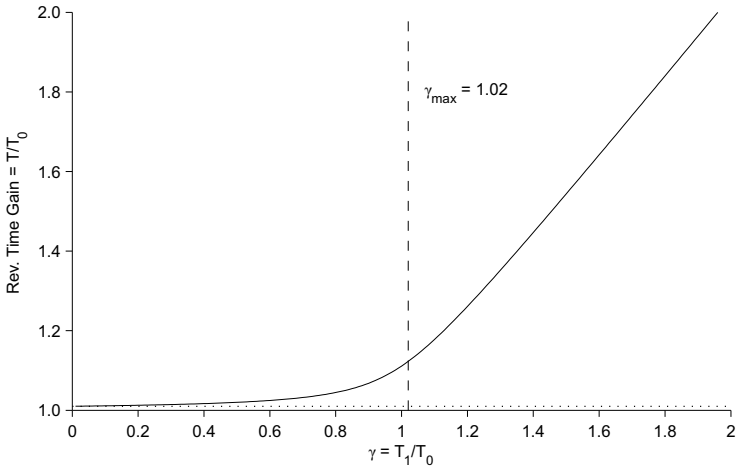

Figure 2.2: Gain in reverberation time for various values of γ, the ratio between the reverberation times of the electronic reverberator and the unaltered room, for a single channel VRAS with feedback gain of −20 dB. The dotted line shows the gain made by the equivalent MCR system and the vertical dashed line shows the value of γ_{max}.

The limit of double sloped decay can be defined as the point at which the initial amplitude of the two decay components is equal (Poletti, 1994b). The value of γ at which this occurs can be calculated from the gain in energy density

$$G_{VRAS} = \frac{w}{w_0}. \tag{2.1.10}$$

It can be shown that (Poletti, 1994b)

$$\gamma_{\max} = \left.\frac{T_1}{T_0}\right|_{\max} = \frac{G_{VRAS}}{2 - G_{VRAS}} \tag{2.1.11}$$

which is valid for $G_{VRAS} < 2$. Under this restriction, the maximum value of γ for the system in Figure 2.2 is 1.02 which allows a reverberation time gain of 1.13. This is significantly higher than would be possible with an MCR system (a gain of 1.01). As the gain in energy density is restricted by the stability of the system, the number of channels must be increased in order to achieve a desired reverberation time. This channel count will be much lower than required by an MCR system.

2.1.3 Simulation of a system with electronic reverberation

The effect of a reverberation enhancement system which includes electronic reverberation can be simulated in the time domain through the use of FIR filters (Oppenheim et al., 1983) which simulate the room impulse response. This has been implemented in order to test the accuracy of the above derivation and the diffuse field assumption on which it is based. A

simple simulation of a room impulse response can be made by applying an exponential decay envelope to white noise (Moorer, 1979). This should create a generic room impulse response which is very close to an idealised diffuse field. This method can also be used to simulate an electronic reverberator. Implementing these impulse responses as FIR filters is a simple and reliable way to simulate reverberation enhancement as the unaltered reverberation times can be set consistently and will be relatively independent of frequency.

The construction of the simulation is illustrated in Figure 2.3. To find the resultant reverberation time of the simulated room, the primary source outputs an impulse and the signal at the primary receiver (or receivers) is recorded. As this simulation works to double precision, there is negligible background noise so a simple impulsive input signal is sufficient. The impulse responses measured at the receiver 'microphones' are then filtered using octave band filters. The decay traces are obtained through reverse integration (Schroeder, 1965) and then the reverberation times are found by evaluating the gradient of the decay traces (ISO3382-1, 2009).

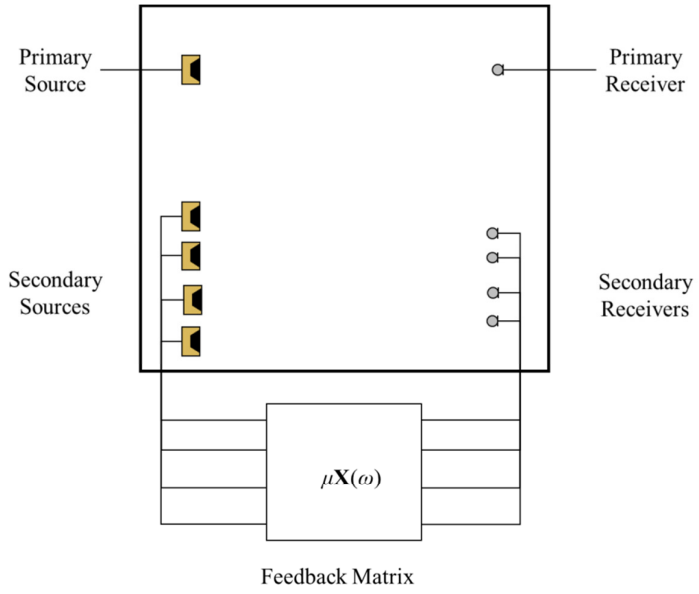

Figure 2.3: Diagram showing the basic layout of the simulation. The secondary sources and receivers make up the reverberation enhancement system whilst the primaries are used to measure the room.

The simulation routine can be easily modified to include different numbers of channels as well as changing the number of primary receivers and producing repeated results. This allows for a wide variety of systems to be simulated with varying degrees of precision, set by the number of primary receivers and repeats, depending on the number of different systems which are to be investigated. In order to test the analysis presented in the previous section the

feedback matrix was represented as an array of reverberators each implemented as FIR filters in the same way as the room impulse responses.

A four channel system has been simulated with a feedback gain of −23 dB which was set to ensure the stability of the system. The unaltered reverberation time of the room was set at 0.5 s for all frequency bands. The maximum value of γ, given by equation (2.1.11), is 1.19 but a wide range of values has been tested. The resultant reverberation times were predicted using equation (2.1.8). These can then be compared against the reverberation times from the simulated impulse response.

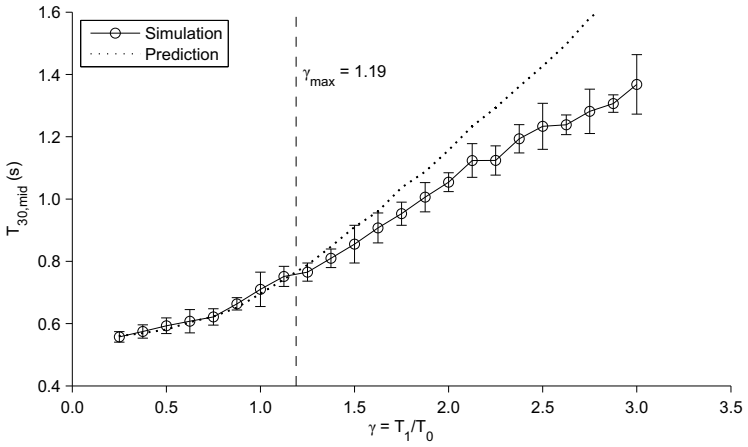

Figure 2.4: Simulation results for a 4 channel system including electronic reverberation in the feedback loop. The solid line shows the results of the simulation whilst the dotted line shows the reverberation times predicted analytically using equation (2.1.8). The errorbars show one standard deviation above and below the mean.

The results of this simulation can be seen in Figure 2.4 which plots the value of T_{30} extracted from the impulse response for various values of γ. This shows that for values of γ less than γ_{max} the analytical results agree well with the simulated result. Above this value the decay trace is expected to become double sloped. The predicted reverberation times in Figure 2.4, calculated using equation (2.1.8), are derived simply from a single term of the modelled decay trace and do not account for curvature of the decay trace. The simulation evaluates the entire decay trace so the curvature will be present. Hence the observed discrepancy between the simulated and predicted reverberation times for values of γ greater than γ_{max}.

It may be possible to predict the reverberation time more precisely for a wider range of values of γ by recreating the entire decay trace as given by equation (2.1.2) and then evaluating the reverberation time directly. This would also allow the difference in T_{20}, T_{30} and EDT to be predicted. The results of using this type of prediction are given in Figure 2.5 showing much better agreement with simulation results for values of γ greater than γ_{max}. At

very large values of γ the predicted reverberation time is too high but at this point the decay trace is highly double sloped and would probably not be useable in a practical system.

The simulations presented in this section support the accuracy of the analytical results presented in the previous section. Further to the work by Poletti, it has been shown that by creating a trace with both the decay terms and then evaluating the reverberation time allows more accurate predictions of the resulting reverberation especially for large values of γ. This implies that the two term decay model is accurate and that it may be possible to use this model to predict other important parameters of the sound field such as EDT. This will be investigated more fully in chapter 5.

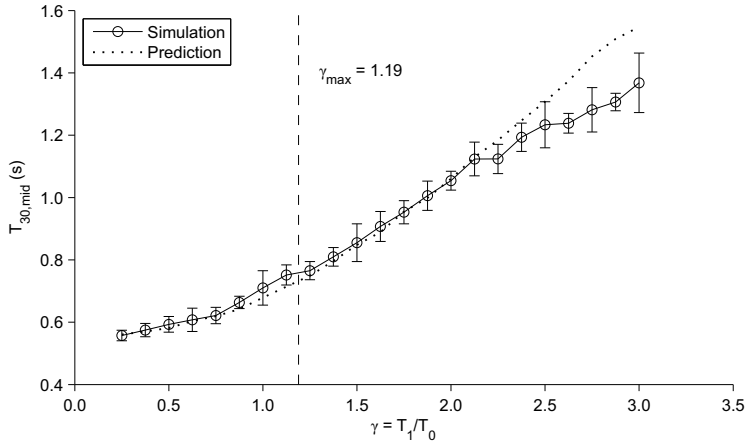

Figure 2.5: Predicting the reverberation time from the two-term decay trace, as opposed to the single term used in Figure 2.4, allows much better agreement with the simulation results especially for values of γ greater than γ_{max}.

2.1.4 Experiments with a system including electronic reverberation

An experiment has been designed to test the performance of a reverberation enhancement system which includes electronic reverberation in the feedback loop. The room used for this experiment is a laboratory space with dimensions of 6 by 5 by 2.5 m and an unaltered reverberation time of 0.53 s. The reverberation time of the room was measured using the integrated impulse response method using deconvolution of a swept sine signal. The test signal was a logarithmic sine sweep from 20 to 3000 Hz lasting 120 s. Six microphones were used simultaneously to measure the room response along with two source positions. The setup is illustrated in the lower part of Figure 2.6. For this experiment, the measured reverberation times are based on the T_{20} in order to avoid problems with background noise.

A single channel system was constructed using a laptop computer with a software reverberation effect as shown in the upper part of Figure 2.6. For each value of reverberation time of the effect, three different positions of the system transducers were used. The open loop gain was measured using a pink noise excitation signal and the amplifier gain was set in order to create a mean value of −22 dB. This procedure was necessary because changing the reverberation time of the processor altered the effective gain. The reverberation time of the processor was measured from its impulse response which was derived using deconvolution of a swept sine signal.

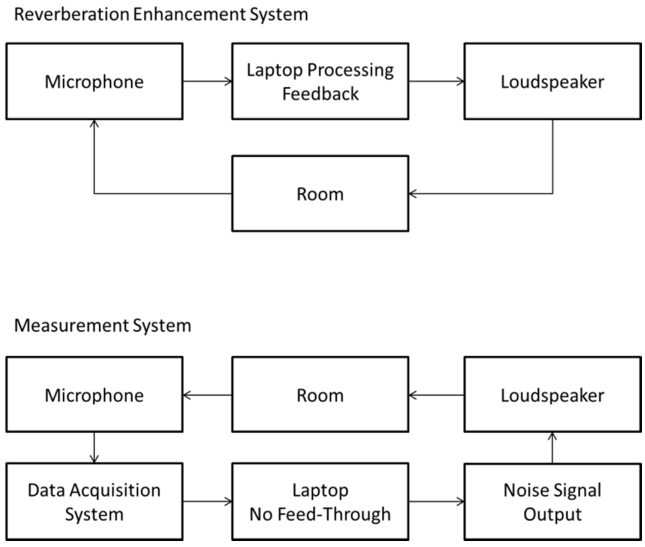

Figure 2.6: Block diagram of the experimental setup.

The results of this experiment are given in Figure 2.7 which shows the increase in reverberation time with increasing values of γ. Values of resultant reverberation time have also been predicted from the measured unaltered reverberation time, reverberation time of the processor and open loop gain. Both the single term model, as used in Figure 2.4 and shown here as a dotted line, and the two term model, as used in Figure 2.5 and shown as a solid line, are given.

Neither model predicts the resultant reverberation time accurately. The change in the reverberation with γ seems to be closer to the trend observed with the two term decay model but the observed values are consistently higher than those predicted. This implies a systematic error but the reason for this offset is unclear. It may have been caused by unexpected behaviour of the reverberation algorithm used to process the feedback signal. As this was commercial software, the details of the algorithm are unavailable. However, the

trend is close enough to imply that the two term decay model provides a useful prediction of the shape of the energy decay trace.

These experiments show the increases in reverberation time made possible through the use of electronic reverberation. There is a large improvement in performance over a system without any processing. Although the predicted values do not match precisely with experimental results, the two-term decay model provides a reasonable estimate of the resulting reverberation time even for values of $\gamma > \gamma_{max}$. This shows that the single term model is a poor predictor of the reverberation time for large values of γ. This does not detract from the accuracy of the single term model which is only designed to be used when $\gamma < \gamma_{max}$. These results imply that the two term model can be used to predict the shape of the entire decay trace and may therefore be used to predict other parameters of the room response such as early decay time.

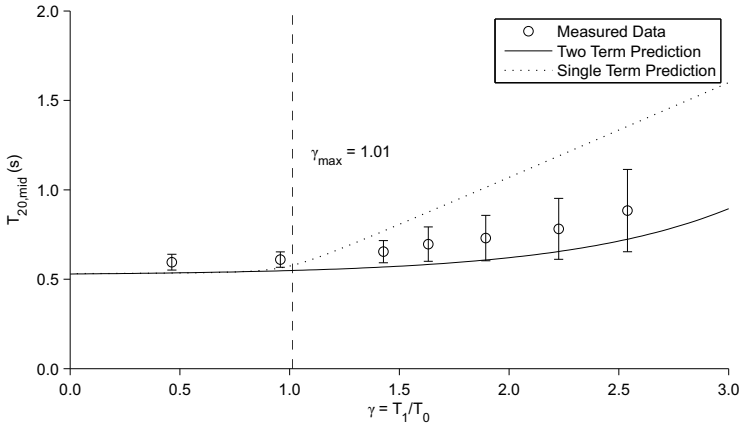

Figure 2.7: Measured reverberation times of a single channel system including electronic reverberation. Two different prediction methods are used; the solid line shows the values predicted using a two term decay model whilst the dotted line shows the values from a single term model. The vertical dashed line shows the value of γ_{max} predicted from equation (2.1.11).

2.2 Non-in-line system including delay

Whilst the previous section was based on the work of Poletti, this section will describe an entirely novel strategy for reverberation enhancement which uses a non-in-line configuration with a simple delay in the feedback loop. Whilst delay has been used in reverberation enhancement before, notably in the in-line Ambiphony system, its use in a non-in-line system has not previously been documented. This section contains an analysis of the behaviour of this system followed by simulation and experimental results which test the accuracy of this analysis.

In traditional feedback control systems, delay is often seen as an undesirable quantity. This is due to the destabilizing effect which occurs when it is introduced in these types of systems. However, in the context of reverberation enhancement, the stability limits will not be affected by the introduction of delay. The stability of reverberation enhancement systems will be discussed in detail in section 3.1. For now it is sufficient to say that since delay only affects the phase response, due to the properties of diffuse field transfer functions, adding delay does not affect the probability of instability.

2.2.1 Analysis of a system including delay

The behaviour of a non-in-line reverberation enhancement system which includes delay can be modelled by simple modification of the energy balance equation (1.1.16). The source term can be suitably delayed so that the equation becomes

$$V\frac{dw(t)}{dt}+\frac{c_0\alpha S}{4}w(t)=P_s+Ng^2w(t-\tau) \tag{2.2.1}$$

where τ is the delay. For simplicity, it is assumed that all channels have the same feedback gain and delay.

As the reverberation time is the only quantity of interest, the source term P_s can be neglected and the homogeneous case can be solved. This is achieved by substituting a trial solution of the form

$$w(t)=e^{-at} \tag{2.2.2}$$

with decay rate a. The reverberation time is related to the decay rate by $T=13.8/a$. Substitution of equation (2.2.2) into equation (2.2.1) leads to the characteristic equation

$$a-\frac{c_0\alpha S}{4V}+\frac{Ng^2}{V}e^{a\tau}=0. \tag{2.2.3}$$

Equation (2.2.3) can be simplified by substituting the unaltered decay rate of the room a_{w0} using the Sabine formula $T=13.8\times 4V/c_0\alpha S$ and defining a normalised feedback gain, which is identical to that used in the analysis of the MCR system, $\mu_{MCR}=g\sqrt{4/c_0A}$ so that

$$a-a_0+a_0e^{a\tau}\mu_{MCR}^2N=0. \tag{2.2.4}$$

As this formula contains linear and exponential terms of a, the solution is not immediately obvious. However, it is possible to solve by using the Lambert function (Knuth et al., 1996).

This is a generalised function which cannot be written in closed form. Instead it is defined as the inverse of

$$ye^{y} = x \tag{2.2.5}$$

so that y is a function of x. This function is multi-valued, but for the purposes of this analysis only real positive inputs and real values of the output will be considered. This function can be approximated with simpler functions (Barry et al., 2000) and implementations are available in several commercial software packages such as MATLAB and Mathematica.

In order to solve equation (2.2.4), it must be rearranged so that it is in the same form as equation (2.2.5). This can be achieved by multiplying through with a factor of

$$\tau e^{\tau(a_0 - a)}.$$

By rearranging the resulting equation into the form of (2.2.5) and then applying the Lambert function to both sides, it can be shown that

$$\mathrm{W}\left[a_0 \tau e^{a_0 \tau} \mu_{MCR}^2 N\right] = \tau\left(a_0 - a\right) \tag{2.2.6}$$

where W denotes the Lambert function. From this it is trivial to show that

$$a = a_0 - \frac{1}{\tau}\mathrm{W}\left[a_0 \tau e^{a_0 \tau} \mu_{MCR}^2 N\right] \tag{2.2.7}$$

which can then be used to predict the resultant decay rate using the unaltered decay rate, delay, feedback gain and channel count. The results of this analysis can be seen in Figure 2.8 showing that the inclusion of delay allows large increases in performance.

By dividing equation (2.2.7) by a factor of a_0 it can be seen that the ratio of the resultant to the unaltered decay rates is a function of the product of the delay time and unaltered decay rate. As the decay rate is inversely proportional to the reverberation time, the gain in reverberation time is a function of the ratio of time delay to reverberation time. Hence it is this ratio that is important to the resulting performance of the system rather than the absolute delay time.

This result implies that a useful increase in the resultant reverberation time is possible by including a simple delay. In order to test the accuracy of this analysis, this type of system will be simulated numerically and also tested experimentally. These investigations are presented in the following sections. It should also be noted that delay may be introduced into

the system simply by increasing the distance between the loudspeaker and microphone and this may have some effect on the performance of the system.

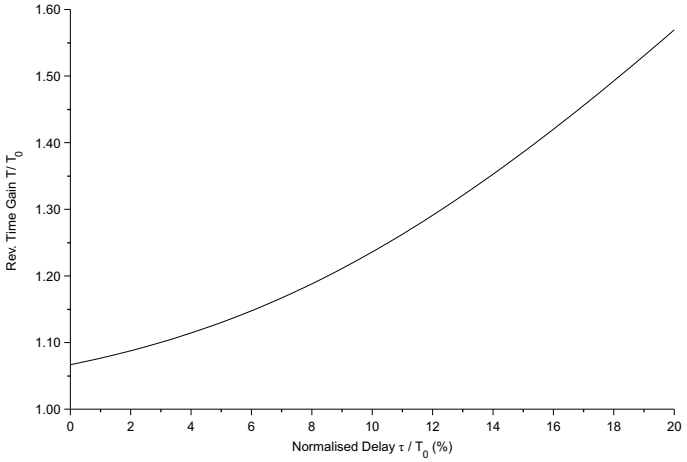

Figure 2.8: Reverberation time gain against delay as a percentage of unaltered reverberation time. The modelled system has a single channel and a feedback gain of −12dB.

2.2.2 Simulation of system including delay

The simulation of this system including simple delay is identical to that used for the simulations in section 2.1.3, the only difference being that no filters are used in the feedback loop (see Figure 2.3). In order to include the delay, the corresponding amount of zeros is simply added to the beginning of the impulse responses which relate to the feedback path of the reverberation enhancement system. The simulated system had four channels and the resulting reverberation time was measured using the integrated impulse response method.

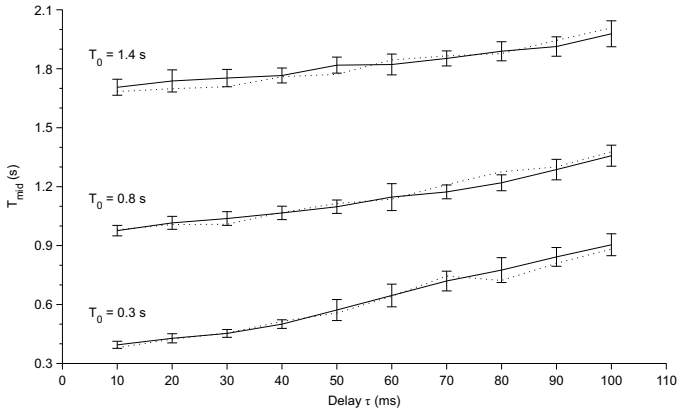

Figure 2.9: Simulation of a system including time delay for several values of delay and unaltered reverberation time. The dotted line shows the times predicted analytically and the solid lines show the simulation results. The errorbars show one standard deviation above and below the mean.

The results of these simulations are shown in Figure 2.9. Several different values of time delay have been tested as well as different values of unaltered reverberation time. The predicted values are calculated using equation (2.2.7) where the unaltered decay rate is measured from the generated impulse responses. The predicted values in the figure seem not to be monotonically increasing with delay time. This is because they are based on the unaltered reverberation times of the generated impulse response which has inherent variability. Overall, the simulation results agree very well with the predicted reverberation times. This implies that the analysis of section 2.2.1 is valid. The following section presents experimental results which test this kind of system.

2.2.3 Experiments with a system including delay

An experiment has been conducted to test the performance of the system including time delay. The methodology and setup was identical to that used in the experiment in section 2.1.4. A single channel system was constructed using a laptop with software to add the delay. For each value of delay, three different positions of the system transducers were used. The open loop gain was measured using a pink noise excitation signal and found to have a mean value of −17 dB. The time delay, including that caused by the separation of source and receiver, was measured directly from the open loop impulse response which was measured using deconvolution of a swept sine signal.

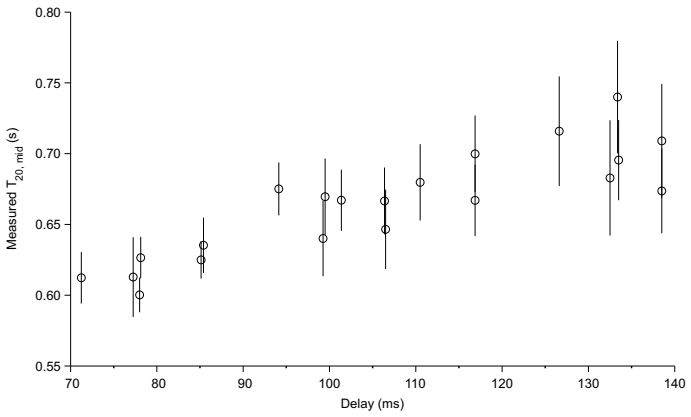

Figure 2.10: Measured reverberation times for a system with time delay in the feedback loop. Various values of delay are shown. The errorbars show one standard deviation above and below the mean.

The results of this experiment are given in Figure 2.10, showing the increase in the room reverberation time with increasing delay. The results are shown separately for different positions of the reverberation enhancement system because the value of delay is slightly different due to changes in the distance between source and receiver. The unaltered mid-

frequency reverberation time of the room was 0.53 s and these results show that, even with a single channel system, a useful increase in the reverberation time can be obtained. It is also worth noting that the spatial variation of reverberation time increases with increasing time delay as indicated by the errorbars. This may be symptomatic of a reduction in the quality of the diffuse field and will be discussed in detail in chapter 5.

The resulting reverberation time can be predicted using the analysis from section 2.2.1. The unaltered reverberation, open loop gain and time delay have all been measured directly and are used to calculate the resultant reverberation time. A comparison of these predictions with the measured reverberation times is shown in Figure 2.11 in which the measured values of T_{20} are plotted against predicted reverberation times. This clearly shows good agreement between the analytical predictions and the experimental results. At large values of delay the measured values are lower than the predictions which may indicate a failure of the analysis for long delay times.

The inaccuracy of the analysis at large values of delay may be because the system cannot affect the early part of the decay trace. As the measured T_{20} ignores the first 5 dB of the decay trace, this should not change the measured results as long as the delay is less than the time taken for the first 5 dB decay. However, for the room which is tested here the first 5 dB decay takes 44 ms which is lower than any of the delay times tested. In fact, the analysis seems accurate up to values of delay of 100 ms. An alternative explanation is that, at high values of delay, the spatial variation is large and the mean values shown in Figure 2.11 do not represent the true mean. Further investigation into the changes in the early part of the decay trace and the spatial variation will be presented in chapter 5.

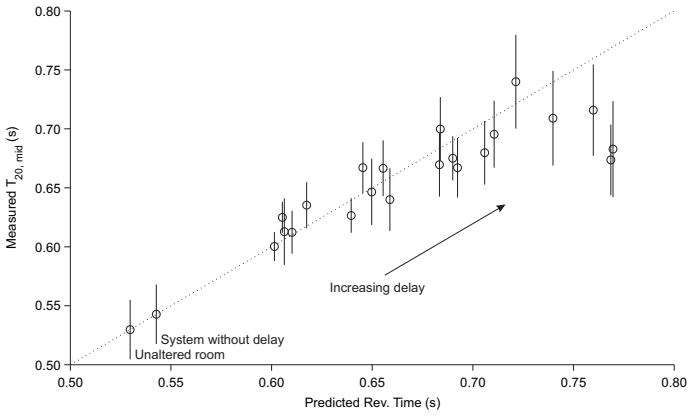

Figure 2.11: Comparison of the measured reverberation time against the value predicted analytically with unity indicated by the dotted line. Points are included, for reference, which represent the unaltered room reverberation time and that which would be possible with a system without delay.

The performance of this system is comparable to that of a system including electronic reverberation (section 2.1). In the configuration of the experiment presented here, a single channel with −17 dB feedback gain, a system with electronic reverberation with a value of γ set to its maximum as given by equation (2.1.11) would cause a resultant reverberation time of 0.63 s. As can be seen in Figure 2.10, this reverberation time can be achieved with a delay of around 90 ms. This value of delay does not cause a significant increase in the spatial variation of reverberation time but further investigation is required to test whether this value of delay has any negative impact on the quality of the reverberation.

2.3 Summary

The techniques discussed in this chapter allow the performance of a reverberation enhancement system to be improved without increasing the feedback gain. The feedback gain cannot be increased indefinitely, as the system will become unstable, so these techniques allow for longer resultant reverberation times without increasing the number of channels. Two methods have been presented here. The first is the use of artificial reverberation, specifically the use of digital reverberators. Several algorithms can be used to simulate reverberation but all of them can be used within reverberation enhancement with similar results.

The other method discussed is the use of simple delay within a non-in-line reverberation enhancement system. The analysis presented in section 2.2.1 shows that this type of system allows significant increases in performance. The accuracy of this analysis has been verified through simulations and experimental results. It is important to consider how this system performs in comparison with systems which use electronic reverberation which is by far the most common configuration. One of the main advantages of using delay is that it is simple to implement and, unlike electronic reverberation, does not affect the stability limit of the system.

It has also been shown that the two systems have comparable performance. Both systems have been shown to increase the reverberation time from 0.53 s to approximately 0.7 s where a similar system without processing would only cause a reverberation time of 0.55 s. However, further investigation is required to test the performance of the system including delay. The useable upper limit of delay time is not revealed by the analysis or the experimental results presented here. Other parameters of the room impulse response and the sound field will be analysed in chapter 5. This will give allow for a more rigorous comparison between the two systems.

3 Increasing the maximum stable feedback gain

The performance of a reverberation enhancement system is dependent on the gain of the system. However, the gain itself is limited by the stability of the system. The feedback from the loudspeaker to the microphone causes the system to form a closed loop and if the signal travels around the loop with a gain greater than unity and in phase then the amplitude will increase exponentially, until limited by non-linearities of the system. This is known as instability.

The stability limit of a feedback system can be predicted using the Nyquist criterion (Nelson and Elliott, 1992). In order to utilise this analysis, the frequency response of the system must be known. However in a diffuse field, the frequency response is modelled statistically and therefore the absolute stability limit cannot be derived. Instead, a probability of instability is used (Schroeder, 1964). This is explained fully in the next section.

Several methods have been devised for increasing the stable feedback gain which should allow an increase in the performance of a reverberation enhancement system. As mentioned at the start of the previous chapter, increasing the performance of a system without increasing the channel count will allow better application in small enclosures. Many of the techniques used to increase the stable feedback gain are only applicable to in-line reverberation enhancement or public address systems. A general overview of the various methods will be presented in section 3.1 and the suitability of application for reverberation enhancement will be discussed.

Having introduced the concept of stability in the diffuse field and the various methods which may be used to improve the stability limits, the techniques which seem most applicable to reverberation enhancement will be analysed in detail. The first of these is the use of time variant processing. A comparison of two time variant algorithms will be presented in section 3.2. Secondly, the claim that distributed mode loudspeakers (DMLs) allow higher gain before instability (Mapp and Ellis, 1999) will be investigated in section 3.3.

3.1 Stability of feedback systems in a diffuse field

The mathematical analysis used to study the stability of feedback systems is well established in the field of control theory. However, as the reverberation enhancement system will be placed in an approximately diffuse sound field some modifications to the normal method are required. This section will introduce the basic concepts of feedback control and then the analysis of the stability of a reverberation enhancement system will be considered.

3.1.1 Introduction to feedback control theory

In order to guarantee the stability of a feedback system a signal travelling around the feedback loop must be attenuated or the phase must be such that the signal will not constructively interfere with itself. A simple feedback system is shown in Figure 3.1 where U and Y are the frequency domain representation of the input and output signals respectively, G and H are transfer functions and g is the feedback gain. The closed loop, frequency domain transfer function of this system is

$$\frac{Y}{U} = \frac{G}{1 - gGH}. \tag{3.1.1}$$

where the capitalisation of U and Y indicates the Fourier transform of the time signals. The term gGH is known as the open loop transfer function and it is this which determines the stability of the system (Nelson and Elliott, 1992). If the open loop transfer function equals unity, the denominator of equation (3.1.1) will become zero and the value of the transfer function will approach infinity. At this point the system will be unstable.

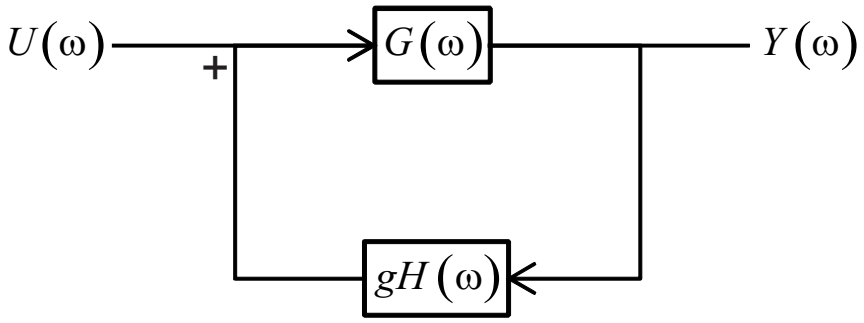

Figure 3.1: Diagram of a simple feedback system.

In order to determine whether the system will be unstable, the Nyquist plot of the system can be examined. This is formed by plotting the open loop transfer function on the complex plane with frequency as a parameter along the curve. The stability of the system is determined by whether or not the curve encircles the point $-1+0i$ for systems which have negative feedback, which is the standard in control system literature. However, reverberation enhancement uses positive feedback and therefore the critical point becomes $1+0i$.

An example of a Nyquist plot is shown in Figure 3.2. The open loop transfer function GH is shown so that the feedback gain g can be set to ensure stability. If negative feedback is implemented with this system then it would be unconditionally stable. This is because an arbitrarily large gain could be applied and the locus would not encircle the point $-1+0i$.

However, if positive feedback is used, the system would be unstable unless the feedback gain was set sufficiently low. In this case a value of 0.5 would ensure that the system is stable.

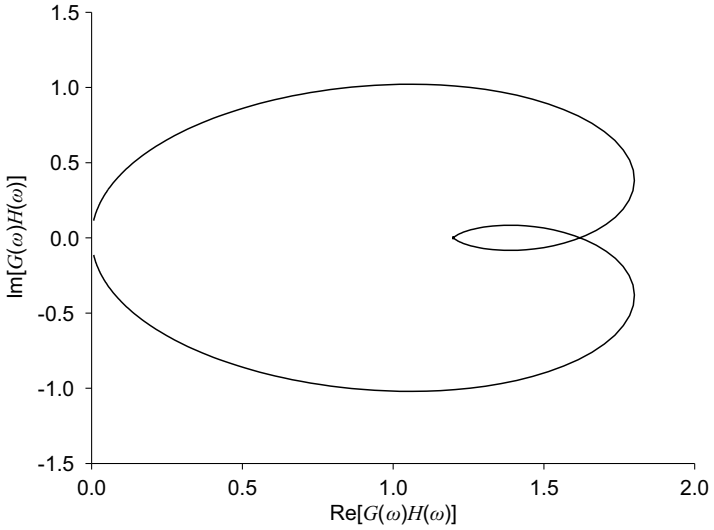

Figure 3.2: Example of a Nyquist plot. This system would be stable if negative feedback was implemented but unstable with positive feedback unless the feedback gain was sufficiently low.

3.1.2 Stability of a reverberation enhancement system

For simplicity, to model the stability condition of a simple single channel reverberation enhancement system without any processing in the feedback loop, the transfer function H can be set to unity. This makes the open loop transfer function gG. As was mentioned in section 1.1.2, it is impractical to model the transfer function in a diffuse field exactly but the statistical properties of the transfer function are known. The real and imaginary parts of the room transfer function are both Gaussian distributed with equal variance σ^2 (Schroeder, 1954; Schroeder and Kuttruff, 1962). This can be used to model the room transfer function G.

The mean value of G will depend on the sensitivities of the transducers but it can be assumed, without loss of generality, that the mean value of the magnitude of G is unity and the feedback gain g can then be replaced by a normalised gain μ. It is assumed that the loudspeaker, microphone and amplifier have perfectly flat frequency responses and their various gains are all absorbed into μ. The relative standard deviation of the magnitude of a diffuse field transfer function is known to be 0.52 (Kuttruff, 2000). Therefore, with the

assumed mean magnitude of unity, the variance of the real and imaginary parts of G will be $\sigma^2 \approx 0.5$.

In order to represent the entire transfer function, it is assumed that there are K independent frequency samples. The risk of instability can then be related to the probability that any one of these samples is in the region of the point $1+0i$. A commonly used method is to assume that if the real part of any sample is greater than unity, then the system is likely to be unstable (Schroeder, 1964). Therefore, the probability of instability can be calculated as the probability that at least one of K independent samples has a real part greater than unity. All of the samples will be Gaussian distributed with variance of 0.5 and are scaled by the normalised feedback gain μ.

The following derivation is adapted from (Poletti, 2000). The probability that at least one frequency sample has a real part, scaled by μ, which is greater than unity can be stated formally as

$$Pr_x\{inst\} = Pr\{\mu x_1 > 1 \quad \vee \quad \mu x_2 > 1 \quad \ldots \quad \vee \quad \mu x_K > 1\} \tag{3.1.2}$$

where $Pr_x\{inst\}$ is the probability of instability, x_k is the real part of the kth frequency sample and $\vee$ is the logical *OR*. This can be equivalently written as

$$Pr_x\{inst\} = 1 - Pr\left\{x_1 < \frac{1}{\mu} \quad \wedge \quad x_2 < \frac{1}{\mu} \quad \ldots \quad \wedge \quad x_K < \frac{1}{\mu}\right\} \tag{3.1.3}$$

where $\wedge$ is the logical *AND*. The probability that x is less than $1/\mu$ can be formulated as the integral of the probability distribution f between $-\infty$ and $1/\mu$

$$Pr_x\{inst\} = 1 - \int_{-\infty}^{1/\mu} \ldots \int_{-\infty}^{1/\mu} f_x(x_1, \quad x_2, \quad \ldots, \quad x_K)\,\mathrm{d}x_1, \quad \mathrm{d}x_2, \quad \ldots, \quad \mathrm{d}x_K\,. \tag{3.1.4}$$

As all the samples are assumed to be independent and identically distributed, the integral term can be simplified to

$$Pr_x\{inst\} = 1 - \left[\int_{-\infty}^{1/\mu} f_x(x)\,\mathrm{d}x\right]^K. \tag{3.1.5}$$

The resulting integral is equivalent to the cumulative distribution function evaluated at $1/\mu$. The cumulative distribution function of a Gaussian is

$$\int_{-\infty}^{y} f_x(x)\,\mathrm{d}x = \frac{1}{2} + \frac{1}{2}\mathrm{erf}\left(\frac{y}{\sqrt{2}\sigma}\right) \tag{3.1.6}$$

where erf is the error function

$$\mathrm{erf}(x) = \frac{2}{\sqrt{\pi}}\int_{0}^{x} e^{-t^2}\,\mathrm{d}t\,. \tag{3.1.7}$$

The known variance, $\sigma^2 \approx 0.5$, can be substituted into equation (3.1.6) and then this function can be used in place of the integral in equation (3.1.5) with the argument being $1/\mu$. This leads to a probability of instability of

$$Pr_x\{inst\} = 1 - \left[\frac{1}{2} + \frac{1}{2}\mathrm{erf}\left(\frac{1}{\mu}\right)\right]^K\,. \tag{3.1.8}$$

Although the frequency samples are assumed to be independent, it is known that the autocorrelation of the frequency response of a room has a finite width (Schroeder, 1962). Therefore the samples must be spaced widely enough to ensure sufficient independence but close enough that the frequency response is properly represented. Numerical simulations have shown that a frequency spacing of $1/T$ gives the most accurate results when using the analysis based on the real part (Poletti, 2000). Therefore, the value of K in equation (3.1.8) can be set to the product of the bandwidth and the reverberation time BT.

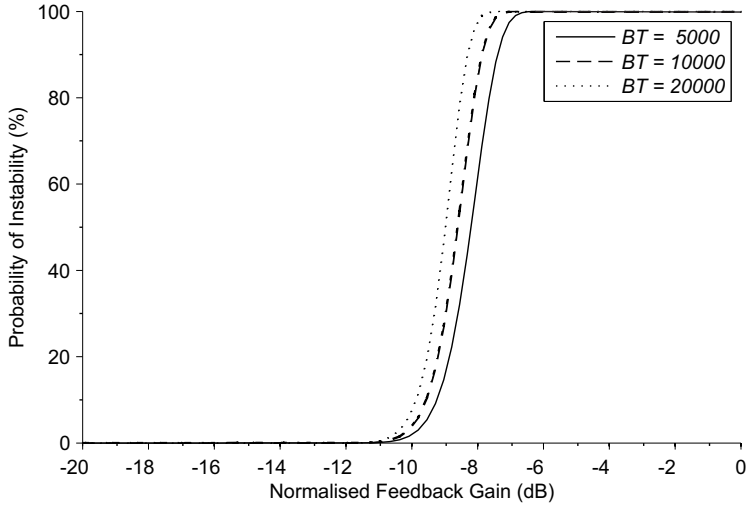

Figure 3.3: Probability of instability for a single channel system in the diffuse field against the feedback gain of various values of the product of reverberation time and system bandwidth.

The predicted probability of instability can be seen in Figure 3.3 which shows the transition between a stable and unstable system. With a feedback gain of −12 dB, there is negligible

probability of instability but with a feedback gain of −7 dB instability is almost certain. Equivalent results to that given by equation (3.1.8) are available for multi-channel systems and systems with additional processing in the feedback loop (Poletti, 2000) but the underlying concept of this analysis is the same throughout. The basic result is that the addition of more channels or extra variance in the processing decreases the stable feedback gain.

For the single channel system in Figure 3.3, a feedback gain of −12 dB ensures a very low probability of instability even for a large value of *BT*. Using equation (1.2.2) the reverberation time gain can be calculated. According to these results, a single channel system should allow the reverberation time to be increased by a factor of 1.07. The feedback gain cannot be increased without significant risk of instability so in order to allow larger gains in reverberation time more channels must be implemented. Alternatively, or in addition, measures for increasing feedback gain without instability could be applied. These methods will be discussed in the following section.

3.1.3 Methods for increasing the stable feedback gain

There are several possible techniques for increasing the feedback gain of a reverberation enhancement system above the normal stable limit. There is a large body of work on increasing the stable gain of public address systems (van Waterschoot and Moonen, 2011). The various methods have varying degrees of application to reverberation enhancement. The simplest method is the use of directional microphones and loudspeakers which are orientated in such a way as to minimise the amplitude of the feedback path. In terms of reverberation enhancement, this technique is only applicable to in-line system as opposed to a non-in-line system which uses omni-directional transducers.

By placing directional microphones close to the performers and orientating directional loudspeakers towards the audience, in-line reverberation enhancement systems increase the level of direct sound from the performers picked up by the microphones and the level of direct sound from the loudspeakers heard by the audience. The amplitude of the feedback via the direct sound path will be reduced due to the directivity of the transducers.

Changes in the directivity of the transducers to improve the stability limit have also been implemented using microphone arrays and signal processing techniques which originate from beamforming technology (Kobayashi *et al.*, 2003). Whilst the practicalities of this method are significantly more complex than the use of directional microphones, the outcome is similar. With either method a significantly higher amplifier gain may be used without risking instability because of the reduction in the effective feedback gain.

By definition, this method is not applicable to non-in-line systems which use relatively omni-directional transducers located remotely from the audience and performer. The feedback path via the diffuse field is the mechanism by which this class of system operates and the direct path is simply attenuated by virtue of the distance between the loudspeakers and microphones. As the direct sound feedback path is negligible, the use of directional transducers or arrays will not significantly alter the stable feedback gain of a non-in-line reverberation enhancement system. However, this technique has been used in "active-wall" systems as described in section 1.2.4 allowing improved non-in-line performance from closely spaced transducers.

A similar problem is evident for a method known as acoustic feedback cancellation. This is designed to eliminate the feedback path through the use of signal processing (van Waterschoot *et al.*, 2004). The basic concept is to model the feedback path as a digital filter and then apply this filter to the output signal. The filtered version of the output signal is then subtracted from the microphone signal such that it is out of phase with the feedback signal and will therefore remove it. This method is not readily applicable to non-in-line reverberation enhancement as it works by reducing the effective feedback gain.

This technique could, theoretically, be used to create systems with in-line style operation while retaining the freedom of transducer placement and homogeneous reverberation enhancement possible with non-in-line systems. However, the implementation of the digital filters modelling a diffuse field transfer function is highly complex and restricts the performance of this technique (Rombouts et al., 2006). For this reason, this technique is normally applied when the feedback transfer function is relatively simple, such as in echo cancellation for hearing aids (Siqueira and Alwan, 2000). Although it may be possible to apply this technology to reverberation enhancement, it has not been considered in this work.

Some methods of controlling acoustic feedback may be applicable to reverberation enhancement but will not generally improve the performance of a system. For instance, notch filters are often used in public address systems to reduce the amplitude of problematic peaks in the transfer function. These filters can be tuned manually or automatically (Leotwassana et al., 2003). This method may allow an increase in the mean feedback gain but its application is limited to transfer functions where there are, at most, a handful of problematic peaks. Total equalisation of a diffuse field transfer function is not feasible. Therefore, this technique may be useful for tuning a particular system but it will not affect the overall performance of a generic reverberation enhancement system.

Another useful technique is to reduce automatically the feedback gain when instability is detected, over the entire audio bandwidth (Patronis Jr, 1978) or in discrete frequency bands (Osmanovic and Clarke, 2010). This is a useful safety mechanism for preventing sustained instability. However, the reduction in feedback gain prevents an increase in the performance of reverberation enhancement. This could be implemented in a reverberation enhancement system, but it would not significantly increase the possible gains in reverberation time.

One of the earliest methods developed for increasing the stable feedback gain was the use of frequency shifting in the feedback loop (Schroeder, 1964). Frequency shifting is a processing scheme which changes the frequency of a signal by a set number of Hertz. The mean distance between consecutive peaks in a diffuse field transfer function is 10 Hz (Schroeder, 1987). By using a frequency shift of 5 Hz in the feedback loop, a signal at a frequency of a large peak in the transfer function will be output with a frequency which will likely correspond to a dip. Therefore the frequency response will effectively be smoothed.

Frequency shifting allows a sustained increase in the stable feedback gain of 10 dB, although only 6 dB is available if audible beating artefacts are to be avoided (Schroeder, 1964). Starting from the stable feedback gain of −12 dB, as assumed in section 3.1.2, the resulting feedback gain including frequency shifting could be −6 dB. A single channel system with this level of feedback gain would increase the reverberation time, according to equation (1.2.2), by a factor of 1.33.

This is a significant improvement over the system without frequency shifting but multiple channels may still be required to achieve the desired performance. It has been shown that the improvement of stable feedback gain with frequency shifting decreases with larger channel counts (Poletti, 2004). However, when considering the small scale systems which are the focus of this work the additional feedback gain may still be useful.

There are several processing options which have similar effects to frequency shifting. These include time-varying delay (Nielsen and Svensson, 1999). The increases in stable feedback gain are of a similar order to those created using frequency shifting. The following section will investigate these methods and compare the available algorithms. It is important to consider not only whether these processing schemes allow additional feedback gain but also whether this gain will translate into additional reverberation time.

3.2 Time variant processing

The use of frequency shifting or time-varying delay as part of a public address system reduces the risk of instability via the diffuse field feedback path. As non-in-line

reverberation enhancement systems have a negligible direct sound feedback path and are entirely limited by the diffuse field path, the inclusion of one of these processes is highly applicable. This section will introduce the processing schemes and detail the way in which they are implemented. Numerical simulations and experimental results will be presented which demonstrate the possible gains in performance through the use of this method.

3.2.1 Digital implementation of time variant signal processing

Although the signal processing under analysis here may be implemented with other means, this section will only describe the digital methods. Frequency shifting is identical to single side band modulation, which is a form of amplitude modulation (Oppenheim et al., 1983). The only difference is in application; frequency shifting is used in audio applications whereas single side band modulation relates to radio transmission. The basis for the digital implementation of frequency shifting, illustrated in Figure 3.4, is an FIR filter which approximates the Hilbert transform. This filter shifts the phase of positive frequencies by 90° and negative frequencies by −90°. The filtered signal and the original signal are modulated by sinusoidal signals which have a frequency which is equal to the desired amount of frequency shift. The modulators are also 90° out of phase.

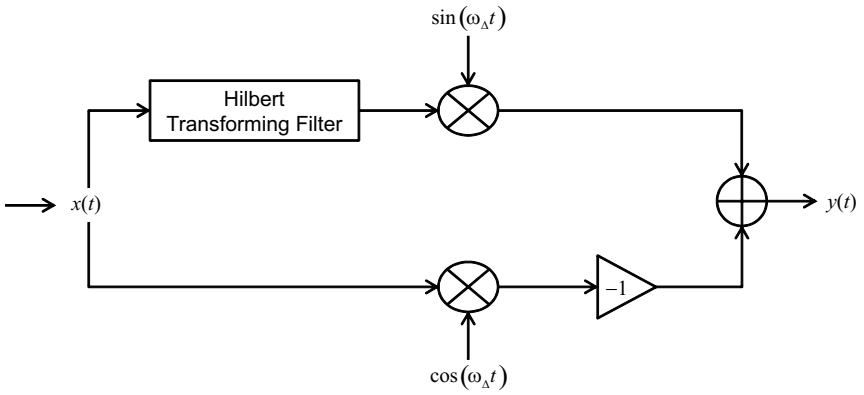

Figure 3.4: Signal flow diagram of a digital frequency shifter where ω_Δ is the desired shift in frequency.

Amplitude modulation creates a signal with frequencies that are the sum and difference between those of the modulator and modulated signals. Due to the phase relation caused by the Hilbert transform and the different modulation signals, the difference tones of the two modulated signals will be in phase and the sum tones will be out of phase. Therefore the difference of these two signals will leave only the sum tone. This means that all frequencies in the output signal will equal the frequencies in the unaltered signal plus the frequency of the modulators i.e. shifted by a constant amount ω_Δ. The necessary phase relations can also

be created using elliptic IIR filters which may be more efficient than the FIR Hilbert transformer (Wardle, 1998).

Another signal processing method which will be investigated here is time-varying delay. The time domain response of a time-varying delay is usually of the form

$$y(t) = x\left[t - \tau_0 - \tau_\Delta \sin(\omega_m t)\right] \tag{3.2.1}$$

where τ_0 is a fixed delay amount, τ_Δ is the amplitude of delay modulation and ω_m is the frequency of modulation. This processing method effectively causes a shift in pitch meaning that high frequencies are shifted more than low ones. A simple delay can be easily implemented digitally using a buffer but the transition between buffer elements required to make the delay time-varying can cause undesirable clicking sounds. For this reason, time-varying delays are often implemented using interpolation between adjacent buffer elements.

Various interpolation schemes can be used for application in digital delay (Cain et al., 1994; Valimaki and Laakso, 2000). The performance of these schemes is generally a compromise between accuracy of delay fraction, frequency response, transient response and complexity of implementation. The simplest scheme is a linear interpolation between adjacent samples (Smith, 2008). The output sample is the weighted sum of two adjacent samples whereby the weighting factors are chosen so the output corresponds approximately to the desired delay fraction.

Both frequency shifting and time-varying delay allow the gain of a reverberation enhancement system to be increased. There are other similar processing schemes, such as phase modulation, these will not be covered in this work as they provide similar performance (Nielsen and Svensson, 1999). The remainder of this section will analyse the benefits of frequency shifting and time-varying delay for reverberation enhancement both in terms of increased stable feedback gain and increases in resultant reverberation time.

3.2.2 Simulations of frequency shifting

A simulation of a reverberation enhancement system including frequency shifting in the feedback loop has been implemented. This is a time domain simulation based on FIR filters which represent the room impulse response. This simulation uses the same impulse response model as described in section 2.1.3. The impulse response is measured directly using an impulsive excitation signal. The resultant reverberation time is evaluated in octave bands using the reverse integration method (Schroeder, 1965).

In order to assess the results of the simulations, these are compared with a predicted value excluding the frequency shift. This value is calculated using the analysis including time delay from section 2.2.1. The amount of delay is determined by the delay in the processing. The FIR filter which approximates the Hilbert transform includes a modelling delay, in order to make the filter causal, and this delay is included in the prediction. The feedback gain is measured from the unaltered impulse responses and this is used in the prediction.

The stability of the system was determined by visual and aural analysis of the response of the simulated room to an impulsive excitation. For a system with frequency shifting, it was found that audible artefacts were present when the feedback gain was greater than −6 dB and the system was unstable for gains above 0 dB. This was determined by listening to the resultant impulse responses. Assuming a stable feedback gain without time variance of −12 dB, these findings are in line with previous studies (Schroeder, 1964).

The mid-frequency reverberation time obtained for the system including frequency shifting is shown in Figure 3.5. The systems which have feedback below −12 dB agree well with the values predicted using equation (2.2.4) including the processing delay of the frequency shift. For gains above −12 dB but below −6 dB, which do not contain audible artefacts but would be unstable without time variance, useful increases in resultant reverberation time are observed in comparison to a time invariant system. For example, with a −6 dB feedback gain, the resultant reverberation time is 0.73 s where a time invariant system with a gain of −12 dB causes 0.58 s. The values are slightly higher than predicted for the nominal feedback gain.

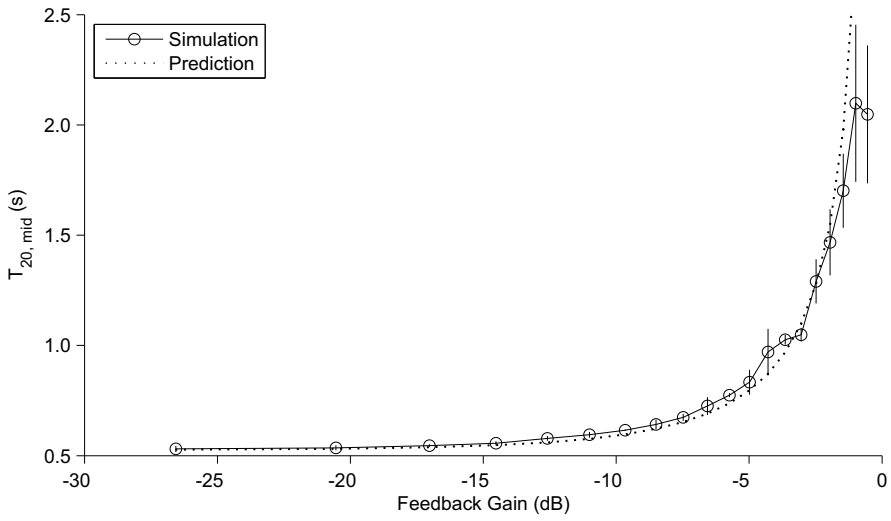

Figure 3.5: Simulated reverberation time gain for a single channel system including 7.5 Hz frequency shifting in the feedback loop. Predicted results are from the analysis in chapter 2 but exclude frequency shifting. Audible artefacts are present above feedback gains of −6 dB. The unaltered reverberation time was 0.53 s.

For values of feedback gain between −6 and −3 dB, the simulated reverberation times are higher than the predicted value. Additionally, the variations in reverberation time are larger than for the systems with lower feedback gain. Although this discrepancy is reasonably small, it has been shown more clearly in other simulations which are given in appendix A. The systems with gain above −2 dB have reverberation times which are lower than predicted by the analysis from chapter 2. Closer inspection of the recorded impulse responses and the resulting decay traces, shown in Figure 3.6, provides further insight into the results shown in Figure 3.5. A periodic artefact, with a repetition rate equal to the amount of frequency shifting, can be seen clearly in the impulse response of the system with a feedback gain of −0.5 dB.

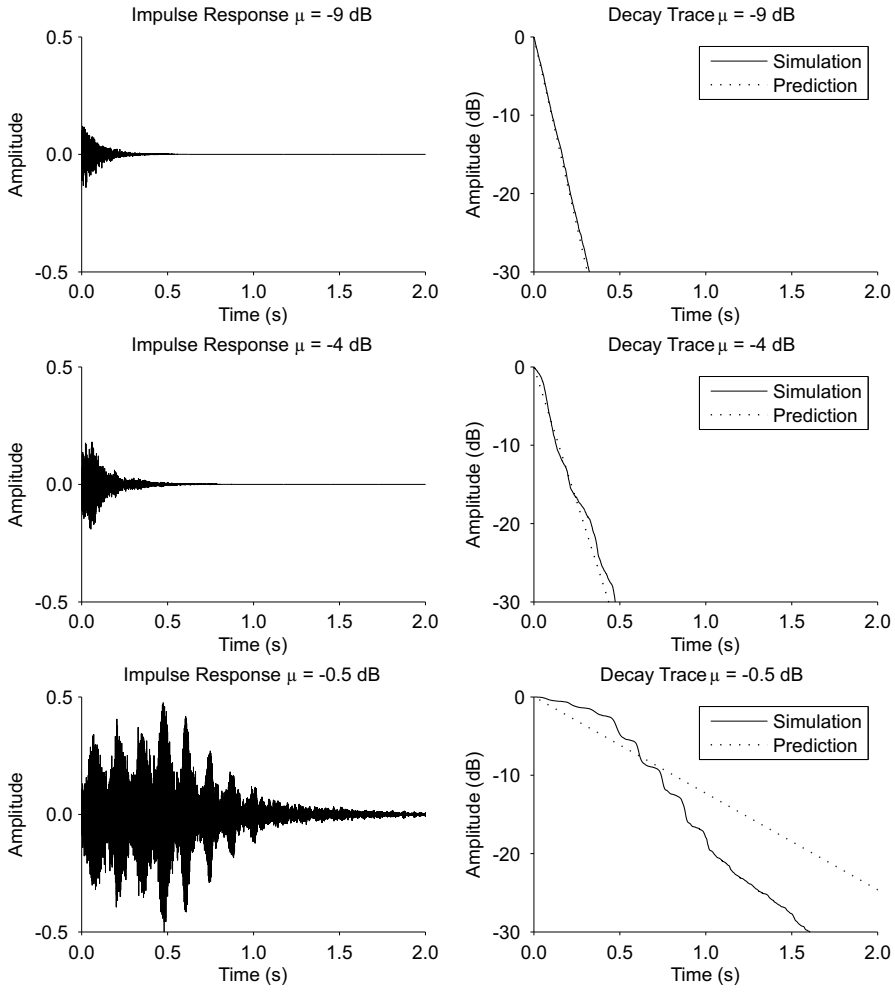

Figure 3.6: Example impulse responses and decay for a single channel system including 7.5 Hz frequency shifting. The dotted lines indicate the decay trace which would be expected from a linear decay with reverberation time equal to the predicted value.

This artefact causes steps in the decay trace which can be seen in the lower right-hand plot of Figure 3.6. This decay trace clearly displays a reverberation time which is lower than the predicted value. However, as the periodic artefact in the impulse response is so strong, this cannot really be classed as a true reverberation time. Some hints of this artefact are also visible in the impulse response of the system with −4 dB feedback gain shown in the middle left panel of the figure. This results in the slight steps in the decay trace in the middle right panel. These steps cause a slight curvature of the decay trace which means that the resultant reverberation time is longer than the prediction. The system with −9 dB feedback gain has no visible artefacts and shows a linear decay trace. This system would be unstable without the use of frequency shifting and the resultant reverberation time with frequency shifting is higher.

This simulation has shown that a reverberation enhancement system including frequency shifting can increase the reverberation time of a room significantly more than a time invariant system. However, it has also been found that with a normalised gain of greater than −6 dB audible artefacts are present and these are thought to increase the measured reverberation time. These artefacts appear periodically, at the same frequency as the modulation signal, i.e. equal to the frequency shift.

3.2.3 Experimental results including frequency shifting

An experiment has been conducted which tests the effectiveness of frequency shifting in the feedback loop of a single channel reverberation enhancement system. The signal processing was implemented using a Texas Instruments real time DSP board using the algorithms described in section 3.2.1. The reverberation enhancement system consisted of a loudspeaker and microphone connected via the DSP board with the various amplifiers required for operation. This was placed in the ISVR listening room which was designed for evaluating hifi systems. This room has a volume of 65 m^3 and an unaltered broadband reverberation time of 0.3 s.

The reverberation time of the room was measured using a Brüel and Kjær building acoustics kit. This consists of an integrated microphone and measurement system, hemi-dodecahedral loudspeaker and power amplifier. As the swept sine measurement method is ineffective for a time varying system, the reverberation time was measured in octave bands using the noise cutoff method (ISO3382-1, 2009). For this method, the room is excited by a noise signal, usually pink noise, and this is abruptly shut off. The decay trace is calculated directly from the recorded signal and the reverberation time is evaluated from this curve. The measured reverberation time of a system with time invariant feedback is shown in Figure 3.7.

In order to evaluate the performance of the system, the feedback gain is evaluated by injecting pink noise into the system without closing the feedback loop. The resulting signal is then measured and the ratio of the amplitude of the output and input signal is calculated. The feedback gain can be used to predict the resultant reverberation time which can be compared against the measured results. The predictions are made including the time delay in the system using equation (2.2.4). Comparison against results for systems without time variance will give an indication of the additional performance provided.

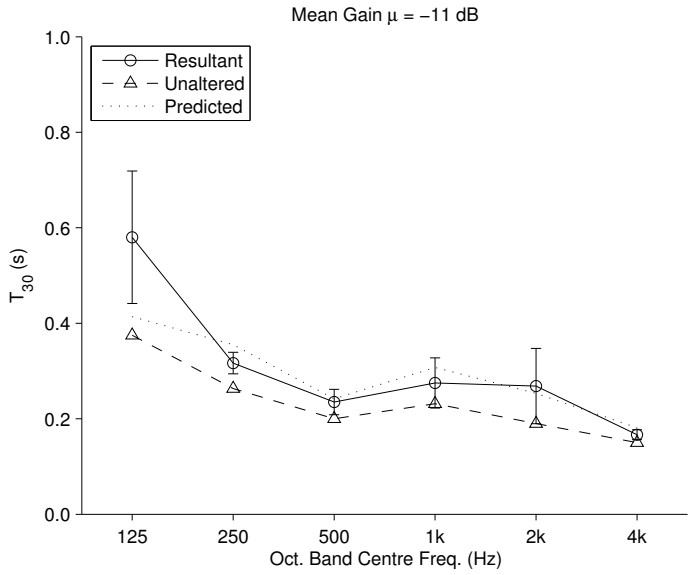

Figure 3.7: Reverberation time for a system with time invariant feedback. The resultant reverberation time is that including the effect of the system. This should be equal to the predicted values which use the analysis from chapter 2. The unaltered reverberation time of the room is included for comparison.

The results of this experiment when frequency shifting is implemented are shown in Figure 3.8. From this it can be seen that the system provides significant increases in the reverberation time compared to the time invariant system shown in Figure 3.7. The upper plot shows a system with a relatively low feedback gain, only slightly higher than would be possible with a time invariant system but with corresponding increases in resultant reverberation time. The measured reverberation times show good agreement with the predicted values, despite the fact that the frequency shifting is not specifically included in this analysis. As the feedback gain varies significantly between octave bands, with nearly 10 dB difference between the 1 kHz and 125 Hz bands, it is expected than the gain in reverberation time is not consistent between bands. However, this could be remedied in a practical system by using a simple graphic equaliser.

The lower plot in Figure 3.8 shows a system with a higher feedback gain which causes artefacts which are just audible. It can be seen that the measured reverberation times in the 1 kHz and 2 kHz bands are significantly higher than predicted. This is due to the artefacts of the frequency shifting as was seen in the simulations in section 3.2.2.

These results imply that the theoretical analysis and the numerical simulations, presented in 2.2.1 and 3.2.2 respectively, are reliable. It also shows that significant increases in the performance of the system are possible through the use of frequency shifting. However, care must be taken to avoid artefacts which exaggerate the measured reverberation time and are undesirable in terms of audio quality.

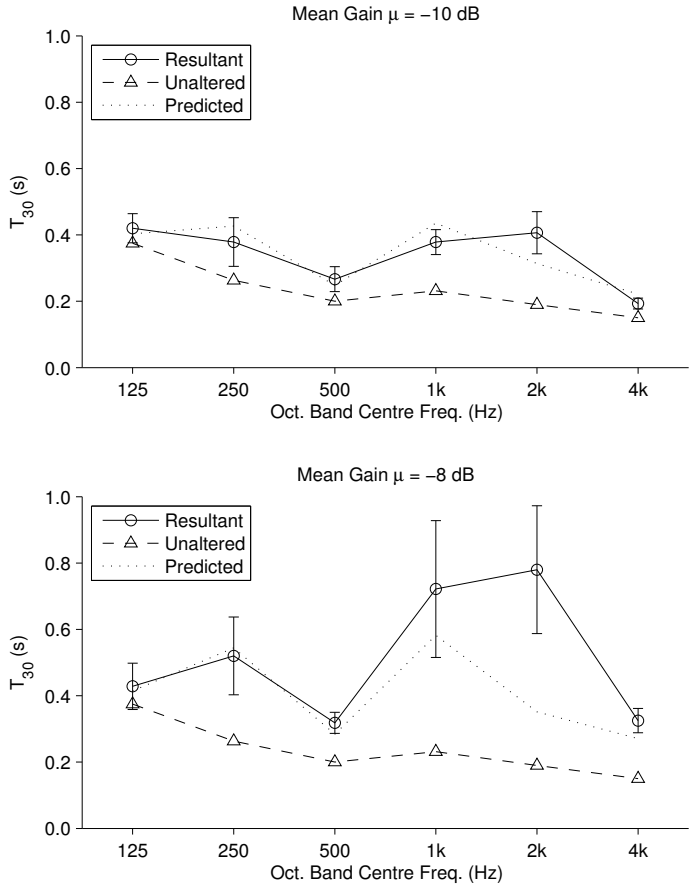

Figure 3.8: Results for a system including frequency shifting. Two gain levels are shown; the lower plot is closer to the stability limit. Legend labels as in Figure 3.7.

3.2.4 Simulations of time-varying delay

In order to assess the performance of a system including a time-varying delay, the simulation routine described in 3.2.2 has been reused with the processing in the feedback loop replaced. A modulation amplitude of 10 ms was used with a delay offset of 30 ms. The frequency of modulation was 1 Hz. These values were chosen such that the processing was inaudible at low values of feedback gain but gave similar performance to the frequency shifting results. The stability limit of this system is approximately −3 dB, which is similar to the performance of the system with frequency shifting from section 3.2.2. Audible artefacts were noticed at gains above −6 dB, determined by listening.

The results of the simulation, shown in Figure 3.9, are similar to those for the system including frequency shifting. The predicted reverberation times are made using equation (2.2.4). These are accurate for feedback gains lower than −12 dB but above this level the simulated values are higher than predicted. The spatial variation of reverberation time, as indicated by the errorbars, increases as the system approaches the stability limit. When the system is unstable, the measured reverberation time decreases rapidly.

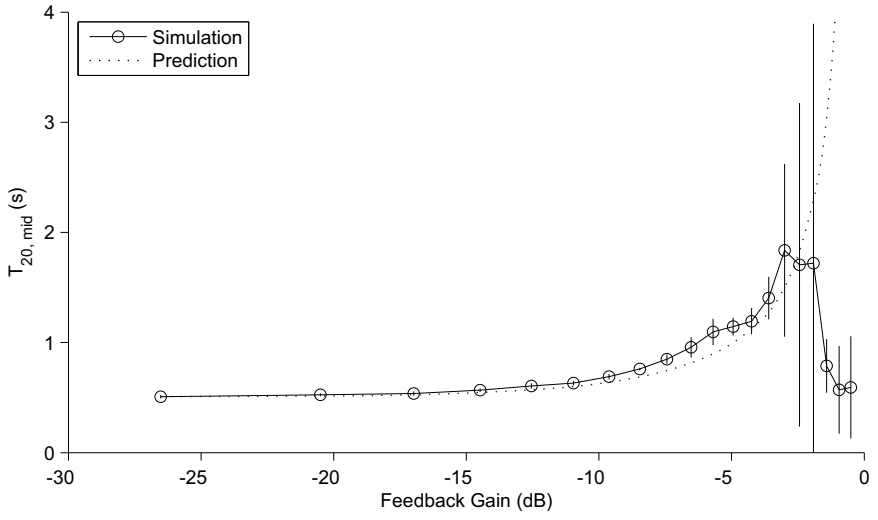

Figure 3.9: Simulated mid-frequency reverberation time as a function of feedback gain in a system including time-varying delay.

The causes of this trend are similar to those identified for the system with frequency shifting. Resultant reverberation times higher than predicted are due to the presence of artefacts. In this case it is difficult to define the true reverberation time. The artefacts may be inaudible, in which case the gains in reverberation time may be useful, even though the measured reverberation time may not properly represent the behaviour of the system. When the system

is unstable, the measured 'reverberation time' is related to the finite integration length used for the measurement method.

The simulations have shown that increases in stable feedback gain are possible through the use of time-varying delay. The resulting reverberation time is correspondingly higher but artefacts cause the measured reverberation time to be higher than that predicted analytically. However, the increase in performance may be useful as long as the artefacts are inaudible. The following section describes an experiment testing a system which uses time-varying delay.

3.2.5 Experimental results including time-varying delay

Alongside the experiment described in section 3.2.3, a system with a time-varying delay in the feedback loop has been tested. The method was identical to the experiment using the system with frequency shifting. The magnitude of the delay modulation was 10 ms and the frequency of modulation was 1 Hz as this gave similar performance to the results with frequency shifting. The predicted values were calculated including the time delay due to the processing and the source-receiver distance. The results are shown in Figure 3.10 comparing the unaltered room reverberation time with the measured and predicted resultant reverberation times.

This figure shows that the predictions are lower than the measured results. This was also found in the simulations in the previous section. The increase in resultant reverberation time is due to artefacts. In this case the usability of the system depends of the audibility of these artefacts. This is highly dependent on the configuration of a particular system, the room in which is to be installed and the purpose of the system. Therefore it is difficult to make general statements on the available performance increase made possible with the use of time-varying delay.

Although the reverberation times for this system appear to be higher than for the system including frequency shifting shown in Figure 3.8, the relative performance of the two algorithms is not immediately comparable. This is because the measured reverberation time is affected by artefacts and may not properly represent the true behaviour of the system. Additionally, the wide variety of possible parameter values complicates the simple comparison of these systems. This is especially true for time-varying delay where the modulation amount, modulation frequency and offset delay will all affect the final performance. However, it can be said that both of these systems allow increases in performance over the time-invariant system.

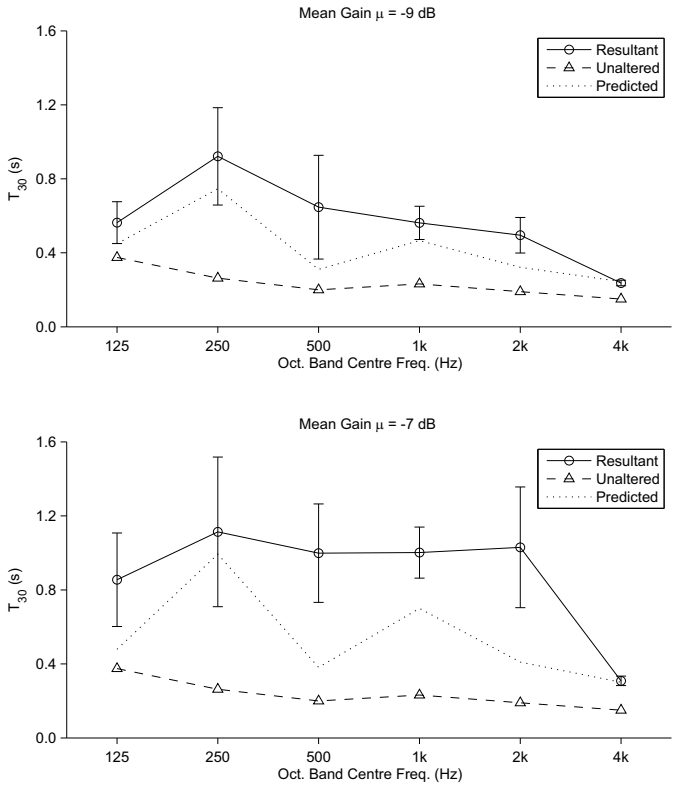

Figure 3.10: Reverberation times of a room affected by a system including time-varying delay. The two plots have different feedback gains with the lower plot having a higher gain. Legend labels as in Figure 3.7.

3.2.6 Summary of time variant reverberation enhancement

The simulation and experimental results from this section have shown that performance increases are possible through the use of time variant processing. This is due to an increase in the stable feedback gain. However, although these systems are stable it has been found that artefacts are present which cause the resultant reverberation time to be measured as higher than is predicted analytically. In this case it is difficult to define the true reverberation time of the room.

Both frequency shifting and time-varying delay have been used here. Similar performance was found for both of these processing schemes. Whilst frequency shifting is slightly more complex to implement, time-varying delay has more parameters which must be specified. It may be more important to consider the audibility of the artefacts caused by these two methods when choosing between them. However, this is beyond the scope of this work.

The use of time variant processing may improve the robustness of a system. If the feedback gain is set near the time invariant stability limit then the addition of frequency shifting or

time-varying delay will almost certainly prevent instability even if there are changes in the feedback path. At this level of feedback gain, there should not be significant levels of artefacts. Time variance could be used for this application but as has been shown in this section, it is unlikely to provide useable increases in the resultant reverberation time due to the presence of undesirable artefacts.

3.3 Distributed mode loudspeakers

There are several types of transducer which are designed to radiate sound. The most common of these is the cone loudspeaker (Newell and Holland, 2007). However, many alternative designs are available such as the electrostatic loudspeaker, ribbon driver and air motion transformers. One alternative design of interest here is the distributed mode loudspeaker (DML). As was discussed in section 1.2.5, these transducers have properties which may make them suitable for application to reverberation enhancement.

One of the benefits of DMLs is the increase in stable feedback gain when they are used within a public address system (Mapp and Ellis, 1999). It has been shown that a 4 dB increase in gain is possible within a certain setup. This increase would allow additional resultant reverberation time when used within a reverberation enhancement system. This aspect of their behaviour will be investigated in this section. First a short introduction to operation of the DML is given.

3.3.1 Operation of distributed mode loudspeakers

The basic idea for a distributed mode loudspeaker is to use a flat panel which is excited by a point force to create bending waves (Harris and Hawksford, 1997). In order to create a broadband radiation with a reasonably flat frequency response, the modal response of the panel to bending must be considered. By constructing the panel such that the modal density is high, the local mean of the frequency response of the panel will be relatively constant. In many ways this is similar to the concept of the diffuse field in that the frequency response is highly variable in detail but flat on average.

One of the advantages of this type of transducer is that each resonant mode of the panel has a different radiation pattern. With a high modal density, the various directivities sum to create a wide overall radiation which is more consistent across the frequency spectrum in comparison to a traditional cone loudspeaker. The sound radiation caused by this behaviour has been claimed to cause a lower ‘correlation’ between points when compared with a traditional cone loudspeaker (Gontcharov and Hill, 2000).

The wide directivity and 'decorrelated' radiation pattern, as well as the variable frequency response, mean that the DML is well suited to the rear channels in a surround sound system which normally deliver ambient effects (Newell and Holland, 2007). Additionally the form factor of these transducers makes them easier to implement in this type of configuration. For these reasons the DML could also be well suited to reverberation enhancement.

Another property of the DML is that, in comparison with a cone loudspeaker, its performance is not significantly affected by reflections (Azima and Harris, 1997; Azima and Mapp, 1998) or room modes (Fazenda et al., 2002). The radiated sound is claimed to suffer less colouration once the effect of the room is included.

The on-axis frequency response of a cone loudspeaker and a distributed mode loudspeaker have been measured and are shown in Figure 3.11. These measurements were taken with a sampling frequency of 44.1 kHz requiring an anti-aliasing filter which is observed as a sharp decrease in the responses above 18 kHz.

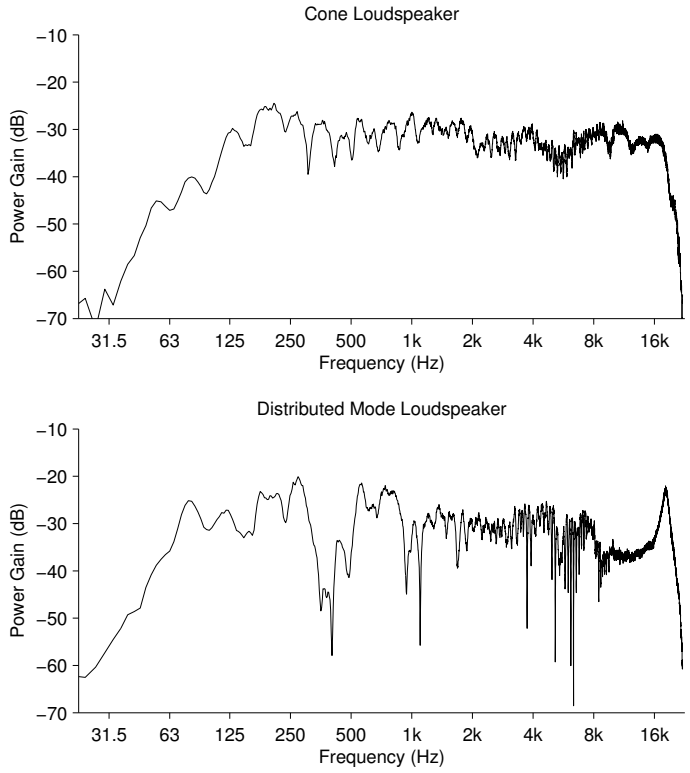

Figure 3.11: Frequency responses of a cone loudspeaker and a distributed mode loudspeaker. The measurements were made on-axis in a hemi-anechoic chamber. Note that the values of power gain include the amplifier gain and so do not represent the sensitivity of the transducer.

The experiment used a Fane MiniPro DML which has a surface area of approximately 0.3 m^2 and a quoted frequency range of 60 Hz – 21 kHz. The cone loudspeaker is a KEF HTS3001 which has a 115 mm woofer and a concentric, 19 mm tweeter. The quoted frequency range is 70 Hz – 55 kHz. The measurement was made in a hemi-anechoic chamber which has a hard floor which creates a single reflection. This creates a comb filtering effect which can be seen in the response of the cone loudspeaker.

The response of the DML does not obviously contain the effects of comb filtering. However, there are several aspects to the frequency response which are undesirable. There are large dips at 400 Hz, 1.1 kHz and 6.3 kHz. There is also a large peak 18 kHz. These features are characteristic of a DML which will show larger variation in the narrowband frequency response.

The power response is also important, especially for reverberation enhancement as it includes the effect of the directivity. A measurement was made in a reverberation chamber using a pink noise excitation signal. Mean values of power gain between the input noise signal and the pressure response, measured at several positions, can be seen in Figure 3.12. This shows that the diffuse field response of the DML is flatter than the cone loudspeaker and this is due to the consistent directivity of that transducer.

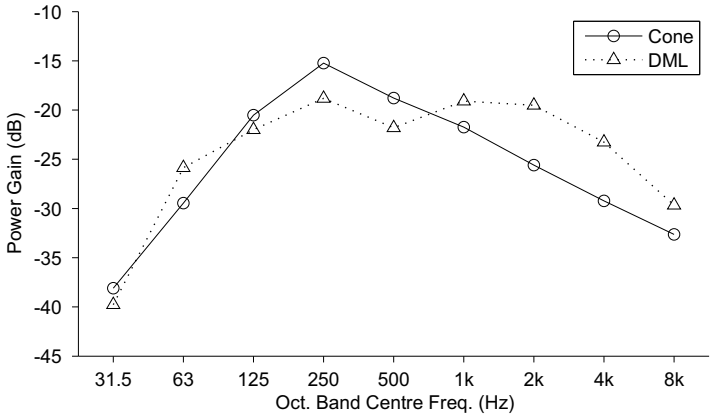

Figure 3.12: Diffuse field sound power measurements made in a reverberation chamber. The measurement is purely for comparison and is neither a sensitivity measurement nor a measure of absolute sound power.

It has been claimed that a public address system using a DML has a higher stable feedback gain compared with a system using a cone loudspeaker (Mapp and Ellis, 1999). The on-axis frequency responses in Figure 3.11 imply a larger variance of the response of the DML which, according to the analysis given in section 3.1.2, would decrease the stable feedback gain. However, the suggested cause of the higher stable feedback gain when using a DML is

the lower colouration due to interaction with the room boundaries and room modes. It may be that once in a room, the DML and cone loudspeaker will have a similar stability limit.

3.3.2 Experiments with a DML

An experiment has been conducted to test the claimed gain in the stability limit and the general performance of a reverberation enhancement system including a DML. The measurement system consisted of a laptop with a soundcard which was used to measure the transfer functions and feedback gains of the system. The reverberation time was measured using the same technique and equipment as in section 3.2. The measurements were made in the same location as that experiment, namely, a 65 m^3 listening room with broadband, unaltered reverberation time of 0.3 s.

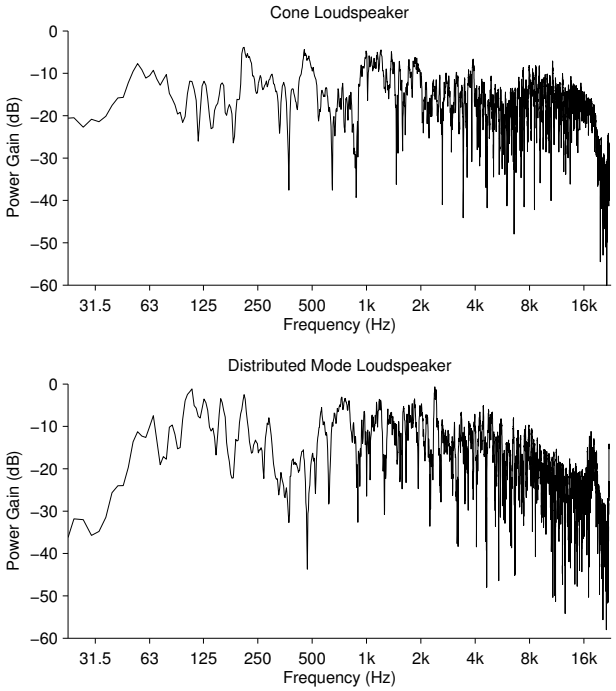

Figure 3.13: Measured transfer function in the listening room. The response at low frequency is misleading due to the presence of background noise in this room below 100 Hz.

The open loop transfer functions of the system with the cone loudspeaker and DML, shown in Figure 3.13, seem to show a similar amount of variance with peaks close to 0 dB and dips of nearly −40 dB which supports the argument that the DML is less affected by interactions with the room. This is because there is less change between the anechoic response in Figure 3.11 and the in-room response of Figure 3.13 with the DML. However, the variance of the in-room response of the DML is not lower than that of the cone loudspeaker. According to

the stability theory derived in section 3.1.2, the variance of the response is the important parameter when deciding the stability limits and therefore the DML can only have a maximum stable feedback gain which is equal to the cone loudspeaker and may be lower.

For this experiment, the broadband feedback gains of the two systems were set as close as possible. The open loop gains in octave bands are shown in Figure 3.14, showing that the feedback gains of the two systems are fairly similar. This should mean that there are similar changes in reverberation time caused by the two systems. As the feedback gains are not identical, it is useful to compare the measured reverberation times to a value predicted from the measured feedback gain. The effect of time delay caused by source-receiver separation is also included.

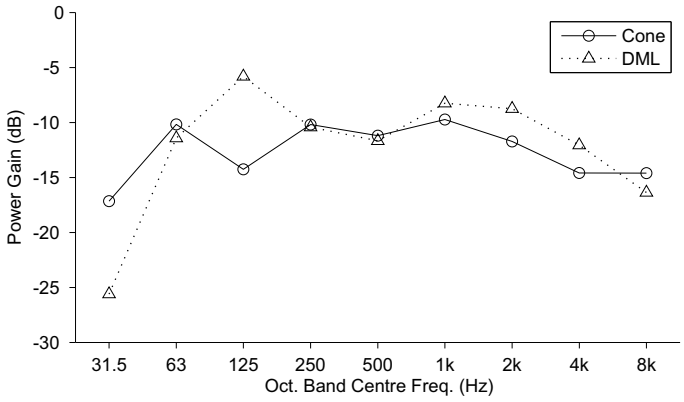

Figure 3.14: Open loop feedback gain in octave bands. The values for the 63 Hz and 31.5 Hz bands are too high because of background noise.

The resultant reverberation times are shown in Figure 3.15 compared against that predicted from the unaltered reverberation time, measured feedback gain and time delay. The systems used for this experiment are the same as those whose open loop gain was analysed in Figure 3.13 and Figure 3.14. The system including the cone loudspeaker causes reverberation times which are close to the predicted values. The values measured for the system with the DML are significantly higher than predicted for several of the octave bands.

One explanation for the high measured reverberation time for the system with a DML is that the effective diffuse field power of this transducer is higher than would be expected from a single point-to-point measurement due to the decorrelated nature of the sound radiation from this transducer. However, if this were the case, it would be expected that the phenomenon would be observed over the entire audio bandwidth, especially at high frequency where the modal density of the panel and the room is higher.

As the bands which have the highest reverberation time gains are those in which the feedback gains are highest and within which the narrowband response has peaks which are very close to 0 dB, an alternative explanation may be the presence of some kind of artefact as found for the time variant systems discussed in section 3.2. At these high feedback gains, a single frequency is being emphasised which may cause the model of the sound field, which is assumed to be diffuse, to be inaccurate. In this case the analysis used to predict the resultant reverberation time would also be inaccurate.

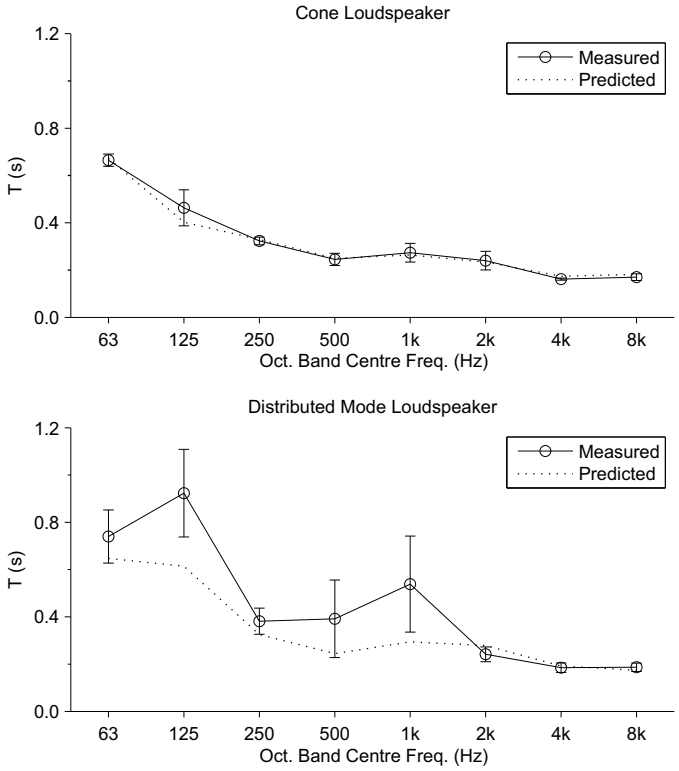

Figure 3.15: Reverberation times (T_{20}) measured with a single channel reverberation enhancement system using two different transducers with similar values of feedback gain.

In order to test the reverberation enhancement system with the DML more thoroughly, a further experiment has been conducted. In this the system was placed in multiple positions to allow a greater averaging over the sound field. The feedback gain was set more conservatively in order to reduce the possibility of artefacts. The resulting reverberation time was then averaged over 6 positions of the measurement system and 5 positions of the reverberation enhancement system. The resultant reverberation time was also predicted from measured feedback gain, unaltered reverberation time and time delay due to source receiver distance.

The results of this experiment are shown in Figure 3.16 and show a very good agreement between the measured result and the predicted reverberation time. This implies that the previous experiment was affected by artefacts and that the DML does not provide additional diffuse field sound power above the measured feedback gain. Along with the fact that the DML does not provide any additional stable feedback gain, this experiment implies that there is no particular advantage to this kind of driver in terms of reverberation time gain. Despite this, it may be that the form factor, wide directivity or some other property would make this transducer suitable for reverberation enhancement.

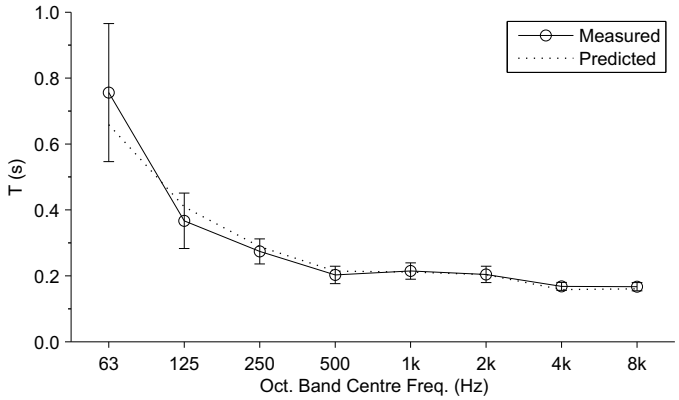

Figure 3.16: Measured reverberation time (T_{20}) of a system using a DML averaged over several positions of the system.

3.4 Summary

This chapter investigated the increases in performance to a reverberation enhancement system made possible by increasing the stable loop gain. Several options were considered including equalisation and echo cancelling but it was decided that the method most suitable for non-in-line reverberation enhancement is time variant processing. This strategy involves the use of signal processing in the feedback loop of the system which causes the open loop transfer function to vary with time. This allows an increase in the stable loop gain of the system.

Two different processing methods were trialled. The first was frequency shifting which alters the frequency of each component of the input sound by a fixed number of Hertz. The other method was a time-varying delay which effectively causes a shift in pitch rather than frequency so that high frequencies are shifted more than low frequencies.

A time domain simulation using these methods was implemented and this showed that significant increases in the stable loop gain were possible. However, the resultant

reverberation time was higher than predicted by standard analysis. This increase was found to be caused by artefacts related to the processing which increased in amplitude as the loop gain was increased.

An experiment was conducted using a real time implementation of frequency shifting and time-varying delay within a single channel reverberation enhancement system. It was found that increases in the stable loop gain of 6 dB were possible with these systems over the time invariant system. The measured reverberation time of the room, including the effect of the system, was found to be higher than that predicted using the unaltered room reverberation time and open loop feedback gain. For instance, a system with frequency shifting with a broadband feedback gain of −8 dB caused a resultant reverberation time of 0.8 s where the predicted value was 0.6 s. This discrepancy is in agreement with the simulation results.

The increase in measured reverberation time, above the predicted values, is due to artefacts. These artefacts may not be audible, in which case the increase in loop gain may still be useful within the context of reverberation enhancement. Additionally, it may be prudent to include some form of time variance in a reverberation enhancement system, without significantly increasing the feedback gain, in order to increase robustness of the system to small changes. There was no significant difference between the performance of the time-varying delay and the frequency shifter.

Another aspect of the reverberation enhancement system, which was thought to affect the stable feedback gain, is the choice of transducers. The cone loudspeaker is used universally in reverberation enhancement systems but it has been claimed that the distributed mode loudspeaker allows an increase in stable feedback gain in public address system. However, in this work it has been found that, within the context of reverberation enhancement systems, the DML performs, at best, the same as a cone loudspeaker in terms of the stable feedback gain. Nevertheless, the DML has other properties such as its wide directivity and low visual impact, which may make it desirable for application in reverberation enhancement.

Whilst there are many possible methods which have been developed to increase the stable gain of an electroacoustic system, it has been shown that many of these options are not applicable to non-in-line reverberation enhancement. Time variant processing, deemed to be the most likely candidate for this application, was found to increase the performance of this type of system. However, the use of time variance introduces undesirable artefacts as the gain is increased which means that this method will not allow large increases in performance.

4 Reverberation enhancement in a modal sound field

It is normally assumed that reverberation enhancement systems will be installed in large rooms, the behaviour of which can be modelled as a diffuse field (Krokstad, 1988). In smaller rooms, which are the subject of this thesis, the sound field at low frequency will not be diffuse (Kuttruff, 2000). Instead there will be isolated modal resonances. The sound field within the enclosure in this frequency region can be designated as a modal sound field.

The effect of the reverberation enhancement system on the modal field will differ from that in the diffuse field. Therefore it may require a different strategy for achieving the desired performance of the system. Moreover, the ideal performance of the system may be different once the modal behaviour is taken into account.

In this chapter, an analysis of a multi-channel feedback system within a modal sound field will be presented. The possibility of improving the performance of this system will be considered via the implementation of a number of performance metrics based on comparisons with ideal behaviour in a diffuse field. The system parameters will be optimised using a genetic algorithm. Although the work in this chapter is entirely based on simulations, considerations will be made towards the construction of a practical system.

4.1 Analysis of the system

The analysis in this section will be based on a non-in-line reverberation enhancement system consisting of a number of microphones and loudspeakers connected via an analogue or digital processor which would allow the feedback matrix to be specified. The system is identical to that shown in Figure 2.3. The effect of this kind of system on the modal sound field can be derived by using standard modal models of an enclosure whereby the response is expressed as a summation over the modes (Nelson and Elliott, 1992).

4.1.1 Derivation of the system response

The basic derivation of the modal response in an enclosure is given in section 1.1.1. This can be extended to model the inclusion of a multi-channel feedback system. To construct the model the equation for the pressure response is used to find the acoustic impedance Z which is the ratio of pressure to volume velocity. The frequency domain acoustic impedance can be derived from the pressure response given by equation (1.1.6).

Defining the primary source as a point source which is constant with frequency, so that $q_{vol} = q_p \delta(\mathbf{y})$, eliminates the integral term and allows direct calculation of the acoustic transfer impedance

$$Z(\mathbf{x}\,|\,\mathbf{y}) = \sum_{n=0}^{\infty} \frac{\omega \rho c^2}{V\left[2\zeta_n \omega_n \omega + i\left(\omega^2 - \omega_n^2\right)\right]} \psi_n(\mathbf{y}) \psi_n(\mathbf{x}). \tag{4.1.1}$$

The pressure at a number of microphone positions can be written as a vector **p** which will be a function of frequency. For the purposes of this analysis, it will be assumed that there is a single primary source at $\mathbf{y}_p$, M_p primary receiver positions at $\mathbf{x}_{pm}$ and a feedback system with M_s secondary sources at $\mathbf{x}_{sm}$ and M_s receivers at $\mathbf{y}_{sm}$. For the sake of simplicity, the case where there are different numbers of secondary sources and receivers will not be considered here. Therefore the length of the vector **p** is M_p+M_s. A vector of the same size $\mathbf{Z}_p$ relates the primary source strength to the resulting pressure and will be frequency dependent. With the system inactive, the pressure at the microphones becomes

$$\mathbf{p} = \mathbf{Z}_p q_p \tag{4.1.2}$$

where $\mathbf{Z}_p = \left[Z(\mathbf{x}_{p1}\,|\,\mathbf{y}_p) \quad \cdots \quad Z(\mathbf{x}_{pM_p}\,|\,\mathbf{y}_p) \quad Z(\mathbf{x}_{s1}\,|\,\mathbf{y}_p) \quad \cdots \quad Z(\mathbf{x}_{sM_s}\,|\,\mathbf{y}_p) \right]^T$ (4.1.3)

The effect of the secondary sources can be included by adding an additional term to the pressure equation

$$\mathbf{p} = \mathbf{Z}_p q_p + \mathbf{Z}_s \mathbf{q}_s \tag{4.1.4}$$

where $\mathbf{q}_s$ is a vector with length M_s and $\mathbf{Z}_s$ is a matrix of dimensions M_p+M_s by M_s. The columns of $\mathbf{Z}_s$ will contain the impedances between the secondary sources and all of the microphones. The elements of $\mathbf{q}_s$ will correspond to the secondary source strengths. Both of these terms will be functions of frequency.

To create a feedback system, the secondary source strengths can be defined in terms of the pressure at the microphone positions. The two vectors will be related by a feedback matrix **X** and a feedback gain *g*. The matrix **X** will have a size of M_s by M_p+M_s but only the right sub-matrix of M_s by M_s elements will be non-zero as these are the elements relating to the feedback paths. This matrix can either have constant elements or can vary with frequency. The pressure response then becomes

$$\mathbf{p} = \mathbf{Z}_p q_p + g \mathbf{Z}_s \mathbf{X} \mathbf{p} \tag{4.1.5}$$

solving for pressure gives

$$\mathbf{p} = \left[\mathbf{I} - g\mathbf{Z}_s\mathbf{X}\right]^{-1}\mathbf{Z}_p q_p . \tag{4.1.6}$$

By substituting equation (4.1.1) for each element of the impedance matrices and defining the other constant values, the pressure can be evaluated for any number of primary receiver positions and an arbitrary feedback system configuration.

The purpose of a reverberation enhancement system is to alter the time domain response of an enclosure so it is useful to derive the time domain response of the system in a modal sound field. The pressure response given by equation (1.1.10) can be used to construct an impulse response by summing over the modes within a given bandwidth. This impulse response can be used within a time domain simulation similar to those in section 2.1.3. Simulations of this kind using modal impulse responses will be used to assess the time domain behaviour of the system in a modal sound field.

If the modal overlap is very low, a simplified formulation can be derived. This is achieved by assuming the microphone signals can be derived from each mode separately. The source term can be defined as a summation of the primary and secondary source strengths which are proportional to the modal amplitude, as opposed to the pressure, at the secondary source positions. In this case the source term becomes

$$\int_V \psi_n(\mathbf{y}) q_{vol}(\omega, \mathbf{y}) \mathrm{d}V = \psi_n\left(\mathbf{y}_p\right) q_p + g\boldsymbol{\psi}_s^T \mathbf{X} \boldsymbol{\psi}_r A_n \tag{4.1.7}$$

where $\boldsymbol{\psi}_s$ is a vector of the value of the modeshape function at the secondary source positions, $\boldsymbol{\psi}_r$ is the equivalent vector for the secondary receiver positions (i.e. the microphone positions) and A_n is the complex modal amplitude as in equation (1.1.2). By substituting equation (4.1.7) into equation (1.1.6) the pressure can be shown to be

$$p\left(\mathbf{x}\right) = \frac{\omega\rho c^2 \psi_n\left(\mathbf{y}_p\right)\psi_n\left(\mathbf{x}_p\right) q_p}{V\left[2\omega\left(\omega_n\zeta_n - g\frac{\rho c^2}{2V}\boldsymbol{\psi}_s^T\mathbf{X}\boldsymbol{\psi}_r\right) + i\left(\omega^2 - \omega_n^2\right)\right]} \tag{4.1.8}$$

From equation (4.1.8) it is apparent that the feedback system effectively alters the damping of the mode. Depending on the sign of the feedback term, the damping of a particular mode may be increased or decreased. Since the sign of the modeshape functions may vary between modes and positions, the system may increase the damping of some modes while decreasing it for others.

The time domain response of the system can also be derived, from equation (4.1.8), such that the decay constant of the exponential in equation (1.1.10) becomes

$$\omega_n \zeta_n - \mu \boldsymbol{\psi}_s^T \mathbf{X} \boldsymbol{\psi}_r \tag{4.1.9}$$

which can then be used to find the altered impulse response of individual modes. This implies that the reverberation time can be decreased as well as increased. The simplified model is only applicable at very low frequency where there is minimal modal overlap but it allows insight into the process by which the sound field is altered. Namely, it can be seen that the damping of the modes is being increased or decreased depending not only on the sign of the feedback path but also on the sign of the modeshape function.

4.1.2 Stability of a modal feedback system

The feedback gain must be set to ensure the stability of the system. This can be calculated using a generalization of the Nyquist stability criterion for multi-channel feedback systems (Elliott, 2001). For a multi-channel system, this can be generalized as the locus of points of the eigenvalues of the open loop transfer function matrix. The open loop transfer function matrix of this system is $\mathbf{Z}_s\mathbf{X}$. The eigenvalues of this matrix determine the stability of the system. As the feedback gain g is arbitrary, it can be set to ensure the stability of the system after calculating the eigenvalues of $\mathbf{Z}_s\mathbf{X}$.

This transfer function matrix, whether it is modelled as here or taken from measurements of a real enclosure, will be subject to some inaccuracies. In order to ensure the stability of the system in all conditions it is prudent to introduce some constraint so that the system is robust to small changes. This constraint can be introduced by setting a region of the complex plane around the point $1+0i$ which the loci of the eigenvalues are not allowed to enter (Elliott, 2001).

For the system under consideration here, it is not only the stability which must be considered but also the fact that the impulse response may become very long even when the system is stable. This is undesirable and therefore a relatively stringent constraint may be introduced in order to reduce the risk of 'ringing tones'. Therefore g can be set so that the real parts of the eigenvalues of $\mathbf{GX}$ are always less than some positive constant. A value of 0.8 has been used for this constant throughout this chapter which corresponds to gain margin of approximately −2 dB.

4.2 Optimising the system

The performance of the reverberation enhancement system in the modal field is not easily defined. In an active noise control system, for instance, minimisation of the global acoustic potential energy is an obvious goal. Similarly the flattening of the frequency response is the

goal of a room equalisation system. The performance of these two systems may be improved by targeting the local pressure or frequency response at particular points rather than the global response. The decision to use a local control strategy can generally be made with a particular purpose in mind, such as the use of a system in a car where the passenger's positions within the enclosure are well defined.

With a reverberation enhancement system, there are several conceivable goals. It is the intention in this chapter to specify the parameters of the system to maximize its performance in the modal sound field. In order to specify the system parameters, a metric of the performance of the system must be chosen. As the purpose of the system is to increase the reverberance of the room, it would be beneficial to alter the modal sound field so it is closer to that present in a larger, more reverberant room, i.e. a diffuse field.

It was initially thought that it may be possible to synthesise additional modes with the intention of increasing the modal density and simulating a diffuse field. However, as the transfer function between the transducers of the system has a small magnitude at the anti-resonances of the room, the system would have to have an extremely high gain at these frequencies in order to ensure a noticeable change. This would require very sharp filters to be used within the system in order to minimise amplification of the resonant modes which could otherwise cause instability. Initial investigations into this technique were not particularly promising and so an alternative approach was sought.

A diffuse field transfer function can be modelled as a random variable. The real and imaginary parts of this transfer function will both be Gaussian distributed over frequency (Schroeder, 1987). This means that the absolute value of the transfer function will be Rayleigh distributed. The relative standard deviation, the standard deviation normalized to the mean, should be approximately equal to 0.52.

The relative standard deviation of the absolute value of the transfer function in the modal sound field will on average be larger than the value in the diffuse field, indicating a greater variance over frequency. This seems reasonable as the modal sound field is generally characterized by a small number of large peaks which should increase the standard deviation.

The other major difference between the diffuse and modal fields is the variance over space. By definition the diffuse field will be homogeneous and in practice the sound pressure level should have a standard deviation of less than 1.5 dB over 6 microphone positions in a high quality diffuse field such as in a reverberation chamber (ISO3741, 2010). In the modal field, the standard deviation over position will generally be larger than the value for a diffuse field and may be greater than 5 dB for example.

With this in mind, two metrics for the performance of the system in the modal sound field can be defined: the first in terms of the relative standard deviation of the absolute value of the pressure over frequency and the second the standard deviation of the mean sound pressure level in dB over position (Green, 2011). Both of these metrics are independent of overall level i.e. the primary source strength. The calculation processes of the two metrics are illustrated in Figure 4.1.

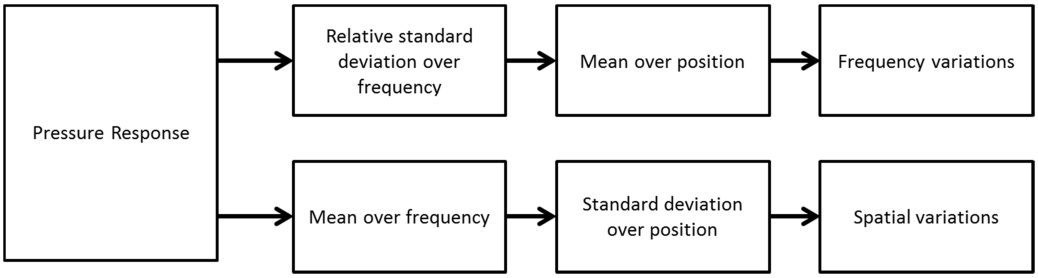

Figure 4.1: Block diagram showing the steps for calculating the metrics used for assessing the frequency variation and spatial variation in the room.

Having defined some metrics of the performance of the system, an optimal system can be sought which minimises these metrics. Due to the complexity of the function, it is not immediately possible to find an analytical solution. In order to check the feasibility of improving the performance of the system it is useful to use a numerical optimisation routine.

It was found that standard optimisation techniques based on gradient descent do not perform well for this problem. Evaluation of either metric over a mesh of points shows that there are many local minima. In order to find the global minimum, or at least a "good" solution, an alternative optimisation routine has been used.

The Global Optimisation Toolbox built into MATLAB features a number of algorithms designed to deal with difficult optimisation problems. The genetic algorithm was chosen for this work because it seemed to find a reasonable solution relatively quickly and robustly. As the current goal is only to test the feasibility of improving the modal field, it is not particularly important to find the true global optimum. Therefore the genetic algorithm is well suited to this problem; although the genetic algorithm is not proven to find the global minimum, it generally finds a "good" solution.

The genetic algorithm built into MATLAB is used to optimise parameters of the system in order to minimize the metrics defined in the previous section. The parameters chosen for optimisation are the coefficients of the feedback matrix $\mathbf{X}$ and the optimisation is done in two different ways. The simplest method is to set the elements of $\mathbf{X}$ as real valued constants.

Alternatively, each element of **X** can be defined as a digital filter and then the filter coefficients optimised. This allows the feedback path to vary with frequency but is easily realisable in a practical system.

For the purposes of this section an enclosure was chosen which would be representative of the kind of room which might benefit from reverberation enhancement but has a significant modal sound field. In this case the modelled enclosure was based on the listening room in the ISVR which has dimensions 6.4x4.1x2.6 m. The broadband reverberation time of this room is around 0.3 s giving a Schroeder frequency, calculated with equation (1.1.15), of around 132 Hz. The first mode of the room appears at 25 Hz. In order to approximate the measured reverberation time of the room in the 63 Hz octave band of approximately 0.5 s, the modal damping ratio was set at 0.06.

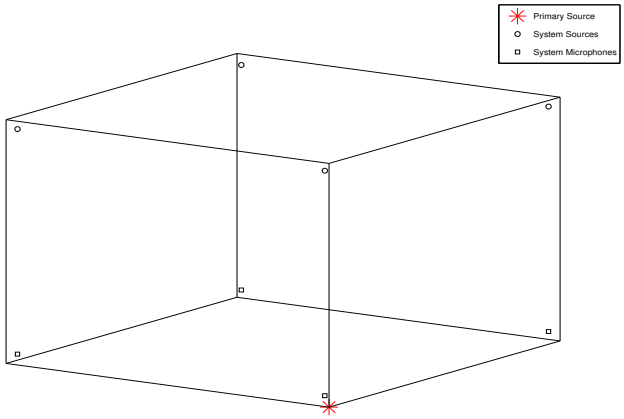

Figure 4.2: Diagram showing the positions of the virtual 'transducers' which have been used for the simulations presented in this chapter.

The results presented here only show optimisation of the feedback matrix so the microphone and loudspeaker positions are fixed. In this case a four channel system was specified with the four loudspeakers spaced 10 cm from each wall in each of the lower corners of the enclosure and the microphones placed in symmetrical positions in the upper corners. This ensures good coupling with all the modes of the enclosure. The primary source was placed in the apex of one corner in order to ensure that every room mode was excited fully. A volume velocity of 1×10^{-4} m^3s^{-1} was assigned to the primary source. The placement of the transducers is shown in Figure 4.2.

The system is optimised by changing the coefficients of the feedback matrix or the coefficients of an array of FIR filters. For the system including digital filters, FIR filters with 8 coefficients were used for each feedback path. This allows variation of the feedback gains with frequency which can be easily realised in a practical system. The resulting performance of the optimised system can be compared against the value of the performance metrics produced by the unaltered room response and that caused by including a feedback system with standard feedback matrices such as the identity matrix or a matrix of ones. These represent each microphone being connected to a single source or every source respectively.

It should be noted that the simulations in this section are entirely based on this particular room and this particular system. The results presented here may not translate to other setups. This is a practical limitation as a general overview of a large number of rooms or systems is beyond the scope of this work. The aim of this work, however, is to give an indication of the possibilities of the technique.

4.2.1 Frequency variation

In order to optimise the system to reduce the variance over frequency, 30 random microphone positions were defined within the enclosure and then the pressure response at each of these positions was evaluated over the frequency range of the modal field (14 – 132 Hz). The relative standard deviation (RSD) over frequency of the absolute value of each of these pressure responses was found and then the mean value of these was calculated.

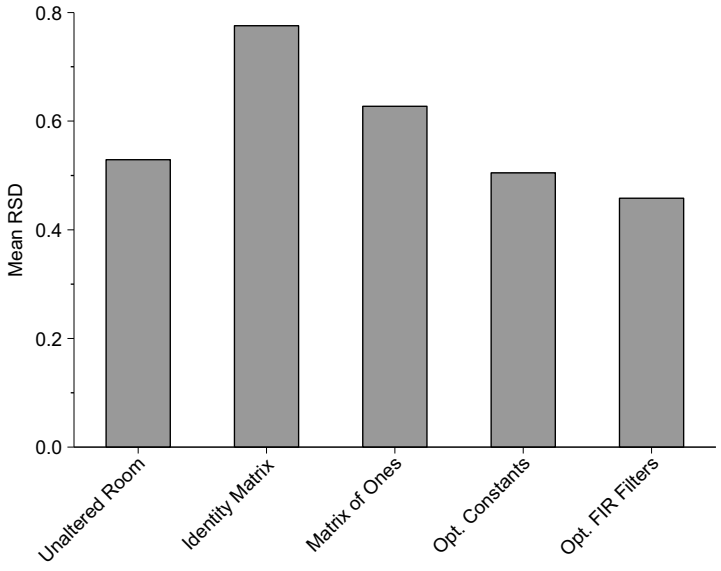

Figure 4.3: Relative standard deviation over frequency averaged over 30 microphone positions. Values are given for the unaltered room, that including a system using an identity matrix or matrix of ones as well as an optimised system using either a constant coefficient matrix or an array of FIR filters.

The calculated mean RSDs are shown in Figure 4.3. The mean value of RSD for the unaltered room is 0.53 which is almost the same as it should be in an ideal diffuse field. This is due to the relatively high damping present in this model. Therefore it is more important to notice the change in RSD when the system is introduced. The optimised feedback matrices perform significantly better than the identity matrix and the matrix of ones. The matrix with constant coefficients is close to the variance of the unaltered room, while the matrix of FIR filters is slightly lower.

In order to gain an impression of the global behaviour of the room the squared pressure amplitude can be calculated and averaged over the microphone positions. Three examples of this quantity are shown in Figure 4.4. This shows that the identity matrix introduces several large peaks into the response of the room. The optimised array of FIR filters effectively reduces the peaks present in the unaltered room response by increasing the mean amplitude of the response without affecting those peaks. Some peaks are reduced, notably the peak at 49 Hz.

It is not immediately obvious whether the optimised system produces a response which is preferable to the unaltered response. However, the response is clearly superior to that produced by the identity matrix. Analysis of the time domain response of the system will determine whether this benefit can be obtained in conjunction with an increase in the reverberation time.

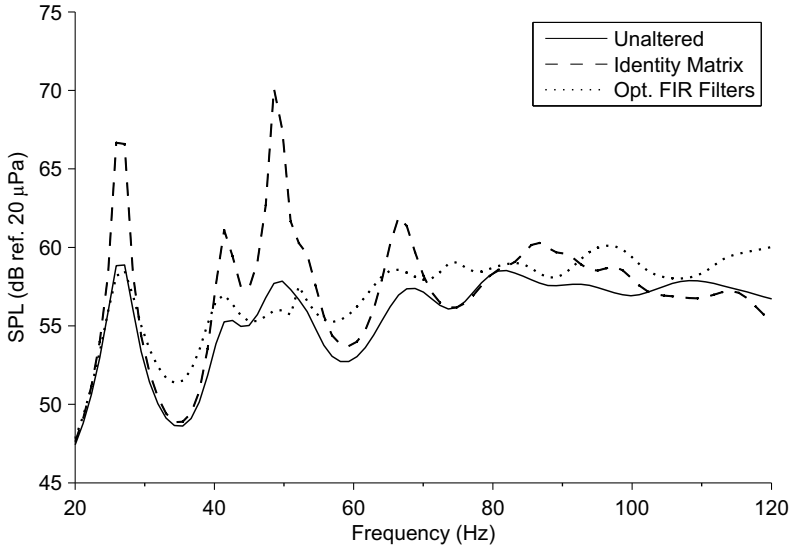

Figure 4.4: Frequency response averaged over 30 microphone positions showing the difference between the response of the unaltered room (solid) and that including a system which uses an identity matrix (dashed) and a system which uses an array of FIR filters optimised to reduce frequency variations (dotted)

4.2.2 Spatial variations

The optimisation routine can also be applied to reduce the variation of the modal sound field over space. A mesh of 30 random microphone positions was generated. These were used consistently during optimisation. The pressure response was calculated at these positions and the average sound pressure level over frequency is found for each microphone. The value of the metric is then defined as the standard deviation across these microphone positions.

The values of the metric are shown in Figure 4.5. The introduction of the feedback system, even without optimisation of the feedback matrix, reduces the variations in SPL over the microphone positions. The optimised systems provide even better performance with the system using an array of FIR filters producing the lowest value of the metric. These results imply that significant improvements to the homogeneity of the sound field are possible through optimisation of the processing in the feedback loop.

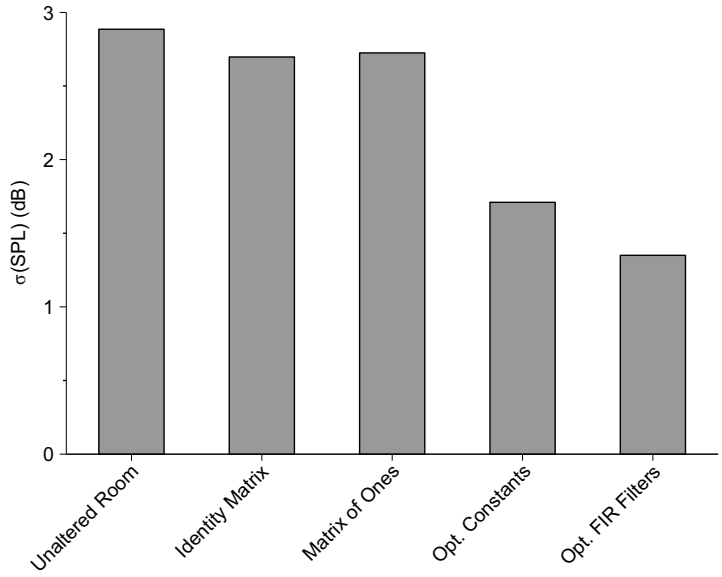

Figure 4.5: Standard deviation of SPL over 30 random microphone positions for the unaltered room and several systems.

Unlike the frequency deviations, where the unoptimised systems performed significantly worse than the unaltered room, the unoptimised systems display some improvement. This could imply that the spatial performance of the system in a modal field is not as important as the frequency considerations. This will inevitably vary between cases so optimisation may still be useful in particular situations.

It is important to test whether these improvements are local to the microphones used for the optimisation. That is, although variations in SPL between the 30 randomly generated

microphone positions have been reduced, this may not represent the true change in the global sound field. In order to test this, additional sets of microphone positions have been generated and used to evaluate the cost function. This should be a fairer test of the true performance of the optimised systems.

To test the global performance of the optimised systems, 10 sets of microphone positions are generated with 30 microphones in each set. The pressure is evaluated at the microphone positions for each system of interest. The cost function is then evaluated for each set of microphones as described above. The mean value and standard deviation of the value of the cost function can then be found across the 10 sets of positions. These results can be seen in Figure 4.6.

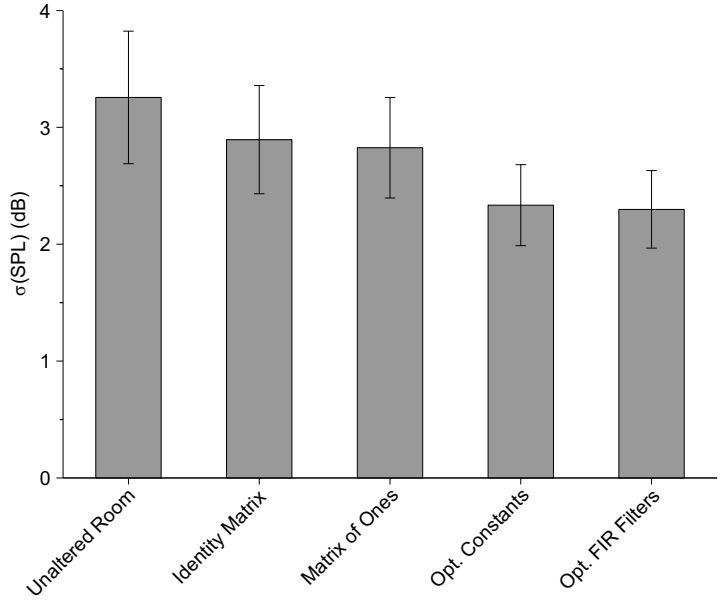

Figure 4.6: Spatial standard deviation of SPL evaluated with 10 sets of 30 random microphone positions.

The results shows that the general trends in the mean value of the cost function are similar to those in Figure 4.5 which were evaluated at the same microphone positions as those used for the optimisation. This implies that global reductions in spatial variations have been achieved. The variations in the measured cost function show that there is little true difference between the performance of the system with optimised constant coefficients and that with optimised FIR filters. Similarly there is not a significant difference between the identity matrix and matrix of ones. However, the change from the unaltered room to the unoptimised systems and then to the optimised systems is significant.

Some impression of the effect of the system on the spatial variance of the sound field can be seen in Figure 4.7 which plots the sound pressure level evaluated over a horizontal plane of

positions at a height of 1.65 m (approximately listening height whilst standing). The value of SPL is averaged over the bandwidth of interest (14-132 Hz) and so includes the effect of several room modes. The plot shows the general increase in level caused by the optimised system but the difference in the spatial variations is not immediately obvious in these plots.

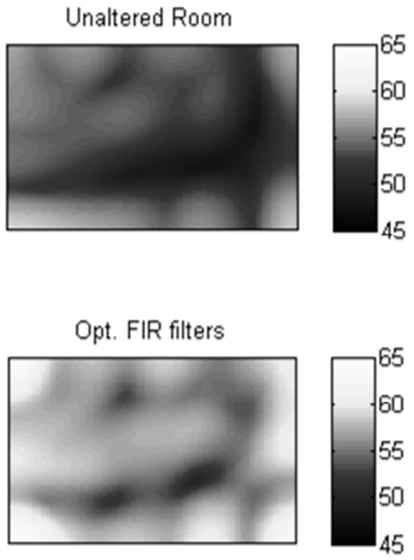

Figure 4.7: Average sound pressure level in dB from 14-132 Hz evaluated over a grid of positions at head height whilst standing for the unaltered room and that including a system using an optimised array of FIR filters.

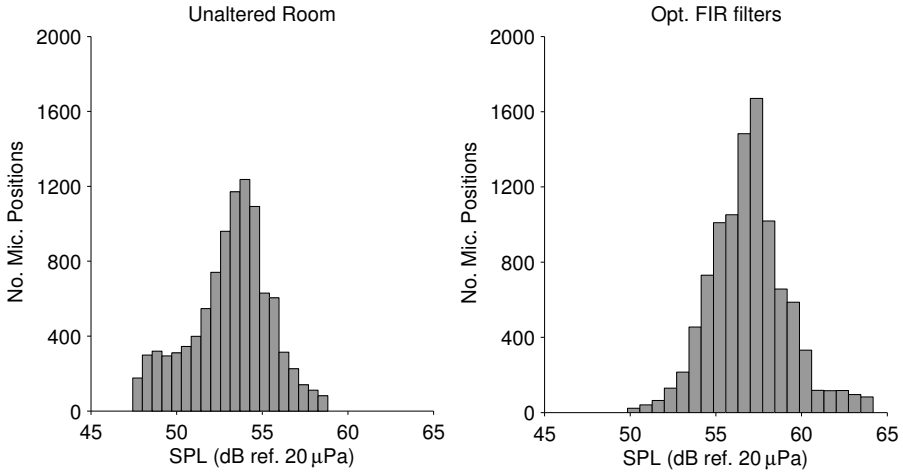

Figure 4.8: Histogram of SPL at a grid of microphones at approximately standing head height. This is the same data as Figure 4.7.

In order to illuminate the change in the spatial variations, histograms of the SPL are given in Figure 4.8. The larger peak in the histogram of the optimised system shows that many more of the microphone positions have values of sound pressure level close to the mean. This indicates a more homogeneous sound field. However, there also seems to be a slight increase in the number of extreme outliers and the range. This means that on average the sound field has lower variations over space, but there are a greater number of individual positions which have a value significantly lower or higher than the average. More complex optimisation routines which may combat this sort of problem will be discussed later in this chapter.

The results in this section have shown that spatial variation in the modal field can be reduced by the introduction of a feedback system. Optimisation of this system's feedback matrix produces further reduction in variation. It is not immediately apparent whether the change in the spatial variation is enough to produce a subjectively improved sound field.

4.2.3 Time domain response

As this system is designed to enhance the reverberation time of the room, it is important to consider the time domain response. The impulse response of the unaltered room can be constructed by summing over all of the modal impulse responses given by equation (1.1.10). This results in a band-limited impulse response where the bandwidth is dependent on the number of modes which are included.

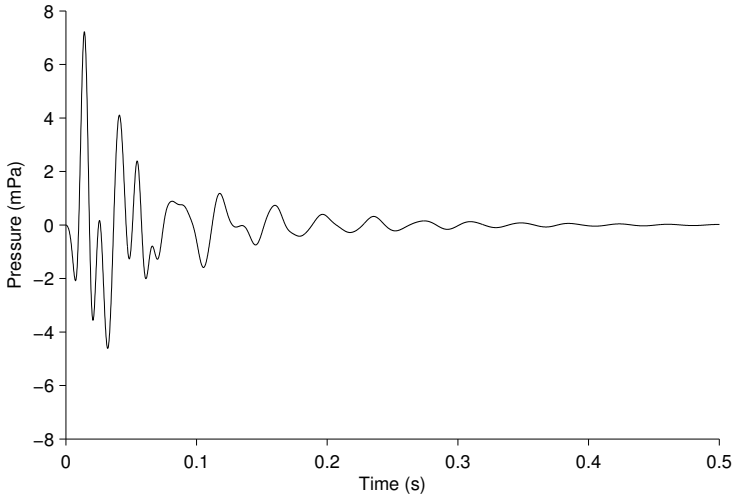

Figure 4.9: Example impulse response using the time domain model introduced in chapter 1. This is the response between the primary source and one of the measurement microphones.

An example of an impulse response calculated using this method is shown in Figure 4.9. The bandwidth used here is 14- 132 Hz and this is used throughout this chapter. Using a time

domain simulation based on FIR filters, the resulting impulse responses between the primary source and the primary receiver microphones including the feedback system can be calculated. The reverberation time can then be calculated using Schroeder's reverse integration method (Schroeder, 1965). These results are shown in Figure 4.10.

The results show a reduction in the reverberation for the system employing the identity matrix. This is unexpected because, as can be seen in Figure 4.4, this system causes large increases in the amplitude of the low frequency peaks. This would normally be associated with a reduction in damping which would create a longer reverberation time. This could indicate an inaccuracy in the time domain simulation method.

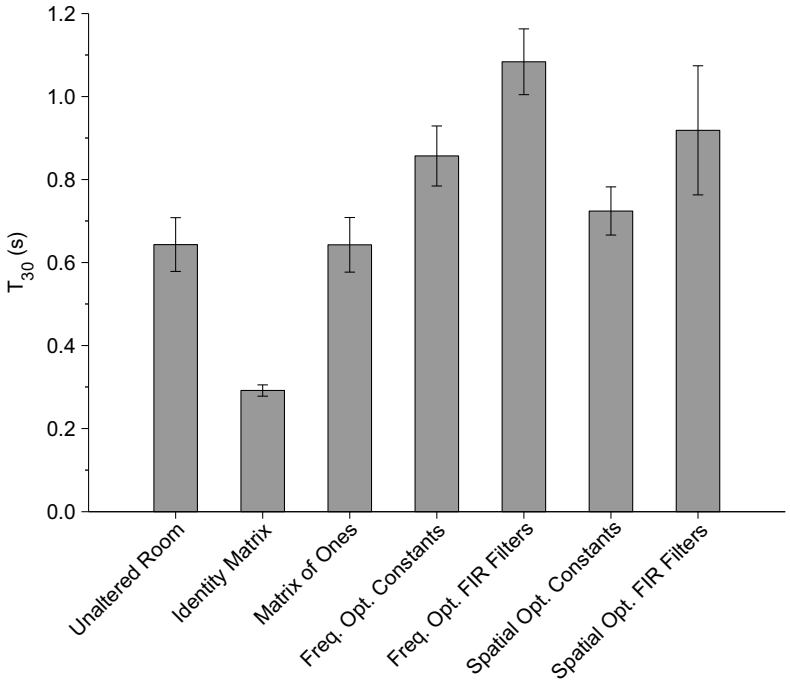

Figure 4.10: Simulated reverberation times for the unaltered room and that including a selection of reverberation enhancement systems. The errorbars shows one standard deviation, calculated across 30 microphone positions, above and below the mean.

The two optimised systems increase the reverberation time. The systems which employ FIR filters increase the reverberation time significantly more than the system using simple constant feedback matrices. If these results are correct, it would seem that optimisation of the system processing is extremely useful because these systems not only increase the reverberation time, which is their original application, but also provide additional benefits by reducing the spatial and frequency variations.

The system with FIR filters optimised to minimise spatial deviations of SPL seems to have greater spatial variation of reverberation time compared with the other systems, as indicated

by the errorbars in Figure 4.10. As the purpose of the optimisation is to make the sound field seem more like a diffuse field, which should have minimal spatial variations of reverberation time, this may indicate poor performance of this particular system. A further optimisation which seeks to minimise the spatial variations of reverberation time will be implemented later in this chapter.

4.3 Consideration of more complex performance metrics

The performance metrics defined in the previous section were based on the expected variations in the sound pressure over frequency and space in a diffuse field. Although this method has been successful in reducing those variations, some secondary effects have been observed which are not addressed by these optimisations.

It was shown in section 4.2.3, that the various systems, whether optimised to a particular performance metric or using a simple matrix, cause a wide range of resultant reverberation times. As the purpose of these systems is reverberation enhancement, control over the resulting reverberation time is an important consideration. This could also be defined as a performance metric which is then used to optimise the system.

Another aspect of the performance of the system optimised to spatial variation revealed by Figure 4.8 is that, although the standard deviation is reduced, the range of sound pressure level is actually increased. Therefore the range of SPL over positions could be used when optimising the system. In a similar vein, it may be useful to give greater weight to large peaks in the frequency response which could be achieved using measures other than the relative standard deviation.

Finally it seems likely that a system optimised to frequency variation, for instance, may perform poorly in terms of spatial variation. Therefore, it is useful to investigate a generic metric which combines several of the terms which have been discussed here. This may be problematic as the weighting of the individual terms or some other aspect of the definition of this method may affect the final results significantly.

In this section, the use of performance metrics which measure additional parameters of the sound field will be investigated. The efficacy of these methods and their independence will be considered. A generic metric, combining several of the individual performance metrics, can also be defined. The use of this kind of metric will be investigated.

4.3.1 Alternative individual performance metrics

Before attempting to define a generic performance metric, it is useful to investigate alternative metrics which may address some of the issues which have been observed earlier in this chapter. As mentioned above, it would be useful to be able to set the resultant reverberation time as part of the optimisation routine. In order to achieve this, a metric can be defined as the absolute value of the difference between the observed reverberation time and a desired value. This can then be averaged over several positions.

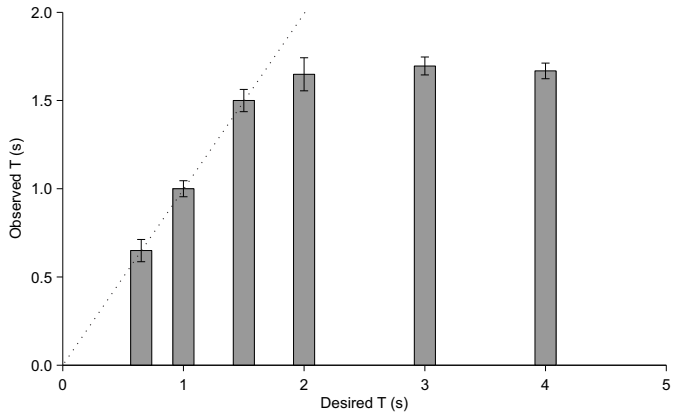

Figure 4.11: Observed reverberation times for systems optimised to various values of desired reverberation times. The bar at 0.65 s relates to the unaltered enclosure and the dotted line shows unity. The errorbars show the standard deviation of reverberation time over position.

An optimisation has been performed using the same method as in the previous section but using the metric designed to achieve a desired reverberation time. The resulting reverberation times are shown in Figure 4.11. The unaltered reverberation time of the room is 0.65 s and this is shown for reference. The systems optimised to create reverberation times of 1.0 and 1.5 s achieve these times with a high degree of precision. Above this value the stability limit of the system prevents any additional gain in reverberation time. The maximum value of reverberation time is approximately 1.6 s which is still a significant increase.

The frequency response of the system optimised to cause a reverberation time of 1.5 s is shown in Figure 4.12 along with that of a system optimised to reduce the frequency variations. This shows that there are very large peaks in the frequency response of the system optimised to the reverberation time. This is probably undesirable and gives further motivation for a generic performance metric which can optimise several parameters of the sound field.

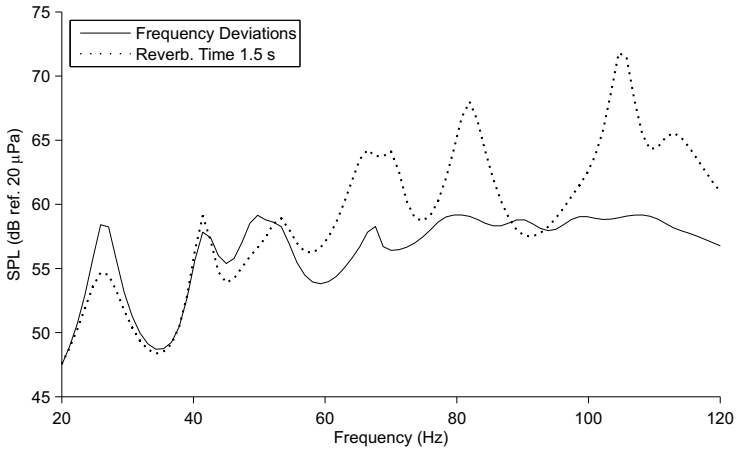

Figure 4.12: Frequency response of a system optimised to reduce frequency variations and a system optimised to achieve a reverberation time of 1.5 s.

Another metric which may be useful is to use the range or another similar measure of the spatial variation of SPL rather than the standard deviation used in the previous section. This is because the system optimised to the standard deviation actually increased the range of values of SPL (see Figure 4.8). A system has been optimised to reduce the range of values of SPL but this system actually has a greater range of values than the system optimised to the standard deviation as can be seen in Figure 4.13.

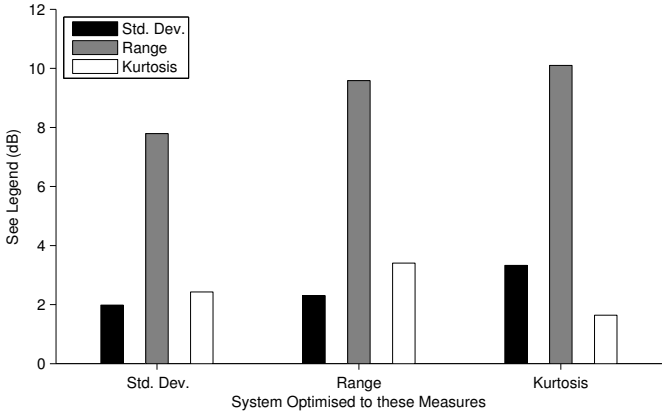

Figure 4.13: Values of standard deviation, range and kurtosis of SPL over position for three systems which are each optimised to reduce one of these parameters. The different optimisations are shown as three groups of bars and the bars within each group relate to the different measured parameters.

This highlights the inherent variability of the genetic algorithm and its dependence on the choice of cost function. As the range of SPL will be strongly affected if the single point chosen has a particularly high or low value, it may stop the algorithm from finding a reasonably good solution which would then be optimised further to find the best solution.

Instead of the range of SPL, the kurtosis can be used. This is a statistical measure which is strongly affected by outliers, i.e. the presence of a small number of points which have a value much higher or lower than the mean, although not as strongly as the range.

The system optimised to reduce the kurtosis of SPL over space does have a low value for kurtosis, as shown in Figure 4.13, but the values of standard deviation and range are significantly higher than the other systems. Also the kurtosis of the system optimised to the standard deviation is not particularly greater than the system optimised to the kurtosis. The objective of these measures is to reduce spatial variations of SPL and it was hypothesised that an alternative to the standard deviation may achieve better results with the genetic algorithm. The results here imply that, contrary to that hypothesis, the standard deviation is the best measure to use in the optimisation. This also discourages the use of alternative measures for assessing the variations over frequency.

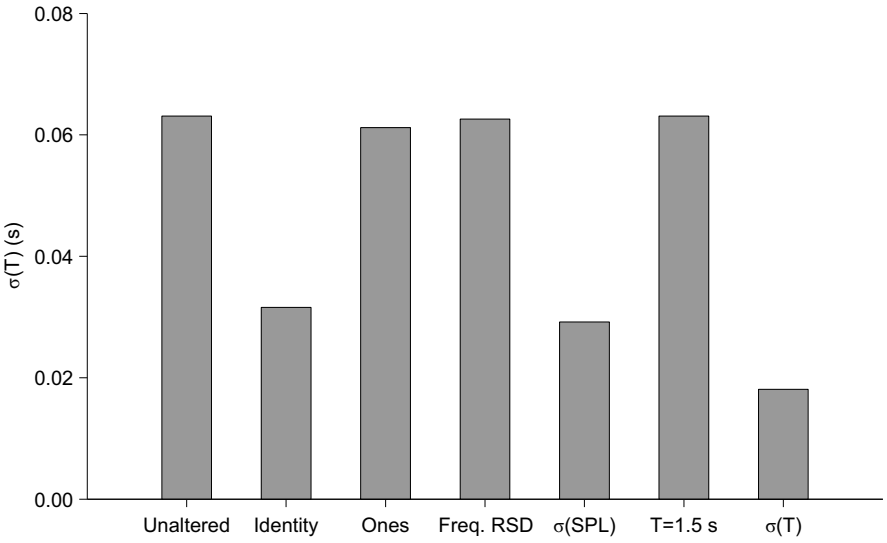

Figure 4.14: Spatial variation of reverberation time for several systems. The bars, from left to right, show the value for the unaltered room, for systems using the identity matrix and a matrix of ones and for systems with matrices optimised to the relative standard deviation over frequency, the standard deviation of SPL over position, the absolute difference of the mean reverberation time with 1.5 s and the spatial standard deviation of reverberation time.

One other parameter which could be considered is the spatial variation of reverberation time. Values of the standard deviation of reverberation time, measured over 30 microphone positions, can be seen in Figure 4.14 for four different optimisations as well as the unaltered room and the systems with 'standard' matrices. The systems optimised to frequency variation and to a reverberation time of 1.5 s show reasonably high spatial variation of

reverberation time which is comparable to that of the unaltered room and that including a system with a matrix of ones.

The system with the identity matrix reduces the spatial variation of reverberation time. Even lower values of spatial variation are achieved by the system optimised to spatial variation of SPL and, predictably, the system optimised to spatial variation of reverberation time. The spatial variation of reverberation may be correlated to the variation of SPL. If that were the case, only one of these terms would be required within the generic metric which will be discussed later in this section.

4.3.2 Generic performance metric

The purpose of a generic performance metric is to allow optimisation of a system such that it has relatively good performance in a number of parameters rather than in a single parameter which may cause undesirable effects in other measures. The evidence seen earlier in this section suggests that it would be useful to combine a term which will set the reverberation time with terms which control the spatial and frequency variations of the sound field. Complex methods have been developed for multi-parameter optimisation using a genetic algorithm (Lis and Eiben, 1997) but this section will consider a basic implementation using a simple sum.

Therefore a generic performance metric can be defined as an unweighted sum of the RSD of pressure magnitude over frequency, the standard deviation of SPL over position and the absolute value of the difference between the reverberation time and the desired value. This quantity is physically meaningless as the terms have different units, but its only purpose is to serve as input to the genetic algorithm. It should cause a reduction in all three values. As the sum is not weighted, one quantity may have a greater effect on the outcome. However, since all of the terms are within the same order of magnitude the use of simple sum may be justified in this case.

An optimisation has been run using this performance metric using both a constant coefficient feedback matrix and an array of FIR filters. The desired reverberation time has been set at 1.5 s as this should be the most challenging in terms of achieving good performance of the other metrics. The optimised systems both achieved the reverberation time accurately with all positions having a value between 1.4 and 1.6 s. The performance of the systems which have been optimised to the generic performance metric can be compared against the system optimised to the reverberation time alone.

The values of frequency and spatial deviations for the system optimised to the reverberation and the systems optimised using the generic metric can be seen in Figure 4.15. This shows that the optimisation has produced significant improvements in performance for both metrics. Comparing these results to those for the system optimised to the individual frequency and spatial metrics in Figure 4.4 and Figure 4.5, respectively, shows that the generic optimisation does not perform quite as well as the system optimised to a single metric in terms of that metric, which is to be expected. The generic optimisation provides reasonably good performance for all the parameters. These results imply that a simple sum of the individual metrics creates an optimised system with good overall performance and that complex multi-parameter optimisation is not required for this situation.

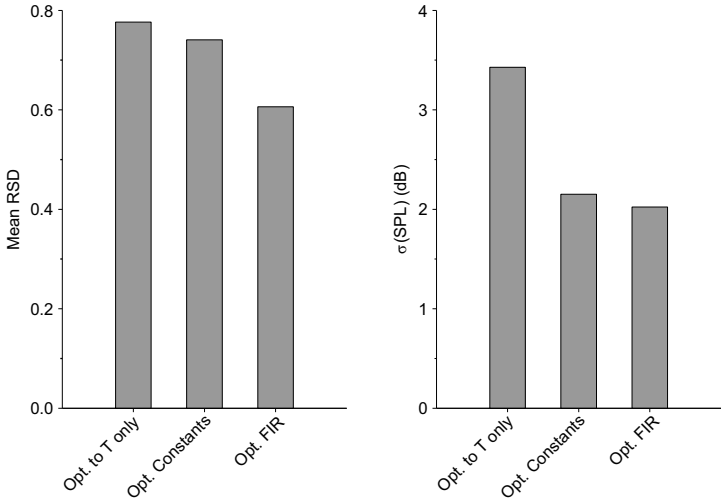

Figure 4.15: Values of RSD over frequency and standard deviation over space for a system optimised to create a reverberation time of 1.5 s and two systems optimised using the generic performance metric including a term to set the reverberation time to 1.5 s.

4.4 Effect of source and receiver positions

In the previous sections, the source and receiver positions were fixed as the investigations were centred on the optimisations of the feedback matrix. The only variation in the positions of the transducers was for the results given by Figure 4.6 as these were specifically related to spatial variations. This section will extend that work to include changes in the primary source positions as well as changes in the number of microphones used to evaluate the cost function.

4.4.1 Primary source position

The primary source is used to excite the sound field. In the previous section, the position has been fixed at the apex of a corner in order to maximally excite all of the modes. In this section, the effect on the systems discussed in the previous section by varying the primary source position will be investigated. Additionally, a system will be optimised to alternative primary source positions; this is a more realistic simulation of a practical optimisation.

The values of frequency and spatial variation evaluated at 20 randomly generated primary source positions are given in Figure 4.16 for the systems which were optimised to the original fixed primary source as well as the unaltered room and systems with standard matrices. This shows that the difference in the measured variations between the unaltered room and the systems using the identity matrix or matrix of ones is similar to that observed with a fixed primary source position. However, the optimised systems have significantly higher variation compared with the simulation using the fixed primary source as seen in Figure 4.3 and Figure 4.6.

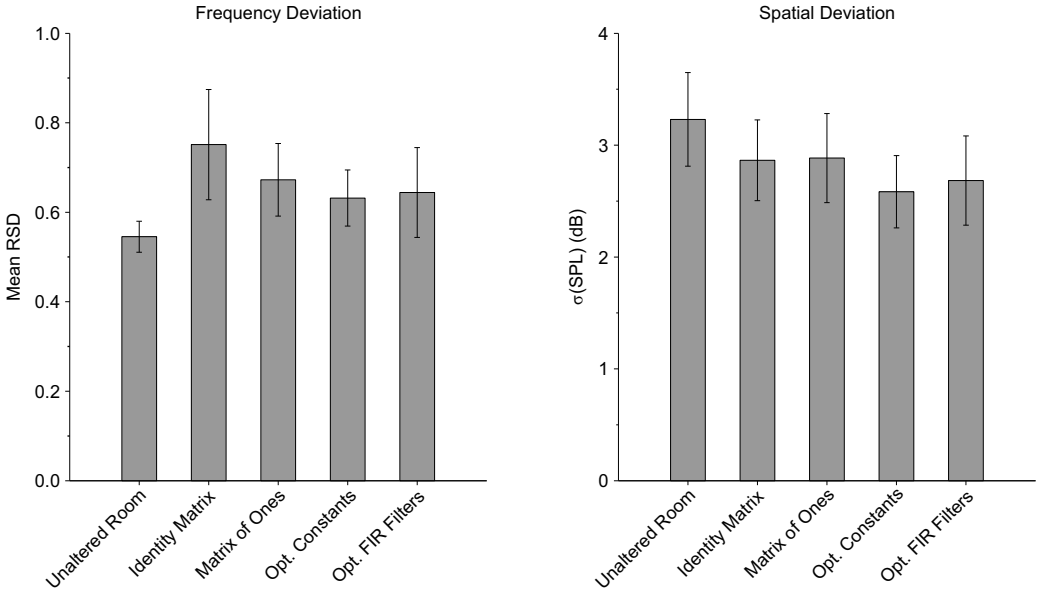

Figure 4.16: Varying the primary source position significantly alters the observed performance of the systems which were optimised to a fixed primary source. The metrics have been evaluated over 30 microphone positions at each of 20 primary source positions. The bars in this plot show the mean and standard deviation of the metric over the primary source positions.

This degradation of the performance of these systems implies that optimisation to a single primary source position is not robust to changes in the source position. Since there is a larger change for the systems which use FIR filters, it could be hypothesised that these systems are less robust to changes to the setup used during the optimisation process. In situations which

utilise a fixed source position, perhaps for room equalisation for audio reproduction, this may not reduce the efficacy of this method. However, for the applications of interest here an alternative optimisation method may be required.

The system can be optimised by evaluating the pressure at the microphones using several primary source positions and then evaluating the spatial and frequency variations over all of these simulated responses. This should allow for a better global performance of the system. This can be seen in Figure 4.17 which shows the performance of the system optimised to 6 primary source positions which are then subsequently evaluated with 20 primary source positions.

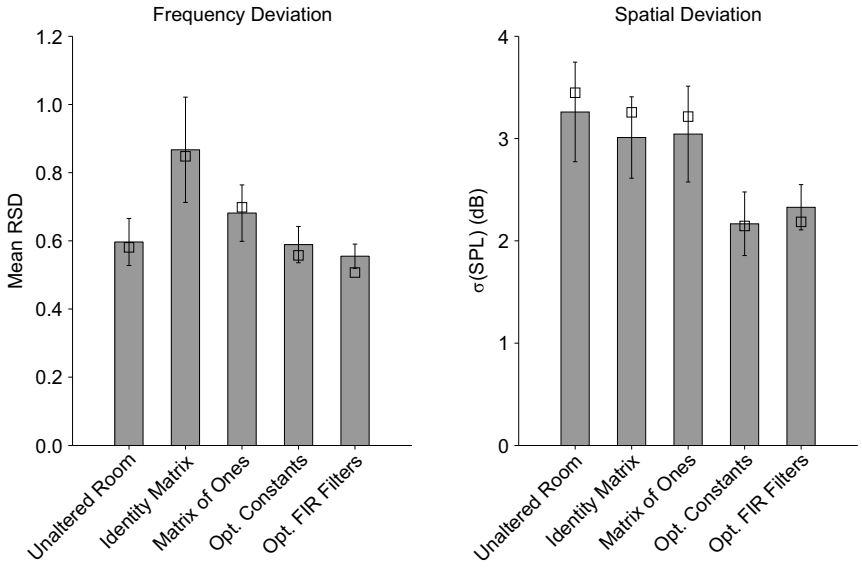

Figure 4.17: Values of frequency and spatial variations for a system optimised with multiple primary sources. The squares show the values of metrics evaluated over the 6 primary source positions which were used to optimise the system and the bars show those metrics evaluated over 20 primary source positions.

This plot shows significant improvements in the global performance of the systems optimised to multiple primary source positions in comparison to those optimised to single positions as seen in Figure 4.16. There is a slight increase in the metrics evaluated over the source positions used for the optimisation (shown as squares in Figure 4.17) and the 20 separate primary source positions, particularly for the system with FIR filters optimised to frequency deviations. This is not particularly significant as the general trend is very similar between these two sets of primary source positions.

These results show that, in order to achieve an effective global optimisation, several primary source positions must be used along with several microphone positions. In order to construct a practical system, it is useful to investigate the minimum number of source and receiver

positions which could be used and still provide a reasonable result. The prescribed number of positions for precision measurement of reverberation time is 12 independent positions with at least 2 source positions and at least 3 microphone positions (ISO3382-2, 2008). The results in this section imply that this is probably too few source positions to optimise the modal response of the system robustly.

4.4.2 Altering the number of microphone positions

As mentioned in the previous section, it is useful to investigate the minimum number of transducers required for an effective optimisation. This relates not only to the implementation of practical systems but also to the simulations presented here as a reduced number of transducers would allow the simulation to be executed in less time. A simulation has been run testing the effect of altering the number of microphone positions on the measured value of spatial and frequency variations. The metrics were evaluated over 2 to 128 random microphone positions which were each tested 50 times. The results for the unaltered room and that including a system with an identity matrix are shown in Figure 4.18.

The mean value shown in the figure effectively has 50 times the nominal number of positions and so the resulting value is relatively consistent for all sets of microphone positions. The errorbars, which show the standard deviation measured over the 50 measurements above and below the mean, clearly show significant variations in the measured value of the metrics when there are a small number of microphone positions.

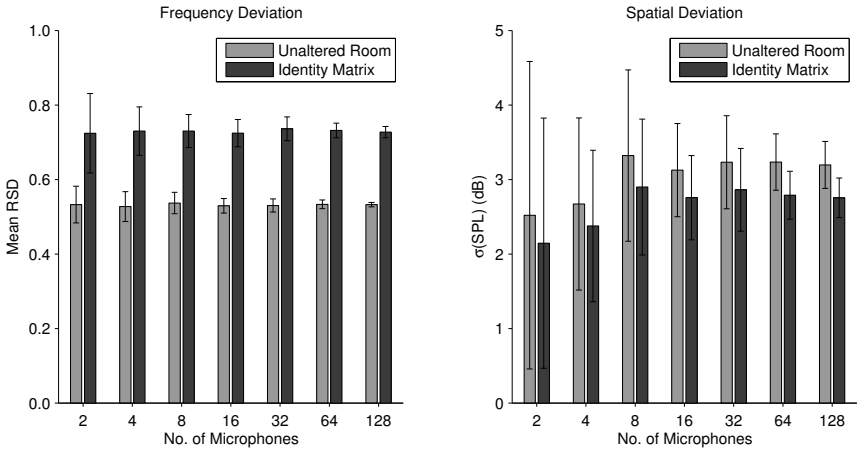

Figure 4.18: Evaluating the frequency and spatial variations over a changing number of microphone positions.

The variation over different sets of the same number of microphones decreases significantly as the number of microphones is increased, especially for the measurement of spatial

variation. Although there is still some overlap for the measured spatial variation even with 128 microphone positions, closer analysis of the data shows that for each of the 50 sets of microphone positions the correct trend is reflected, i.e. a slight reduction of spatial variation when using the system with the identity matrix.

Analysing the difference between the unaltered room and the room including the system for each set of microphone positions can reveal the number of positions which is required to identify the correct trend. For frequency deviation, the correct trend is identified for every point even with only 2 microphones. This is partly because the difference between the true values is quite large. Identifying the correct trend of the spatial variation requires significantly more microphone positions. The arrays of 16 and 32 microphone positions are reasonably reliable with around 90% of these arrays giving the correct trend. With 128 microphones, every set provides the correct trend.

These results show that although the exact position of the microphones will affect the measured value of the metric, more often than not the difference between the systems can be identified with a reasonably small number of microphone positions as long as they are used consistently between measurements. The exact number is dependent on the actual difference between the two quantities as a very large number would be required to measure a small change. An array of 16 or 32 microphones seems to provide reasonable results for present simulation.

4.4.3 Optimising to a practical number of source and receiver positions

The practical implementation of this kind of optimisation would require a significant amount of measurement effort. Although the optimisation would probably be performed off-line it would still need to be based on measured data. The optimisation requires the transfer function between all of the primary and secondary sources. In section 4.2 there is a single primary source, 30 primary receiver positions and 4 secondary sources and receivers which means that 170 transfer function measurements are required.

It has been shown that a single primary source position is inadequate but that the number of microphone positions may be reduced. For a practical system to be easily implemented it would be useful if the secondary source and receiver positions could be used as primary sources and receivers to reduce the number of transfer function which must be measured. Additionally, it would be useful if the microphones could be reused between source positions without having to be moved. This would create additional independent measurement paths without having to increase the number of actual transducers.

Finally, it would be desirable for a practical system to have the ability to perform routine monitoring of its performance. In this case the transducers should be positioned so that they do not have to be removed from the room for it to be used for its primary function. For this reason, any additional microphones which are not part of the feedback system itself should be positioned close to the ceiling of the room.

This section will optimise a system using secondary source positions as the primary source position along with using the secondary receivers as primary receiver positions in addition to a small number of additional microphones. These transfer functions will be used for the optimisation but the performance of the system will be compared with the other systems discussed in the chapter by evaluating them using a much larger array of transducers. This should reveal the true performance of the system.

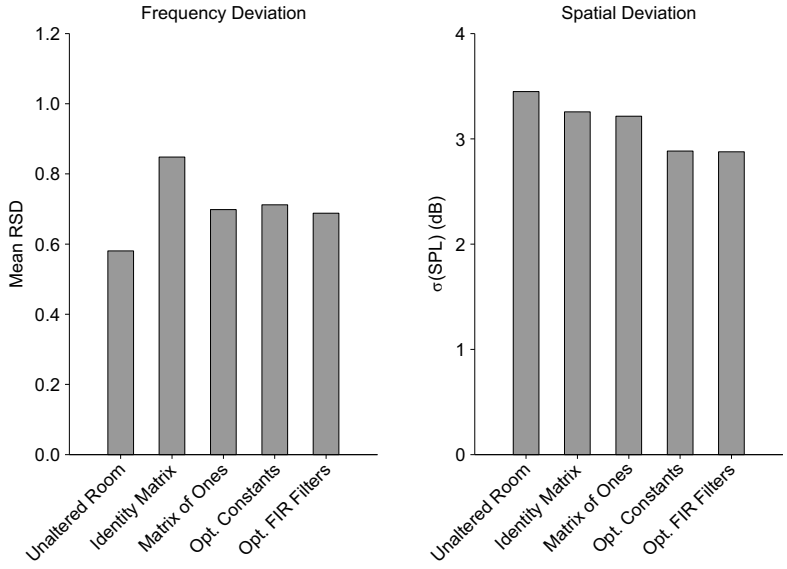

Figure 4.19: Simulated frequency deviations and spatial deviations for a system optimised to four source and 8 receiver positions which are positioned to allow simple practical application. The performance is measured over the 6 source and 30 microphone positions used in section 4.4.1 and Figure 4.17.

Optimising a system using the four secondary source and receiver positions and four additional receiver positions, placed 10 cm below the ceiling, should be implementable practically. The performance of this system, evaluated over the array of 6 sources and 30 receivers discussed in section 4.4.1, is shown in Figure 4.19. This shows that this system performs significantly worse than the system optimised to the 6 source and 30 receiver array as seen in Figure 4.17. This may be because of the low number of transducers or it could be that the positions are affecting the result.

4.4.4 Summary

The investigations in this section have shown that the number of source and receiver positions can significantly affect the resulting performance of the system. Particularly, it has been shown that optimising to a single primary source position may create poor performance for other source positions. In order to improve the global performance of the sound field, the system should be optimised to several primary source positions. Using six random source positions in the room has been shown to provide excellent performance.

The effect of changing the number of microphone positions has also been investigated. It has been found that the exact position of the microphones will affect the value of the performance metric. In order to compare a measurement between two different sets of microphone positions, a large number of microphones must be used to identify the correct trend. However, if the positions are used consistently, the trends are found with fewer microphones.

It has been shown that when measuring the variance over frequency, the correct trends can be identified with only two microphone positions. However, more positions are required when measuring spatial variations. It has been found that the correct trends can be identified with 16 microphone positions with slight improvements in precision as the number is increased. This may need to be altered for different rooms.

4.5 Summary

This chapter has sought to investigate the effect of a reverberation enhancement system on the modal response of a room. The motivation for this stems from the overall goal of this work which is to improve the performance of reverberation enhancement systems in rooms with relatively small volumes. These rooms have a Schroeder frequency well into the audible frequency range and therefore the band below that frequency should be considered when specifying the system.

The impact of a reverberation enhancement system on the modal response can be derived using the standard modal summation technique which was first introduced in section 1.1.1. This theory can be used to model both the frequency and time domain responses of the enclosure. It has been shown that the interaction of the reverberation enhancement system with the room response is more nuanced than in a diffuse field as the sound pressure level or reverberation time can be increased or decreased by the system depending on the frequency, positions of the transducers and feedback processing.

In order to assess the performance of the system, the modal response can be compared to a diffuse field response as it is assumed that this is closer to the desired enhanced room response. Two simple metrics have been defined which can be related to known properties of the diffuse field. Firstly, it is known that the pressure amplitude should be Rayleigh distributed over frequency in a diffuse field and this should create a relative standard deviation, the ratio of standard deviation to mean, equal to 0.52. Initial investigations showed that the modal response often had an RSD higher than this value. Therefore, the RSD over frequency was defined as one of the performance metrics with a lower value indicating better performance.

The spatial variation of SPL within a diffuse field is reasonably low and should ideally have a standard deviation of between 1 and 2 dB over a number microphone positions. In the modal sound field this will be higher. The standard deviation of SPL over position was defined as the second performance metric with a lower value indicating better performance. It was hypothesised that the performance of the system could be improved by altering the processing in the feedback loop.

Due to the complexity of the problem, an analytical solution could not be found and numerical optimisation using a gradient descent algorithm could not find a solution. In order to avoid this problem, an alternative numerical optimisation method was sought. The genetic algorithm was found to provide reasonable improvements in performance although it is not guaranteed to find the absolute global minimum. This has been subsequently used to optimise the processing in the system throughout the remainder of the chapter. The optimised parameters are either the constant coefficients of the feedback matrix or the coefficients of an array of FIR filters of order 8. The feedback gain of the system was set to ensure stability of the system.

The system has been optimised, initially, to the two performance metrics individually. These optimised systems have been compared against the measured performance of the unaltered room response and that created when a system is implemented using the “standard” feedback matrices: the identity matrix and the matrix of ones. It has been found that the standard matrices increase the frequency deviations above those observed in the unaltered room response. The optimised system significantly reduces these variations, with the system optimised FIR filters having lower frequency variation than the unaltered room.

The systems optimised to spatial variations show similar improvements in performance. The standard matrices show slightly lower spatial variation than the unaltered room with the optimised systems having lower variations again. The optimised systems were tested with a

set of microphone positions different from those used to optimise the system and similar levels of performance were observed which shows that global reductions in the spatial variation of the SPL have been achieved.

The time domain response of these systems was calculated and the reverberation time measured using the integrated impulse response method. As predicted in the analytical model, the reverberation time was shown to decrease for some systems, notably the system with an identity matrix, but increase dramatically with others. Significantly, the resultant reverberation time had no obvious correlation to the design of each system. As the underlying function of the reverberation enhancement system is to increase the reverberation time it would be useful to have control over the resultant reverberation time.

Following these initial investigations, the possibility of using alternative performance metrics has been considered. Most successful of these was the optimisation of the feedback processing to create a desired resultant reverberation time. It was found that the reverberation time could be set with a high degree of accuracy as long as the desired value was not too ambitious. Due to the stability limit of the system, the reverberation time could not be increased beyond a certain point.

It was found that the system optimised to create a specific reverberation time had poor performance in the other metrics which were used earlier in the chapter. Therefore a generic performance metric was defined which was an arithmetic sum of the three metrics mentioned above. It was found that the system optimised to this metric still achieved the desired reverberation time but with significant improvements in the frequency and spatial variations. These were not quite as good as the system optimised to the individual metrics but the overall performance of this system is a reasonable compromise between each of the metrics.

The simulations up to this point all featured a fixed primary source position and fixed number of measurement positions. This was out of necessity due to the large number of simulations which was being run. The effect of changing these quantities has also been investigated which should provide some insight into the measurement effort which would be required to perform this kind of optimisation in a real room.

It has been found that varying the primary source positions significantly affects the measured value of the performance metric, but that the trends are reasonably similar to those seen with a single primary source. However, the performance of the systems optimised using a single primary source is significantly reduced when they are measured using multiple primary source positions. It has been found that optimising to several primary source positions improves the global performance of the systems. Optimisation with 6 primary source

positions was found to create a more consistent change in the room response, although fewer may provide sufficient performance. A single primary source is not recommended due to the low robustness of the resulting system.

Following this, an investigation has been carried out into the effect of varying the number of measurement positions. It has been found that this does not significantly affect the measured performance in terms of frequency deviation but does have an effect on the measured spatial variation. It is important to note that the underlying trends can be identified with fewer microphones if their positions are used consistently between measurements. The correct trend for spatial variation is identified with between 16 and 32 measurement positions. Note that this was simulated using a single source position so the number of microphone positions will probably be lower than this number as it is the number of independent measurement paths which will determine the accuracy of the measurement.

The performance of a measurement system which could be realised reasonably easily has been investigated. This uses the transducers of the reverberation enhancement system with a handful of additional measurement positions. It has been shown that a system optimised using this measurement system provides reasonable performance when evaluated using a more thorough measurement system. Although these investigations have been carried out in simulation, this result implies that optimisation of a real system is practically realisable. However, there may be additional practical complications which have not been considered in this work.

This chapter has sought to improve the performance of a reverberation enhancement system in the modal sound field. It has been shown that numerical optimisation of the feedback processing of the system using a genetic algorithm can improve the performance of the system significantly. This allows the reverberation time of the room to be set and the frequency and spatial variations of the room response to be reduced. It has been shown that the optimised performance of the system is affected by the number and the positions of the transducers which are used to evaluate the performance during the optimisation. However, by following certain guidelines, global improvements in the room response can be achieved.

5 Diffusion and early energy

The performance of a reverberation enhancement system can be measured using a single parameter: the resulting reverberation time of the room. However this may not be sufficient to explain the complex behaviour of the room and its interaction with the reverberation enhancement system. As discussed in the previous chapter, the modal sound field may become important at low frequency. Even when considering the diffuse field frequency region, the room will not perform as an idealised diffuse field. This chapter will consider other characteristics of the room response other than the reverberation time and will analyse the effect of the reverberation enhancement system on these characteristics.

5.1 Diffusion of the sound field

The extent to which the sound field approximates a diffuse field can be called the "diffusion". Considering this feature of the sound field is especially important in a small room as it may already suffer from relatively poor diffusion. The introduction of a reverberation enhancement system may improve or degrade the diffusion of the sound field. This section seeks to observe this change in the diffusion.

Several quantities have been proposed for objective measurement of the diffusion. These are based on the properties of a theoretically ideal diffuse field. As discussed in section 1.1.2, the sound pressure level in a diffuse field should be independent of position and the intensity should be independent of direction i.e. the field is homogeneous and isotropic. Additionally the energy density should decay exponentially after a sound source is suddenly cut off. When the resulting decay trace is plotted on a decibel scale, it should be a straight line.

Several methods have been proposed which attempt to measure the degree to which a real sound field displays these properties (Bodlund, 1976). A naïve approach is to measure directly the spatial variation of sound pressure, the directional variation of intensity and the discrepancies of the decay trace from a straight line. As it is known that a room is only an approximation of an idealised diffuse field, it is expected that these measures will not be zero. In order to achieve a reliable measure of diffusion, these quantities can be compared to a prediction based on a more realistic analysis of a room response and the measurement equipment. This should allow a more consistent measurement and facilitate comparison between rooms.

A complementary pair of diffusion measures has been proposed which takes the ratio of a measured quantity to a predicted value based on the uncertainty of the measurement equipment and the statistical variations of a room response (Green et al., 2011). These

measures are the normalised standard deviation of reverberation time, NSDRT, (Davy, 1979) and the normalised standard deviation of level, NSDL. In each case the standard deviation of reverberation time or sound pressure level is measured across a number of microphones and this value is then normalised to the theoretical value.

These measures require a theoretically predicted value for the standard deviation of reverberation time and level in order to provide a reference for the normalisation. The expected standard deviation of reverberation time in a diffuse field can be calculated as

$$\sigma\left(T_{20}\right) = 0.88 T_{20} \sqrt{\frac{1+1.90/n}{NBT_{20}}} \tag{5.1.1}$$

where n is the number of decays averaged at each microphone position, N is the number of independent positions and B is the bandwidth. When using the integrated impulse response measurement, the value of n should be set to 10 (ISO3382-1, 2009). The value of NSDRT is the ratio of the sample standard deviation to the value given by equation (5.1.1).

To calculate the NSDL the measured standard deviation of sound pressure level between positions is normalised to the value predicted using the formula

$$\sigma\left(L\right) = \frac{4.34}{\sqrt{1+\frac{BT_{20}}{6.9}}} \tag{5.1.2}$$

which has been shown to have good agreement with measured values in reverberation chambers (Lubman, 1968). However, for rooms with higher levels of absorption, it has been suggested that the mean value over time of the standard deviation of instantaneous level of the decay trace be used in place of the simple standard deviation of sound pressure level. This is calculated by aligning the decay traces in time and finding the standard deviation of level at each time sample. The arithmetic mean is taken over time across each of the values of standard deviation. A time window of between 100-200 ms is usually chosen to average over (Green, 2011). Using this measured value as part of the NSDL has been shown to give closer agreement with experimental data (Chiles, 2004).

Some example decay traces are shown in Figure 5.1 using experimental data from the single channel system with 135 ms of delay as originally presented in section 2.2.3. These decay traces show significant curvature. As the amount of curvature is different for different positions, the measured reverberation time will differ between positions. This should be measured by the NSDRT which implies that this measure relates to the linearity of the decay trace. Additionally, it has been shown by Green (2011) that the NSDRT is affected by

uneven spatial distribution of absorbing or scattering elements. This result implies that the NSDRT should measure the isotropy of the sound.

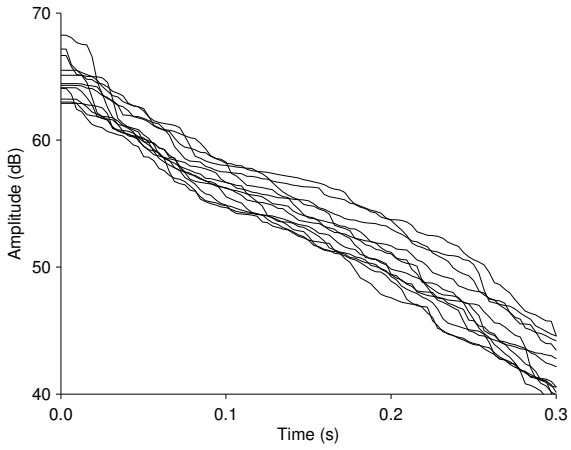

Figure 5.1: Decay traces measured at 12 independent positions using a single channel reverberation enhancement system with 138 ms of delay in the feedback loop.

The decay traces in Figure 5.1 also show some large steps which correspond to strong early reflections in the impulse response. As the NSDL measure used here is based on the standard deviation of instantaneous level, it will be affected by these reflections. This means that the NSDL not only measures the homogeneity of the sound but also the degree of short term deviation of the decay traces from linearity. This is supported by previous experimental work (Green, 2011). Combining the NSDRT and the NSDL should give a good picture of the state of diffusion of the sound field.

This section investigates the changes in NSDRT and NSDL which occur when a reverberation enhancement system is introduced. Equations (5.1.1) and (5.1.2) show that the value of standard deviation of reverberation time is expected to increase with increasing reverberation time whilst the standard deviation of level should decrease. The normalised values should reveal whether these expectations are fulfilled and if not then these measures will show that the system has altered the reverberation time without the expected change in diffusion.

5.1.1 Diffusion analysis of the experimental data

The experimental results discussed in sections 2.1.4 and 2.2.3 can be used to test the effects of the reverberation enhancement system on the diffusion of the sound field. These experimental results show that the measures NSDRT and NSDL are highly variable. The

uncertainty in these measures is a significant proportion of the mean value. This means that it is difficult to identify trends with changing reverberation time.

If the data are analysed in individual octave bands, the correlation is low and the p-value is high. This implies that there is a significant statistical possibility that the observed trends occur by chance. This is because of the high uncertainty in the measures and the relatively low number of observations. However, the data from separate octave bands can be taken as independent points within the same dataset and which significantly increases the effective number of observations. These results are shown in Figure 5.2 for systems with electronic reverberation and Figure 5.3 for systems with delay. Results are shown for the octave bands 250 Hz through to 2 kHz. The Schroeder frequency of the room is approximately 150 Hz so the results for the 125 Hz octave band and below have been ignored. Note that values of NSDRT and NSDL greater than unity indicate there is greater than expected spatial variation.

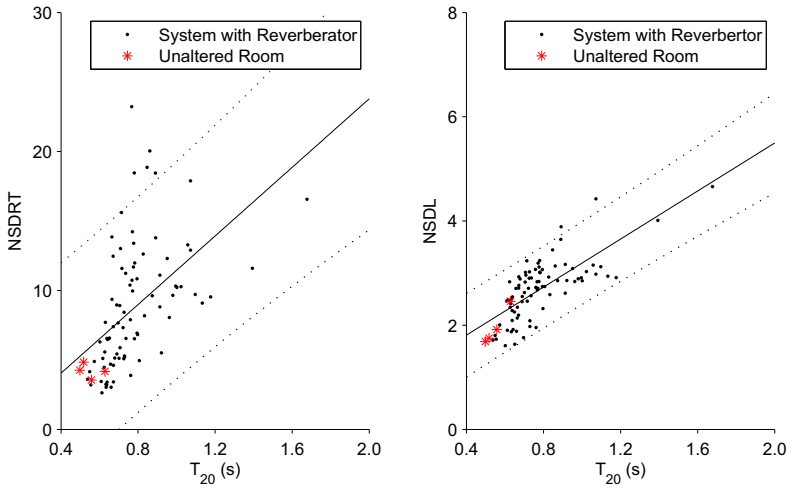

Figure 5.2: Measured values of (a) NSDRT and (b) NSDL for various values of reverberation time caused by a reverberation enhancement system with electronic reverberation. A line of best fit is shown, solid line, with 95% confidence intervals, dotted. These values are taken from 4 octave bands, hence there are 4 points for the unaltered room.

The results show significant increases in both the NSDRT and the NSDL as the reverberation time is increased. The value of correlation coefficient for the NSDRT in Figure 5.2 (a) is 0.52, which indicates reasonably poor correlation; however the p-value is 2×10^{-7} which shows that this correlation is unlikely to have occurred simply due to chance. This implies that there is a definite increase in the NSDRT with increasing reverberation time, which indicates a reduction in diffusion. The correlation coefficient for the NSDL in Figure 5.2 (b) is 0.74 and the p-value is 9×10^{-17} which indicates much better evidence of a correlation between the reverberation time and the NSDL. This also implies a reduction in

diffusion as the reverberation time is increased. Similar results are found for the system including delay shown in Figure 5.3 with correlation coefficients of 0.46 and 0.42 and p-values of 2×10^{-6} and 2×10^{-5} for the NSDRT and NSDL respectively.

The increase in reverberation time is caused by lengthening the reverberation time or delay time of the processing in the reverberation enhancement system. This implies that these methods of improving the performance of the system come at the cost of a reduction in the diffusion of the sound field. As discussed above, the NSDRT and NSDL can be related to the linearity of the decay trace and the presence of strong early reflections, respectively. It seems that the system with reverberation affects the NSDRT more whereas the system with delay has a greater effect on the NSDL. This may imply that the system with reverberation causes greater curvature of the decay trace whilst the system with delay introduces a significant early reflection. Drawing these conclusions may be unwise due to the high degree of variation in these quantities, however, these results show that there is a measureable increase in the NSDRT and NSDL as the reverberation time is increased through the use of reverberation enhancement.

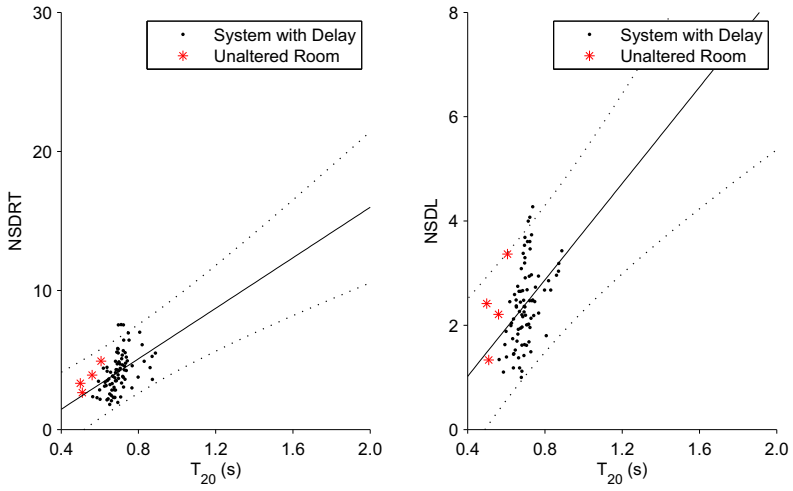

Figure 5.3: Measured values of (a) NSDRT and (b) NSDL for various values of reverberation time caused by a reverberation enhancement system with delay. A line of best fit is shown, solid line, with 95% confidence intervals, dotted. These values are taken from 4 octave bands, hence there are 4 points for the unaltered room. The axes limits are set to match Figure 5.2.

The link between the measures of diffusion and the characteristics of the decay trace can be shown through further analysis of these experimental results. The decay traces in the 1 kHz band of the systems with delay, which show the lowest and highest values of NSDRT, are given in Figure 5.4. The decay traces related to the low value of NSDRT are shown in the left hand plot and correspond to a value of 78 ms of delay used in the system processing. The

plot on the right shows the decay traces of the system with 139 ms of delay which causes a high value of NSDRT.

In each plot, the traces which correspond to the longest and shortest reverberation times of the 12 measurements positions are shown as dotted and solid lines respectively. The two decay traces for the system with a low value of NSDRT are nearly parallel, indicating a consistent reverberation time across positions. However, the system with a high value of NSDRT has decay traces which cross and this is due to the curvature of the decay trace.

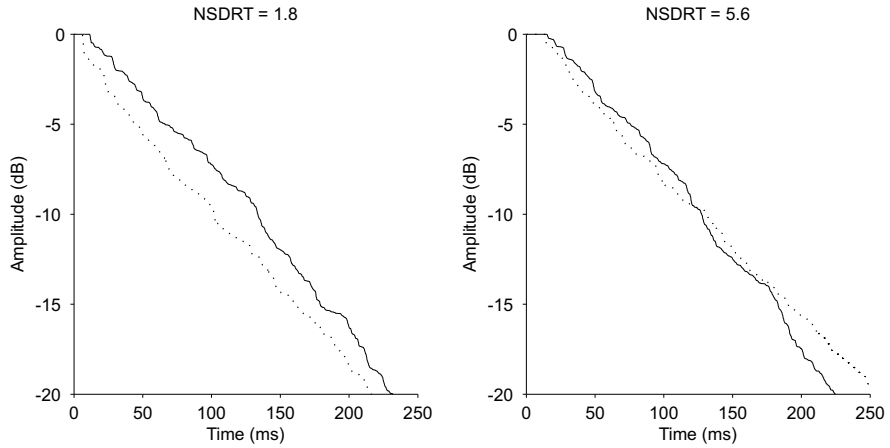

Figure 5.4: Decay traces in the 1 kHz octave band for the systems with delay which have the lowest (a) and highest (b) values of NSDRT. The solid lines show the position which has the lowest measured reverberation time whilst the dotted line shows the position with the longest.

The two decay traces in Figure 5.4 (b) seem to have opposite curvature, i.e. the solid line has a gradient which increases with time where the gradient of the dotted line decreases. This implies that a low value of NSDRT may be observed if the decay traces were curved consistently over position. Therefore, it could be more accurate to link a rise in NSDRT to a reduction in the isotropy of the sound field which manifests itself as curvature of the decay trace. In this case, these results imply that, while a set of curved decay traces does not necessarily cause a high value of NSDRT, a high value would indicate that the set of decay traces is likely to feature some curvature.

Strong early reflections, or a total lack thereof, are thought to be related to high values of NSDL. The decay traces for the systems including delay with the highest and lowest values of NSDL are shown in Figure 5.5. In this case the trace with the highest mean level is shown as a dotted line whereas the solid line shows the trace with the lowest mean level. In both of these plots the gradients of the main part of the curve, where the T_{20} is evaluated, have similar gradients.

The difference in level between the two curves, in each case, is caused mainly by the extent of the early reflections. The early reflections are most important in the first 5 dB of decay. It can be seen in Figure 5.5 (b) that the system with a high value of NSDL has a large difference in the gradients of the decay traces in the first 5 dB of decay. The difference between the decay traces in the first 5 dB of decay is much smaller for the system with low NSDL seen in Figure 5.5 (a). This can also be described as a curvature of the decay trace but it is specifically isolated to the early part of the impulse response. Therefore, these results show that the NSDL is most strongly affected by curvature of the early part of the decay trace which relates to uneven early reflections.

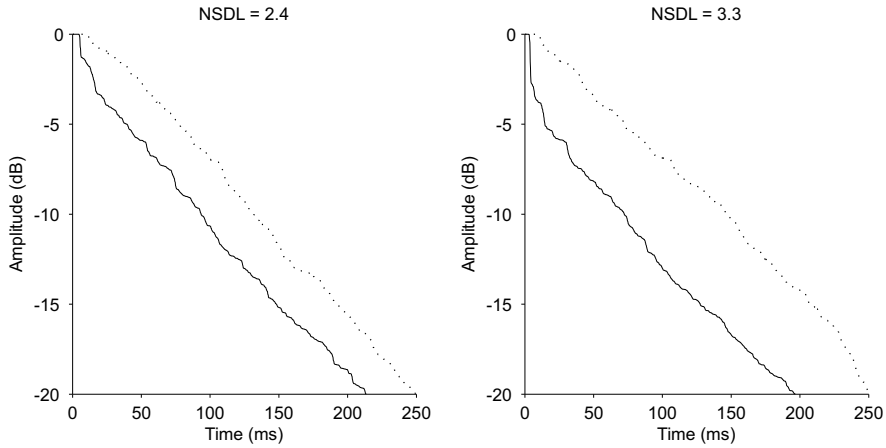

Figure 5.5: Decay traces in the 1 kHz octave band for the system with delay which have the lowest (a) and highest (b) values of NSDL. The solid lines show the position which has the lowest mean level whilst the dotted line shows the positions with the highest.

5.1.2 Simulation of diffusion

By using the simulation routine discussed in earlier chapters, see section 2.1.3, a large number of diffusion 'measurements' can be made with a wide variety of reverberation enhancement system configurations. The ease with which a large number of 'measurements' can be made allows the underlying trends to be more easily identified despite the inherent variability of the diffusion measures. This simulation can also be used to compare the performance of the systems with delay or with an electronic reverberator.

The simulation used here is identical to that used in chapter 2. The system consists of 4 channels and all of the transfer functions are modelled as exponentially decaying white noise implemented as an FIR filter. The unaltered reverberation time of the room is set to 0.53 s as this is the same value as the room used in the experiments shown above. The processing in the feedback loop is either a simple delay or a reverberator. Different values of delay time or

reverberation time, respectively, are used to alter the resultant reverberation time. The NSDRT and NSDL are measured across 6 virtual microphone positions.

To observe the change in NSDRT and NSDL more easily, a wider range of resultant reverberation times has been simulated. The system has been modelled including delay times of between 10 ms and 300 ms which causes resultant reverberation times in the 500 Hz band of between 0.56 s and 1.45 s. Similarly, the reverberation time of the reverberator is set to values between 0.05 s and 1.59 s. The reverberation time of the room then changes to values between 0.56 s and 1.54 s.

The standard deviation of reverberation time, over the 6 virtual microphone positions, should then be 0.06 s to 0.10 s. As this change is significantly larger than that observed in the experimental results of the previous section it should be easier to observe deviations from this value measured using the NSDRT. Additionally, many more values of delay time and reverberation time than were tested experimentally are used for the processing within the defined range which should allow greater precision when evaluating the changes in the diffusion measures.

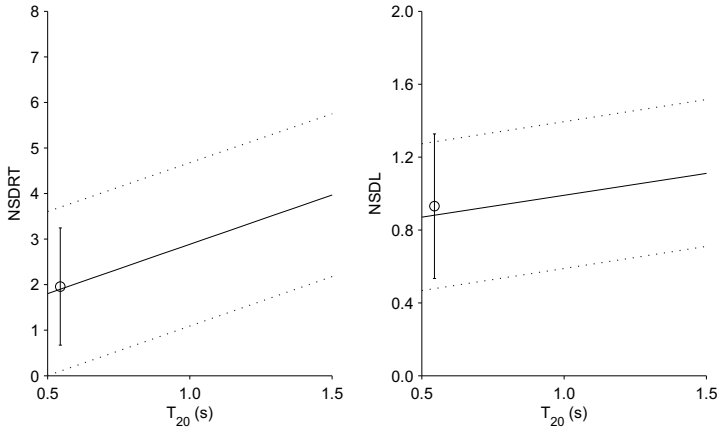

Figure 5.6: Simulated values of (a) NSDRT and (b) NSDL for a 4 channel system with delay in the feedback loop. The reverberation time is increased by increasing the delay time whilst the feedback gain is fixed. The line of best fit is shown as a solid line with 95% confidence intervals shown as dashed lines. The circular point with errorbars shows the mean value and confidence interval for the unaltered room.

The results shown in Figure 5.6 relate to a system with delay in the feedback loop. The individual data points are not shown as there are too many for clear visualisation. This figure shows clear increases in the NSDRT and NSDL with increasing reverberation time corroborating the experimental results given above. However, the gradient of the lines of best fit is much greater for the experimental results than for the simulations shown here. The

reason for this discrepancy is not immediately obvious as it may be a flaw in the simulation routine or an inherent property of the room used for the experiment.

The results for the system using an electronic reverberator are shown in Figure 5.7. Similar to the results for the system with delay, increasing the reverberation time increases the measured value of NSDRT and NSDL. This implies that both systems reduce the diffusion of the sound field. Whilst the trends for NSDL are very similar between the two systems, the system with electronic reverberation does not increase the NSDRT as much as the system with delay for a given change in mean reverberation time.

As the NSDRT is related to the linearity of the decay trace, this result would imply that the system with delay causes greater curvature of the decay trace for an equivalent value of resultant reverberation time. This would contradict the trends observed in the experimental results. In all likelihood, this discrepancy is due to the condition of diffusion of the unaltered room in which the experiments were conducted rather than an underlying property of either reverberation enhancement system.

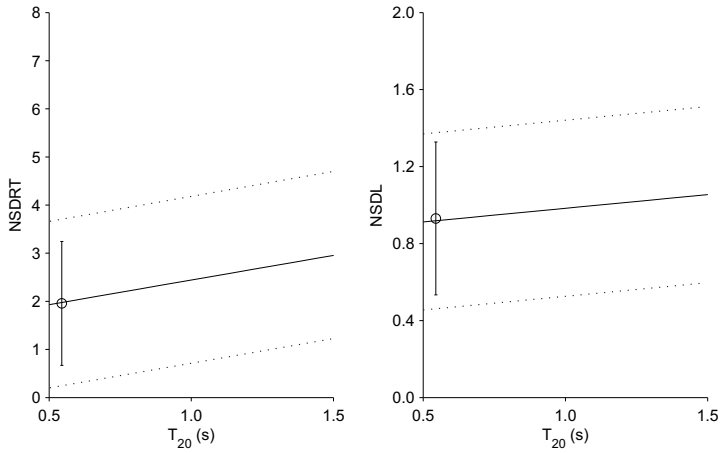

Figure 5.7: Simulated values of (a) NSDRT and (b) NSDL for a 4 channel system with an electronic reverberator in the feedback loop. The meaning of the different line styles is identical to Figure 5.6.

5.1.3 Relationship of diffusion to subjective preference

Although it is generally accepted that diffusion is a desirable property of the sound field, the subjective perception of the measures used in this section, NSDRT and NSDL, is worth considering. A subjective experiment is beyond the scope of this work but previous work on the perceptible differences of sound pressure level and reverberation time may be used to interpret the results from this section. The values predicted by equations (5.1.1) and (5.1.2) are relatively low for any reasonable values of reverberation time and may be imperceptible.

With larger values of NSDRT and NSDL the changes in reverberation time and level between positions may become noticeable.

It has been shown that the just noticeable difference (JND) in reverberation time is approximately 4% of the initial reverberation time with a minimum of 0.024 s for low reverberation times (Cremer and Muller, 1982). This result was derived by having subjects listen to the raw impulse responses so the sensitivity is likely to be different with other programme material. The values given by equation (5.1.1) are generally lower than the JND. This is illustrated in Figure 5.8 (a). Each dotted line shows the difference in reverberation time between two positions which would cause the value of NSDRT indicated by the text adjacent to each line on the figure if it had been calculated from only those two positions. This is found by calculating the value of expected standard deviation from equation (5.1.1), multiplying by the required value of NSDRT and then, due to the definition of standard deviation, dividing by the square root of two. The solid line shows the JND varying with reverberation time. This figure implies that, if the NSDRT is equal to 2, the differences in reverberation time between positions in a room will not be perceivable.

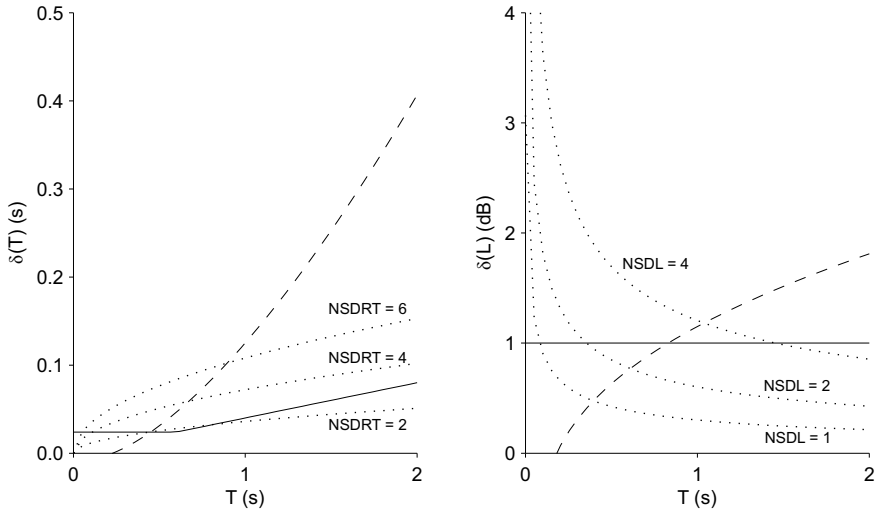

Figure 5.8: Estimated difference between 2 positions of the reverberation time (a) and sound pressure level (b), dotted lines, compared against the just noticeable difference, solid line. Values of the estimated difference are shown for various values of NSDRT and NSDL which were observed experimentally in section 5.1.1. The dashed lines show the expected difference between positions with values of NSDRT and NSDL which vary with the reverberation time according to the lines of best fit from Figure 5.3.

When the sound field has a greater value of NSDRT, there is greater variation between positions. It could, therefore, be hypothesised that for large values of NSDRT the spatial variation of reverberation time would be noticeable. Figure 5.8 would imply that an NSDRT of 4 would create enough spatial variation to be noticeable. This is not a desirable quality for

a room response. However, it is difficult to assess, without extensive subjective testing, the point at which the spatial variance of reverberation time becomes noticeable or unacceptable.

Without investigating the subjective effects, recommendations can be made assuming the worst case scenario. In this case, an NSDRT of lower than 4 is required. The line of best fit for the experimental results given in Figure 5.3 (a) shows an increase in the NSDRT from 2.6, for the unaltered mid-frequency reverberation time of 0.53 s, to 4.7 for the maximum observed value of mid-frequency reverberation time: 0.75 s. Limiting the maximum value of NSDRT to 4 would restrict the maximum useable resultant reverberation time to 0.69 s.

The dashed line in Figure 5.8 (a) shows the expected difference in reverberation time between positions when the value of NSDRT varies according to the line of best fit shown in Figure 5.3 (a). From this it seems that, even with the unaltered reverberation time of 0.53 s, the difference in reverberation time between positions may be noticeable. The limitation of NSDRT to 4 occurs at the point where the dashed line crosses the middle dotted line which corresponds to that value of NSDRT. At this point the spatial variation is only slightly higher than the JND so therefore it should be acceptable subjectively.

The just noticeable difference of sound pressure level is highly dependent on the nature of the signal; both the frequency content and the initial amplitude affect the JND significantly. For example, at an initial SPL of 30 dB, at 3 dB change is required to notice a difference in the level of a 1 kHz sine wave. But if the same tone has an initial SPL of 80 dB, the ear can detect a change of merely 0.3 dB (Howard and Angus, 2009). For the purposes of this section a value of 1 dB will be used as a rule of thumb.

As can be seen in Figure 5.8 (b), which is created with the same method as Figure 5.8 (a) but using the NSDL, the predicted level difference between two positions is significantly lower than 1 dB for all realistic values of reverberation time when the NSDL is equal to unity. For higher values of NSDL, however, the difference in level between positions may become noticeable. As the expected level difference between positions decreases with increasing reverberation time, it is not as simple to set an upper limit for the NSDL as it was for the NSDRT.

The dashed line in Figure 5.8 (b) shows the expected difference in level between positions with a value of NSDL which varies with mean reverberation time according to the line of best fit shown in Figure 5.3 (b). This crosses the threshold of 1 dB at a reverberation time of approximately 0.8 s which implies that, above this value of reverberation time, the spatial variation of SPL would be noticeable. As this value of reverberation time is higher than the

maximum value which was observed experimentally, it seems unlikely that any difference in level between positions would be perceived for the system tested in section 5.1.1.

The values of NSDRT and NSDL which cause a predicted difference between positions which equals the JND are shown in Figure 5.9. This implies that the limits for these parameters are reasonably similar. Ideally, the NSDRT and NSDL should be lower than 2 as this would guarantee an imperceptible spatial variation of reverberation time and level. Even higher values may be acceptable if a different model of the JND is used.

An alternative measurement of the JND of reverberation time has been made using anechoic recordings of musical phrases affected by a processor with variable reverberation time (Meng et al., 2006). This experiment showed a JND of reverberation time of 26%. Comparing this value to the predicted difference of reverberation time between positions would imply that the spatial variations of reverberation time would be inaudible for all values of NSDRT which have been observed experimentally in this section. In this case, the NSDRT could have a value greater than 4, increasing with greater mean reverberation time, in order for spatial variation of reverberation time to be just noticeable.

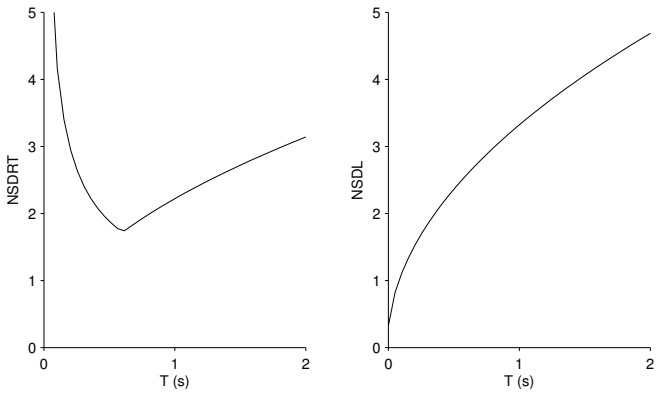

Figure 5.9: Value of NSDRT (a) and NSDL (b) which causes an expected spatial variation of reverberation time or level, respectively, equal to the JND.

In terms of the spatial variations of level, alternative values for the noticeable difference could be used. If the JND of SPL was assumed to be 0.3 dB, as mentioned above for a 1 kHz tone with initial SPL of 80 dB, the values in Figure 5.9 (b) would simply scale by 0.3 implying that a much more stringent condition must be met. In this case, the NSDL would need to be unity or lower. Additionally, it can be imagined that for a speech or music signal, which contain continuous changes in level, the audibility of the spatial variation of level caused by the room will be different from that found using steady state tones or broadband noise.

Clearly, the condition which is selected will have a major effect on the recommendations for restricting the maximum value of NSDRT and NSDL. Assuming the worst case scenario, a value of less than 2 for the NSDRT and NSDL is desirable. However, the results discussed here imply that higher values are unlikely to be audible especially when the signal is programme material and not a test signal such as an impulse or a sine wave. Therefore, values of NSDRT and NSDL of up to 3 should be acceptable when the mean reverberation time is less than 1 s increasing to 5 when the reverberation time is above 1 s.

5.1.4 Discussion of the utility of the measures of diffusion

This section has investigated the use of the NSDRT and NSDL as measures of the diffusion of the sound field within the context of reverberation enhancement. This should give insight into the effect that the system has on the sound field in addition to that which can be gained through measuring the reverberation time. It has been observed in experiments and numerical simulations that the values of these measures increase when the reverberation time is increased through the use of reverberation enhancement. This implies a reduction in the diffusion of the sound field.

It has been shown that the NSDRT is related to the linearity of the decay trace, which is in turn related to the isotropy of the sound field. This could be affected, for instance, by uneven placement of absorbent material (Green, 2011). The NSDL on the other hand is affected by short term discrepancies in the decay trace which can be attributed to the presence of strong, specular early reflections. This relates to the homogeneity of the sound field and could be caused by a lack of diffusing elements (Green, 2011).

In terms of the reverberation enhancement system, it is known that the decay trace may become curved. Using the NSDRT allows the curvature to be assessed without scrutinising the individual decay traces. Another issue with reverberation enhancement systems, especially those applied in small rooms, is the acceptable number of channels. With a small channel count, the sound field may become more spatially varied and this would be indicated by the measured diffusion. Therefore, these measures may be used to check the acceptable channel count beyond the simple goal of achieving a particular reverberation time.

It has also been shown in this section that the diffusion measures can be related to the just noticeable difference of reverberation time and sound pressure level. In this way, they can be used to assess whether a person would be able to hear differences in these quantities between positions in the room. As the JNDs are dependent on the programme material, an absolute limit is not easily defined but guidelines can be recommended. Ideally, the NSDRT and

NSDL would have values of 2 or below. However, it is probably acceptable for the value to reach 4 or even greater if the mean value of reverberation time is high.

This section has shown that the estimated state of diffusion, quantified using the NSDRT and NSDL, can be useful for evaluating the sound field. Properties of the room response are revealed which would otherwise be difficult to measure. This is especially useful in the context of reverberation enhancement, where the sound field is altered artificially. By using the measures of diffusion, the resultant sound field can be compared directly with that which would be expected in a room and this will give a good indication of the performance of the system in simulating a new sound field.

5.2 Early energy in the impulse response

The reverberation time is the parameter most commonly used to characterise the response of the room. As this quantity is measured over a large portion of the decay trace, it is not sensitive to the early part of the impulse response. However, as mentioned in section 1.1.2, this part of the impulse response is important subjectively (ISO3382-1, 2009). There are two main methods for measuring the early part of the impulse response. The first is the early decay time which measures the slope of the decay trace over its first 10 dB of decay. The time taken for this decay interval is multiplied by 6 in order to facilitate comparison with the reverberation time.

The other important consideration is the amount of energy in the early part of the impulse response which can be measured in several ways. The clarity is the ratio, in decibels, of the energy in the first 50 or 80 ms of the impulse response to that in the remainder. With a time limit of 80 ms, the clarity is calculated as

$$C_{80} = 10\log_{10}\left(\int_{0}^{0.08} p^2(t)\,\mathrm{d}t \Big/ \int_{0.08}^{\infty} p^2(t)\,\mathrm{d}t \right) \tag{5.2.1}$$

where p, in this case, refers to the impulse response. A similar measure is the definition which is the ratio of the energy in the first 50 ms against the total energy of the impulse. This is directly related to the clarity and it is therefore unnecessary to measure both quantities (ISO3382-2, 2008).

If the decay trace of the room is linear, then these quantities can be found directly from the reverberation time. The EDT will equal the reverberation time and the clarity will be

$$C_{80,\mathrm{lin}} = 10\log_{10}\left[\exp\left(\frac{1.104}{T}\right)-1\right] \tag{5.2.2}$$

which is illustrated in Figure 5.10. This shows that, for most rooms with fairly linear decay traces, the clarity should have a value between −10 dB and 20 dB. Clearly, if decay traces were almost always linear then there would be no reason to measure either EDT or C_{80}. Therefore, by comparing the observed EDT or C_{80} with that predicted by a linear decay, some measure of the curvature of the decay trace may be achieved.

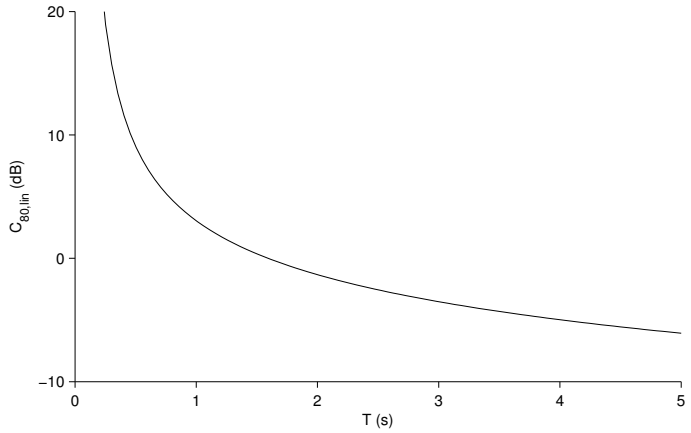

Figure 5.10: Values of clarity which would occur if the decay trace was linear for various values of reverberation time.

5.2.1 Preferred values for early decay time and clarity

Recommended ideal values of reverberation time, early decay time and clarity ratio are given by Beranek (1996). For orchestral music the recommended values of mid-frequency reverberation time are given for occupied concert halls as 1.8 to 2.1 s. These values are found from measured data in concert halls which are subjectively highly rated by musicians and conductors. The ideal values of early decay time and clarity are given for unoccupied halls as 2.2 to 2.6 s and −3.0 to 0.0 dB respectively. Values of EDT and C_{80} for occupied halls are not widely available. In order to compare these ideal values to these predicted by a linear decay, the values of EDT and C_{80} in occupied halls should be estimated.

Relations between occupied and unoccupied quantities are given by Hidaka et al. (Hidaka et al., 2001) where the regression coefficients have been calculated from measured data. The regression coefficients used here are mean values over the octave bands between 125 and 1000 Hz. The occupied early decay time is calculated as

$$EDT_{occ} = 0.57 EDT_{unocc} + 0.41 \quad (5.2.3)$$

which gives recommended occupied early decay times of between 1.7 and 1.9 s. The equivalent calculation for the clarity ratio is

$$C_{occ} = 0.88 C_{unocc} + 1.29 \quad (5.2.4)$$

such that the recommended occupied clarity ratio is between −1.4 and 1.3 dB. If the decay was linear then the clarity, calculated directly from the recommended reverberation times, would be between −1.6 and −0.7 dB.

These recommended values relate specifically to concert halls designed for classical music, but the general trends can be applied to other situations. The recommended EDT is approximately 90% of the reverberation time and the clarity is between 0 and 2 dB higher than that predicted from a linear decay. Therefore the recommendations can be interpreted as requiring an EDT which is as close as possible to the reverberation time and a clarity which is higher than that expected from a linear decay.

These recommendations have been derived for concert halls designed for orchestral music. For other programmes, there are different requirements for the optimal reverberation time. Venues intended for speech and drama require the lowest reverberation time, between 0.5 and 1 s, whilst traditional churches need significantly longer reverberation time, from 2 to 5 s, in order properly to support sacred choral or organ music (Cremer and Muller, 1982). Halls designed for opera have a slightly lower reverberation time than those used for orchestral music, between 1 and 1.5 s.

In these cases the requirements of early energy may also be different to those for orchestral music. Although it would be useful if a reverberation enhancement system could cater for all of these eventualities, discussion of all of these is beyond the scope of this work. For the purposes of this section, the recommended values for orchestral music shall be used. It should be noted, however, that this is not the only possible use of the technology and that different requirements may be introduced depending on the application. For the remainder of this section it will be assumed that the EDT and clarity should be as high as possible and the absolute minimum is, for the EDT, 90% of the reverberation time and, for the clarity, that which would be expected from a linear decay.

5.2.2 Early decay time and reverberation enhancement

As discussed above, the early decay time is a crucial parameter when considering the subjective quality of a room response. Therefore, it should be used when measuring the

performance of a reverberation enhancement system. The systems including electronic reverberation have been shown, in section 2.1, to allow large increases in reverberation time. Several commercial applications of this configuration include a separate in-line system designed to enhance the early energy implying some deficiency in the non-in-line system, see section 1.2.3. In order to test the limitations of the non-in-line part of the system, the results from section 2.1 can be reanalysed using the early decay time.

The simulations in section 2.1.3 showed that significant increases in reverberation time were caused by the system including electronic reverberation with greater increases with larger values of γ, the ratio of the reverberation time of the processor to that of the unaltered room. This cannot be increased indefinitely as the decay trace is expected to be double sloped when $\gamma > \gamma_{max}$ which is subjectively undesirable. The value of γ_{max} for this simulation, calculated using equation (2.1.11), was 1.19.

When $\gamma < \gamma_{max}$ the decay trace should be linear and the EDT should be approximately equal to the reverberation time. If this were the case, the EDT should be equal to the reverberation times predicted using equation (2.1.8) which was found to agree well with the simulated reverberation times when $\gamma < \gamma_{max}$. This equation only uses one of the two decay terms of the predicted decay trace. It was found that evaluating the reverberation time from the predicted two-term decay trace gave better agreement with the simulation results when $\gamma > \gamma_{max}$. The EDT could also be predicted using this method.

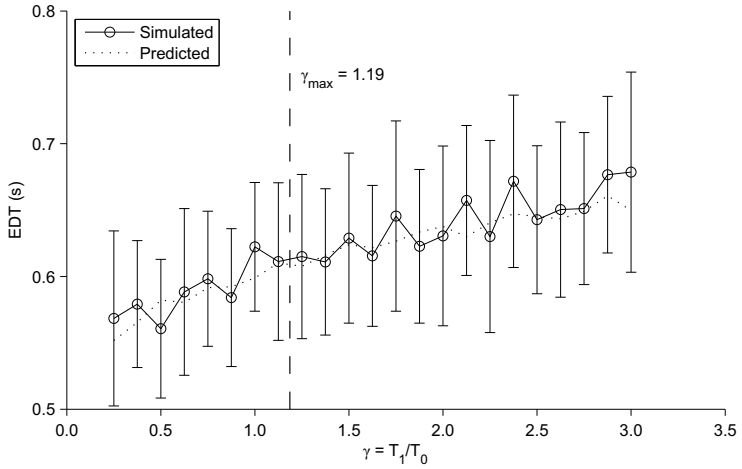

Figure 5.11: Simulated values of EDT for a 4 channel system including electronic reverberation time. This system is simulated with various values of reverberation time of the processor. The unaltered EDT is 0.5 s. The predicted values, dotted line, are evaluated from the analytically predicted decay trace with two decaying exponentials. The value of γ_{max} is shown as a dashed vertical line.

The simulated values of EDT are shown in Figure 5.11 for various values of γ showing some increase in the EDT with increasing γ. Comparing this figure with Figure 2.4, where the predicted values are based on equation (2.1.8), show that even below γ_{max} the reverberation time is significantly higher than the EDT which implies a curved decay trace. This also means that the values from equation (2.1.8) are poor predictors of the EDT. The predicted values shown as a dotted line in Figure 5.11 are those evaluated from the two-term decay trace which show good agreement with the simulated values.

The errorbars in Figure 5.11 are much larger than those for the reverberation time seen in Figure 2.4. As the impulse responses in this simulation are based on exponentially decaying white noise the large variations of these values cannot be linked to a spatial variation of early reflections which may be the case for experimental data. However, the variations do highlight that the shorter time span over which the EDT is evaluated causes much greater uncertainty in the measurement.

The degree of curvature of the decay trace can be assessed using the ratio of EDT to reverberation time as shown in Figure 5.12. As mentioned above, the minimum recommend EDT is 90% of the reverberation time, which is shown in the figure as a dotted horizontal line. This shows that the EDT is too low for all values of γ above 0.8. As this value is lower than γ_{max} a more stringent upper limit for γ may be required when there is no additional system which can separately enhance the early energy. At γ_{max} the ratio of EDT/T is approximately 80%.

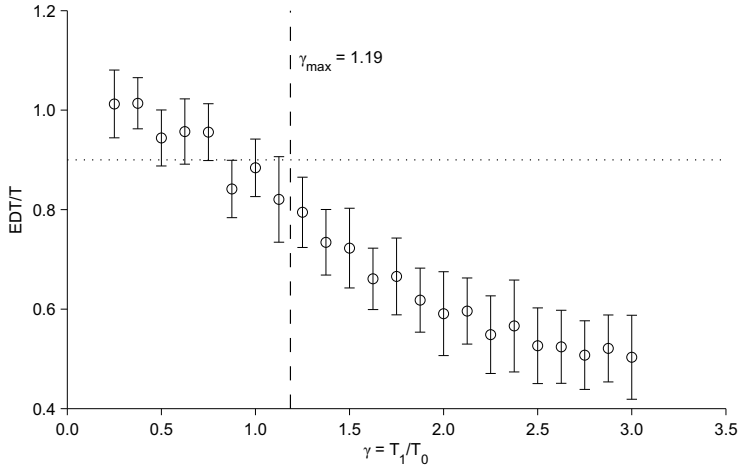

Figure 5.12: Ratio of EDT to reverberation time from a simulated 4 channel system with electronic reverberation. The dotted line shows the minimum recommended value of EDT and the dashed line shows the value of γ_{max}, below which the decay trace should be linear.

The performance of the system including delay, which was introduced in section 2.2, can also be assessed using the early decay time. Both the simulation results and those from the experiment can be used. The analysis from section 2.2.1 predicted that the resultant decay trace would be linear but the experimental results, such as those in Figure 5.1, show that this is not necessarily the case.

The simulated reverberation times of the system including delay in the feedback loop are shown in Figure 2.9. As the length of the delay is increased, the resultant reverberation time is also increased. The reverberation times predicted using equation (2.2.7) agree well with the values found by the simulation. The simulated early decay times can be seen in Figure 5.13. These values are higher than the unaltered 'room' but they do not change with the value of delay. As the reverberation time is increasing whilst the EDT remains constant the decay trace must become curved with greater curvature at higher values of delay. This also shows that the EDT cannot be predicted from equation (2.2.7).

The predicted values shown in Figure 5.13 ignore the delay in the system and use equation (1.2.2) which agrees well with the simulated early decay times. This result implies that the early energy is affected as if the system had no delay. It may be expected that with a delay longer than the time window over which the EDT is measured, the system should have no effect at all and the resultant EDT may decrease compared with the value observed for smaller values of delay. For the system with an unaltered EDT of 0.3 s, the −10 dB point should occur at 0.05 s. These simulation results show that even with a delay larger than the EDT time window, the EDT is still increased by the same amount as for smaller values of delay.

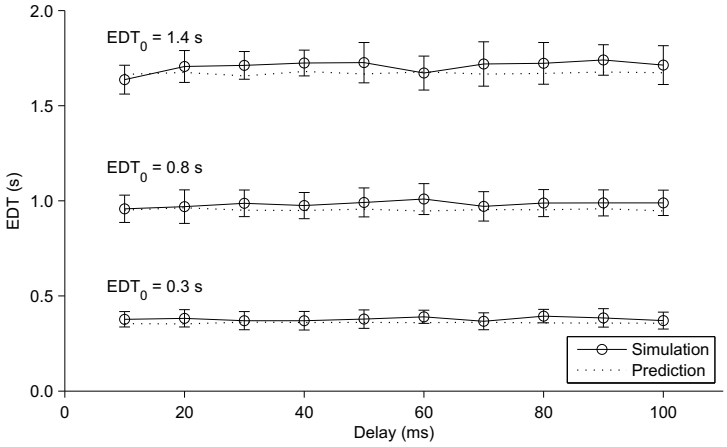

Figure 5.13: Simulated early decay times for a 4 channel system including delay in the feedback loop for three different values of unaltered EDT. The dotted lines show values predicted assuming no delay by using equation (1.2.2).

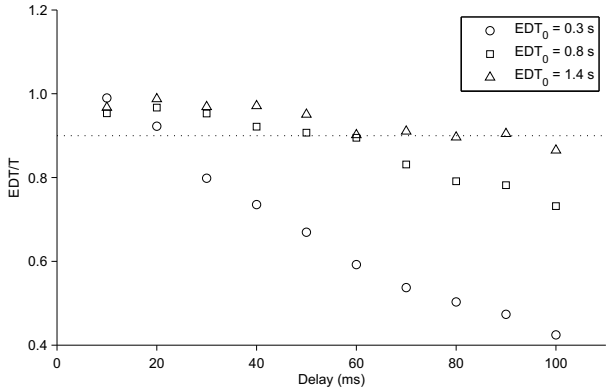

Figure 5.14: Simulated values of the ratio of EDT to reverberation time for a 4 channel system including delay. Three different values of unaltered EDT were simulated. The horizontal dotted line shows the minimum recommended value of this quantity. Errorbars have been omitted from this figure for the sake of clarity.

The ratio of EDT to reverberation time for this simulated system is shown in Figure 5.14. The ratio is near unity for small values of delay, showing that the EDT is nearly equal to the reverberation time. As the delay is increased, the ratio decreases because the reverberation time is increased but, as seen in Figure 5.13, the early decay time stays constant. This effect is exaggerated for the system with low unaltered reverberation time as this has the largest increases in reverberation time.

The dotted line in Figure 5.14 indicates the minimum recommended value of EDT. This shows that for large values of delay, the resultant response may be subjectively unacceptable. The value of delay at which the ratio becomes less than 90% depends on the unaltered reverberation time. From the figure it seems that the maximum allowable delay, for this particular system configuration, is approximately

$$\tau_{\max} = 0.06T \tag{5.2.5}$$

where $\tau_{\max}$ is the estimated maximum value of delay which would create a subjectively acceptable resultant room response. For the four channel system of this simulation, this value of delay would cause a reverberation time gain of 1.41 where the same system without delay would cause a gain of 1.19. Whilst this is a useful increase in performance, it is not as great as would be expected by simply looking at the resultant reverberation times in Figure 2.9.

The experimental results from sections 2.1.4 and 2.2.3 can also be reanalysed to test the effect of the system on the EDT. These results are given in Figure 5.15 and Figure 5.16, respectively. The system with electronic reverberation shows a slight increase from the unaltered value. Changing the reverberation time of the processor does not significantly change the EDT. The predicted values, calculated using the two term decay mode, rise

slightly with γ but this is not reflected in the measured result. However, as the spatial variation of EDT is much larger than the predicted change, it is unsurprising that the trend is not observed.

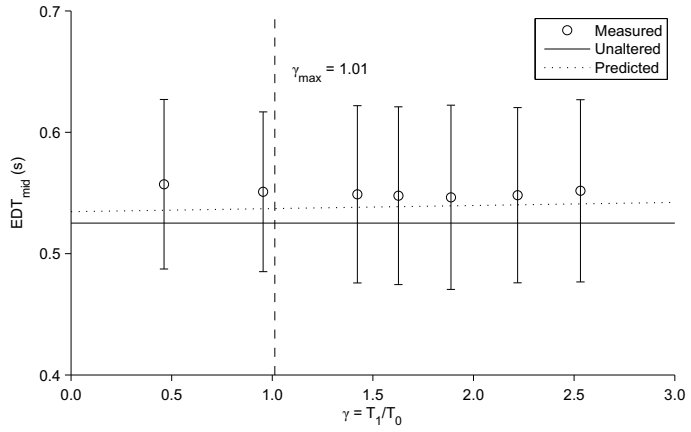

Figure 5.15: Measured values of early decay time for a system with electronic reverberation. The unaltered EDT is shown as a horizontal solid line whilst the dotted line shows a predicted value using the two term decay model.

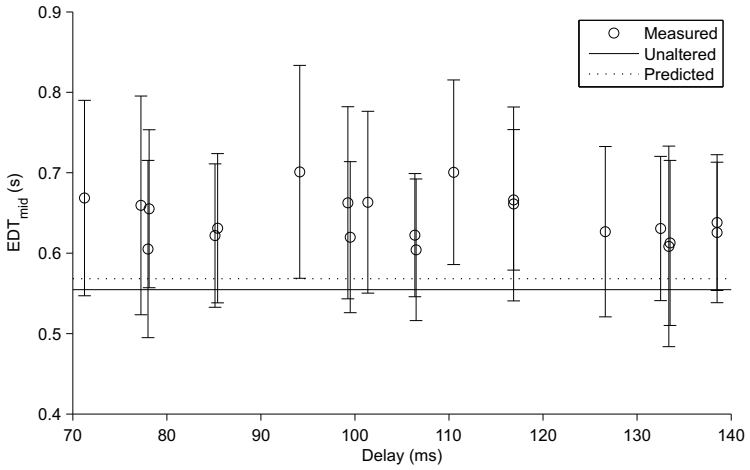

Figure 5.16: Measured early decay time using a single channel system including delay. The solid line shows the unaltered EDT and the dotted line shows a value predicted assuming no delay as in Figure 5.13.

As the EDT is constant with γ but the reverberation time increases, the ratio between them decreases dramatically as the reverberation time of the processor is increased which can be seen in Figure 5.17. The point at which the ratio of EDT to T becomes lower than the minimum recommended value is close to the value of γ_{max}. This would indicate that this is a reasonable upper limit for the value of γ. It has been claimed that for all values of $\gamma < \gamma_{max}$

the decay trace should be linear (Poletti, 1994b). These results show that the decay trace becomes slightly curved even for small values of γ.

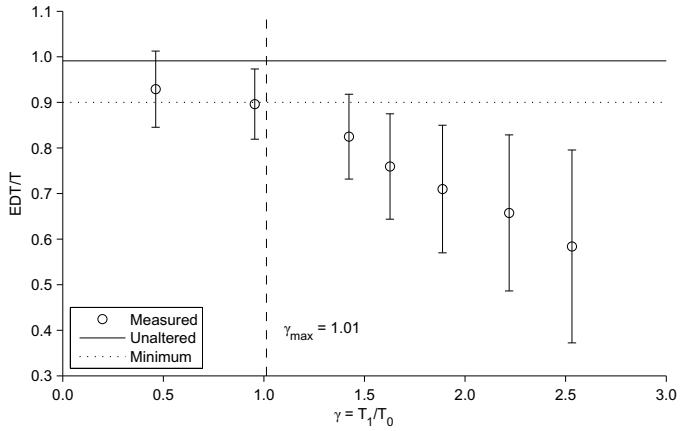

Figure 5.17: Ratio of measured early decay time to reverberation time shown against γ. The solid line shows the value for the unaltered room and the dotted line shows the minimum recommended value. The vertical dashed line shows the value of γ_{max}.

As in the simulation results, the EDT of the system including delay is higher than the unaltered room but increasing the delay time does not significantly alter the EDT. In fact, the EDT is consistent even for values of delay which are greater than the EDT time window which in this case is 88 ms. One way in which these experimental results contradict the simulation results is that the value predicted by assuming that there is no delay in the feedback loop does not match with the measured EDT. Instead, the measured EDT is higher than the value predicted with that method. This discrepancy between simulation and experimental results may be caused by the structure of the unaltered impulse responses.

The simulations use exponentially decaying white noise, which is a good approximation of an idealised room impulse response but does not model the fine structure of the early reflections. The density of reflections in this model is consistent throughout the time history of the impulse response. In the experimental case, the real room response will have isolated reflections in the early part of the impulse response. Introducing the system with delay may increase the density of reflections in the early part of the impulse response which may have the effect of exaggerating the increase in the early energy.

Figure 5.18 shows the ratio of EDT to reverberation time from the measured data for the system with delay. The unaltered value is shown as a solid horizontal line. For values of delay less than 80 ms, the ratio is greater than that measured for the room in its unaltered state. Around 90 ms, which is approximately the EDT time window, the ratio crosses unity

which would imply a linear decay trace when the value of delay is equal to the EDT time window. For larger values of delay, the ratio continues to decrease.

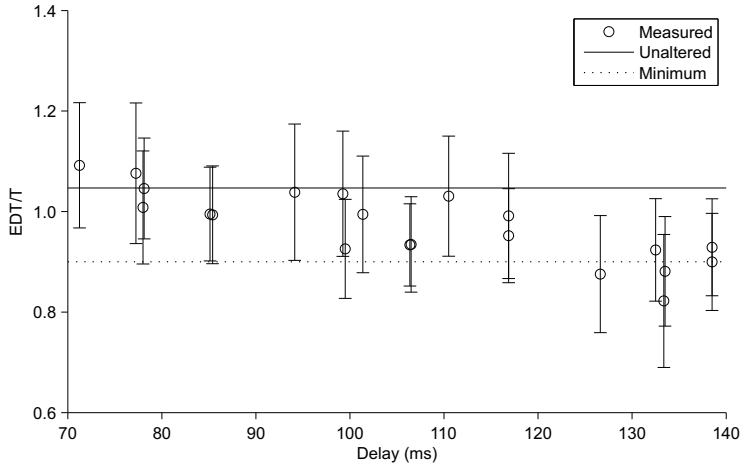

Figure 5.18: Measured ratio of EDT to reverberation time for a single channel system with delay. The solid line shows the value measured for the unaltered and the dotted line shows the minimum recommended value.

The recommended minimum EDT is shown as a dotted horizontal line. This figure shows that, even for large values of delay, the resultant early decay time is always above this minimum. Using these experimental results, equation (5.2.5) can be reformulated as

$$\tau_{\max} = 0.23T \tag{5.2.6}$$

which implies that much higher values of delay, and hence resultant reverberation time, may be used for this particular system configuration. The simulated system had 4 channels and used a simplified model of the room impulse response which may explain the discrepancies between these results and those found experimentally. The trend observed in both simulation and experiment is an initial increase in EDT which then does not change significantly with increasing delay. This leads to a curved decay trace as the reverberation time is increased.

The curvature of the decay trace with increasing reverberation time can be seen in Figure 5.19. This shows several decay traces measured with different values of delay the system. In the first 50 – 100 ms of decay, the traces are very similar but after this point they begin to diverge. Note that this behaviour may change if the experiment was conducted in a different room or if the system had a significant change in configuration, such as using a greater number of channels.

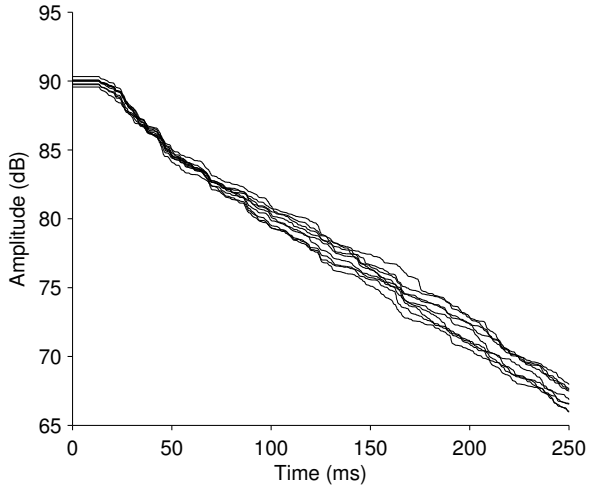

Figure 5.19: Measured decay traces with values of delay in the system ranging from 85 to 133 ms. This shows the consistency of the early part of the decay trace and the change in increase in curvature as the reverberation time is elongated.

5.2.3 Clarity and reverberation enhancement

The measure of early to late arriving sound energy is known as the clarity. The division of the impulse response is normally placed at 50 or 80 ms depending on whether the application is speech or music respectively (ISO3382-1, 2009). The purpose of this measure, along with similar quantities such as the definition and the centre time (Cremer and Muller, 1982), is to find the relationship between the 'useful' early energy, which will enhance subjective loudness, and the 'detrimental' late energy which will reduce intelligibility. As mentioned above, a high value for the clarity is desirable.

The simulated clarity, as affected by the system using electronic reverberation, is shown in Figure 5.20. This shows that the system causes a slight decrease in the clarity compared with the unaltered value with an extremely shallow decreasing trend with increasing γ. For small values of γ, the resultant clarity is approximately equal to that predicted from the resultant reverberation time assuming a linear decay trace. However, as γ is increased, the predicted value decreases much more quickly than the simulation. The prediction using the two-term decay model is closer to the simulated values but still decreases more quickly with increasing γ.

This trend is caused by curvature of the decay trace. As the reverberation time is increased, the energy in the early part of the impulse response should not be significantly affected. If the decay trace was linear, then the energy in the late part of the impulse response should increase and therefore the clarity is expected to decrease as seen in the dotted line in Figure 5.20. As the decay trace in this simulation becomes curved with higher values of γ, the

gradient of the late part of the decay trace is increased, hence the higher values of reverberation time, but the energy is not increased.

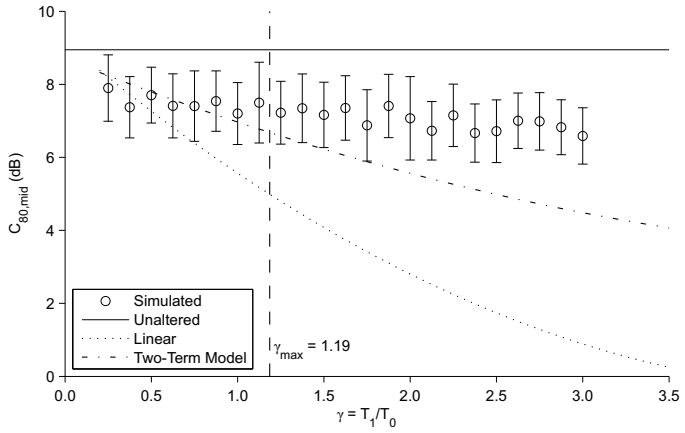

Figure 5.20: Simulated values of mid-frequency C_{80} for a 4 channel system using electronic reverberation. The solid line shows the value of clarity for the unaltered impulse response, which had a reverberation time of 0.53 s. The dotted line shows the value, calculated from the mean mid-frequency reverberation time, which would be expected if the decay trace was linear. The dash-dot line shows a value predicted from the two term energy decay model. The vertical dashed line shows the value of γ_{max}.

Similar behaviour is seen in Figure 5.21 for the simulated system including delay. For each value of unaltered reverberation time, the resultant clarity is lower than the unaltered value. As the delay time is increased, the reverberation time increases resulting in a reduction in the predicted clarity. The simulated value is approximately constant with different values of delay. These effects are much larger when the unaltered reverberation time is low.

It has been shown previously that the decay trace becomes curved as the delay is increased. The resulting values of clarity can be interpreted in a similar way to those observed in the simulated system with electronic reverberation. Namely, the reverberation time is increased by altering the gradient of the late part of the decay trace but total energy in the late reverberant tail is not significantly increased. This causes the resultant clarity to remain constant for all values of delay.

The consequence of this behaviour is that the clarity may actually become too high. It is expected that for a 'passive' room then the clarity will normally be too low. However, the values of clarity in Figure 5.20 and Figure 5.21 are several decibels higher than that expected from a linear decay. The preferred values discussed in section 5.2.1 were between 0 and 2 dB higher than those predicted by a linear decay. The resultant values of clarity observed in these simulations may be perceived as a lack of reverberance. However, the preferred values may be an absolute limit rather than one relative to the reverberation time. In this case, the

reduction in the clarity caused by the system with delay may improve the subjective perception of the room response.

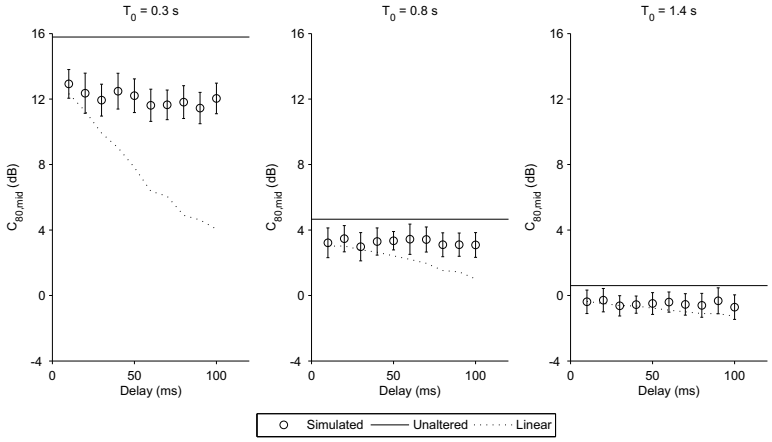

Figure 5.21: Simulated values of C_{80} for a 4 channel system using delay. Three different unaltered reverberation times are shown. The unaltered value of the clarity is shown as a solid line whilst that predicted from the resultant reverberation time assuming a linear decay is shown as a dotted line.

The experimental results, shown in Figure 5.22 and Figure 5.23 for the system with electronic reverberation and delay respectively, have similar trends to those seen in the simulations i.e. the resultant clarity is lower than the unaltered value and does not significantly change with different values of delay or reverberation time of the processor. The clarity predicted from the reverberation time, assuming a linear decay trace, does decrease with increasing delay or reverberation time. The clarity for the system with electronic reverberation is predicted more accurately with the two term decay model.

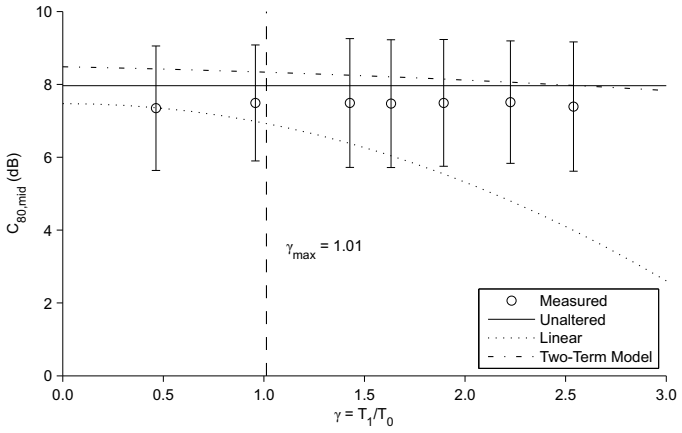

Figure 5.22: Measured values of the clarity with a single channel reverberation enhancement system with electronic reverberation. The solid line shows the unaltered value, the dotted line shows the value calculated from the measured reverberation time assuming a linear decay and the dash-dot line shows a prediction based on the two term decay model. The vertical dashed line shows the value of γ_{max}.

Each of these values is, in fact, within the observed spatial variation of clarity. The errorbars on the measured value are much larger for the experimental results in Figure 5.23 than those in the simulation results given in Figure 5.20 and Figure 5.21 or the experimental results in Figure 5.22. As the clarity is based on a discrete division of the impulse response, it can be sensitive to slight changes in position as a particular strong reflection falls on either side of this division. Although this is the likely cause of the spatial variation of clarity, it is unlikely to alter significantly the observed result due to the reasonably large number of positions which have been used for this measurement.

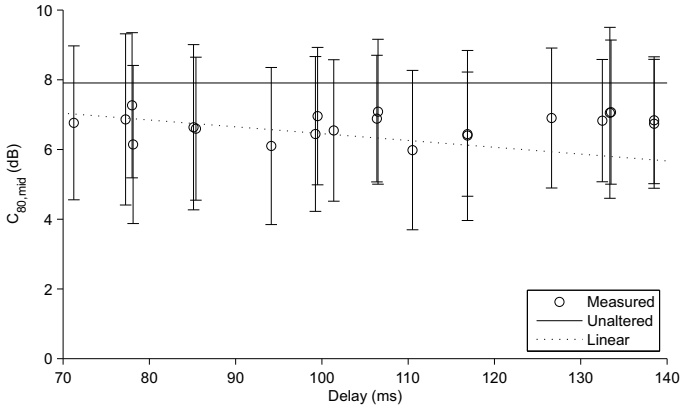

Figure 5.23: Measured values of clarity for a single channel system including delay. The unaltered value of clarity is shown as a solid line whilst that predicted from the measured reverberation time, assuming a linear decay, is shown as a dotted line.

The results in this section show that the introduction of reverberation enhancement causes a slight reduction in the clarity. This reduction is generally less than would be expected from a change in reverberation time if the shape of the decay trace remains linear. As the effect of the system is increased, either through increases in delay time or reverberation time of the processing, the clarity remains constant. This is unexpected as the clarity should decrease with increasing reverberation time if the decay trace is linear. This behaviour is thought to be caused by curvature of the decay trace.

The subjectively preferred values of clarity, as given in section 5.2.1, were between 0 and 2 dB higher than those predicted by a linear decay, although the suggested values could also be interpreted as requiring the clarity to have a value of around 0 dB. In either case, the results given here could be used to suggest maximum values of the delay time or reverberation time of the processing. However, as shown using the early decay time, this is heavily dependent on the configuration of the system and also on the initial room condition.

The important conclusion, which can be deduced from the results given here, is that the curvature of the decay trace, caused by a reverberation enhancement system using either electronic reverberation or delay, may result in a clarity which is significantly higher than would be expected given the reverberation time. This may cause a subjectively poor acoustic due to lack of perceived reverberance but further subjective evaluation is required. The clarity is a useful measure for assessing the degree of curvature and may be used to quantify the necessary system configuration.

5.3 Summary

This section set out to investigate the effect of reverberation enhancement on the secondary parameters of the diffuse field. These quantities allow greater insight into the properties of the room response and allow the performance of the system to be assessed more fully. This is important as a measurement of reverberation time alone does not guarantee a subjectively acceptable room response.

The diffusion of the sound field, in this context, is the extent to which the sound field approximates a diffuse field. As the steady state sound pressure level and reverberation time should be homogeneous throughout a diffuse field, the spatial variations of these quantities can be used to measure the diffusion. The normalised standard deviation of level and the normalised standard deviation of reverberation time are used to improve consistency of the measured diffusion.

These measures are affected by curvature of the decay trace. The NSDRT is affected mainly by double sloping of the decay trace which relates to the isotropy of the sound field. NSDL is affected by short term deviations from linearity of the decay trace relating to the homogeneity of the sound field. As these values are normalised, a value of unity indicates that the sound field has the same spatial variation as would be expected in a diffuse field plus that caused by experimental uncertainty. Values above unity indicate greater spatial variation which is undesirable.

It has been shown that as the reverberation time or delay time of the processing in a system is increased, in order to create a longer resultant reverberation time, the normalised measures of diffusion increase. This implies a reduction in the diffusion of the sound field. This has been shown in simulations and experiments. The simulation results have shown that the system including delay causes greater increases in the NSDRT than the system with electronic reverberation for the same change in reverberation time. This indicates greater curvature of the decay trace.

The normalised measures of diffusion have been compared with known subjective difference limits for sound pressure level and reverberation time. It has been shown that, with a normalised value of diffusion equal to unity, the spatial variation of these quantities is of the same order as that which is just perceivable under ideal conditions. If the normalised measure of diffusion is greater than unity, the spatial variations are increased and there is a greater likelihood that they will be perceived.

These normalised measures of diffusion allow the artificially enhanced room response to be compared with that which would be expected from a naturally different response. As shown in this section, the measures of diffusion may be used to estimate the maximum acceptable limit of reverberation time gain for a given room and system configuration. This limit can be derived assuming either that the normalised measures of diffusion must equal unity or can be related to subjective difference limits.

Another important parameter of a room response is its early energy. This can be evaluated using the early decay time, which measures the decay rate of the early part of the impulse response, and the clarity which is the ratio of early to late energy. These quantities have known recommended values which relate to subjectively good acoustic responses. In general, it is good for these quantities to be close to the value which is expected from a linear decay trace, when they can be entirely predicted from the reverberation time. Preferably, they should be slightly high rather than low.

It has been shown that the system including delay causes an initial change in the early decay time and clarity which then remains constant for all values of delay. This is caused by curvature of the decay trace. Increasing the delay time in the system causes the gradient of the late part of the decay trace to be shallower without altering its amplitude. The early part of the decay trace is affected by the system but changing the delay time does not have any additional effect. These effects manifest themselves as a curved decay trace. It is interesting to note that the early part of the decay trace is affected even when the delay time is longer than the time window of interest, i.e. 80 ms for the clarity or the time taken for the initial 10 dB decay for the EDT.

The system with electronic reverberation shows similar behaviour but with a very gradual change in EDT and clarity as the reverberation time of the processor is increased. This means that the difference between the observed value of these quantities and that expected assuming a linear decay may be smaller for this system configuration than for a given resultant reverberation time. However, the difference in performance in terms of EDT and

clarity between this system and the system using delay may be small compared with the spatial variation of these quantities.

The EDT and clarity can be used to quantify the degree of curvature of the decay trace. The curvature will be higher when the gain in reverberation time is higher. As there are known values of EDT and clarity which are subjectively preferable, these measures can be used to limit the reverberation time gain such that the decay trace is not too curved. This limit will depend on the specific properties of the unaltered room response and the configuration of the system. It may be possible to derive a generic rule for the limit empirically; this may be a possible avenue for future work.

The work in this chapter has shown that the reverberation time alone is a poor measure of the performance of a reverberation enhancement system. Measuring the diffusion of the sound field and the properties of the early part of the impulse response is important to understand the detail of the room impulse response. These quantities can be related to known subjectively preferred values in order to improve the quality of the resultant room response. This is especially important for reverberation enhancement designed for small rooms as the system will likely be required to cause larger changes in the acoustic response than a system in a large hall.

6 Conclusions

This work has investigated the difficulties encountered when applying reverberation enhancement to a small room. This technology was originally designed for improving the acoustics of concert halls where the 'passive' response was subjectively poor. Subsequently, these systems have been used in halls designed for multiple programmes, as drama and different genres of music require different acoustic responses. In each case, the rooms have a volume of hundreds or thousands of cubic metres.

Applying reverberation enhancement to small rooms with volumes less than 100 cubic metres can allow for novel applications of the technology. This includes music rehearsal rooms, interactive auralisation suites and laboratories for testing the subjective effects of reverberation. Whilst reverberation enhancement has been previously applied in music rehearsal rooms with small volume this has generally used identical systems to those applied in large halls and have not specially addressed the differences in the room response.

There are several important differences in the physical properties of a small room compared with a large hall which are of interest when specifying a reverberation enhancement system. Firstly, the lack of space precludes the use of a large channel count and the unaltered reverberation time is likely to be short. This means that the performance, or at least the gain in reverberation time, must be maximised for every available channel.

Secondly, the room response in a small volume room will only approximate a diffuse field, on which the theory of reverberation enhancement is based. This will manifest itself in two ways. In a small room the Schroeder frequency will be high enough to occur well within the audible frequency range. Below this frequency the sound field features separate modal resonances and cannot be approximated as a diffuse field. As this frequency range is audible for small rooms, the modal behaviour of the room in this frequency region must be considered.

Above the Schroeder frequency, the sound field can be approximated as a diffuse field but the accuracy of this approximation is not guaranteed. This is true of all rooms, for instance the steady state sound pressure level is known to decrease with increasing distance from the stage in concert halls. The accuracy of the diffuse field model in small rooms should also be considered when implementing reverberation enhancement. Not only will this affect the accuracy of theoretical predictions of the performance of reverberation enhancement, it can have consequences for the subjective quality of the sound field.

These problems have formed the basis of the investigations into reverberation enhancement. The following section will summarise the results and conclusions. This will include consideration of the consequences of these results and how they might be applied to practical implementations of reverberation enhancement. Finally, possible research topics for future work will be suggested.

6.1 Summary of conclusions

Methods for increasing the resultant reverberation time of the room without increasing the feedback gain of the system were considered in chapter 2. The methods used here were both signal processing schemes which are applied to the signal within the feedback loop of the system. The performance of the system including a simulated reverberation algorithm has been shown to allow significant increases in the reverberation time. It has been shown that the resultant reverberation time can be predicted with a reasonable degree of accuracy using the analysis of Poletti (1994b).

An alternative system utilising a simple delay has also been investigated. A novel analysis of the behaviour of this system has been presented. The system has been shown to allow a significant increase in reverberation time with increasing delay time. The resultant reverberation time agrees well with the values predicted using the analysis. The performance of the system including delay, in terms of reverberation time gain, is comparable to that of the system using electronic reverberation.

It has been shown that significant increases in reverberation are possible through the use of processing in the feedback loop without changing the feedback gain of the system. This means that reasonable performance can be achieved using a relatively small channel count. The resultant reverberation time for both systems tested can be predicted accurately for ‘sensible’ values of reverberation time or delay time of the processing.

Another method for increasing the resultant reverberation time is to increase the feedback gain. This cannot be increased indefinitely as the system will become unstable. There are various methods which can be used to allow the maximum stable feedback gain to be increased. The use of these techniques within a reverberation enhancement system has been investigated in chapter 3. Although there are a large number of techniques designed for this purpose, the use of time variant processing was deemed most appropriate for application in the kind of reverberation enhancement system studied in this work.

Two kinds of time variant processing have been studied: time varying delay and frequency shifting. It has been found that these methods allow an increase in the stable feedback gain.

The resultant reverberation time was found to be higher than would be predicted from the corresponding increase in gain. However, this increase in resulting reverberation time is caused by artefacts which relate to the time varying algorithms.

These artefacts are undesirable but may be accepted if they are inaudible. As the level of the artefacts increases with increasing gain, the time varying algorithms can only be used to create small increases in the gain and therefore marginal increases in the resultant reverberation time. However, it may be useful to include this type of processing without significant increases in the feedback gain because the robustness of the system would be improved. No difference in performance has been observed between the time varying delay and the frequency shifting although their subjective response may be different.

Another method for increasing the stable feedback gain, suggested by Mapp and Ellis (1999), is the use of distributed mode loudspeakers. These transducers are based on a flat panel whose dimensions and materials are chosen to maximise the modal density which is excited by an electro-mechanical motor. This should create a 'diffuse' radiation characteristic with a wide directivity and a frequency response with small scale variations but a consistent local mean.

It has been shown that, despite the observed increase in stable feedback gain in the experiment by Mapp and Ellis, in the context of reverberation enhancement the DML can actually cause a reduction in the stable feedback gain. This is due to the additional variance of the frequency response of the transducers. Due to the wide directivity and slim form factor, the DML may still be a useable option within a reverberation enhancement system.

The work in chapters 2 and 3 focussed on maximising the performance of the reverberation enhancement system. This has been achieved through processing in the feedback loop. The use of these processing techniques allows large gains in reverberation time with a relatively low channel count. This is useful in small rooms which have limited space so a large system with many loudspeakers and microphones would be impractical.

The ability of the diffuse field model to predict the resultant reverberation times accurately has been demonstrated in simulations and experiments. However, it is known that the reverberation time is not the only characteristic of the room response which will affect the performance of the reverberation enhancement system. In small rooms, the modal frequency region is audible and this cannot be modelled using diffuse field theory; this is investigated in chapter 4. Moreover, there are additional characteristics of a room response which are not described by diffuse field theory but which can significantly affect the perceived quality as shown in chapter 5.

The performance of a reverberation enhancement system in the modal frequency region has been considered in chapter 4. The time and frequency domain responses of a room, affected by reverberation enhancement in the modal frequency bandwidth have been derived. This has shown that, in the modal frequency region, the system can decrease as well as increase the reverberation time depending on the positions of the transducers and the setting of the feedback gain.

The modal sound field shows greater variation of pressure between positions and over frequency than a diffuse field. This is affected by the feedback processing of the reverberation enhancement system. The processing in the feedback loop can be optimised numerically to improve the modal response of the room. Due to the complexity of this optimisation problem, gradient descent algorithms perform poorly. To avoid this problem, a genetic algorithm has been used which should find a 'good' solution even if the global optimum is not found.

It has been found that, by optimising the constant coefficients of the feedback matrix or the terms of low order FIR filters, the spatial variation of sound pressure level and the variance of the pressure amplitude over frequency can be significantly reduced. The optimised values are lower than those of the unaltered room and those produced using 'standard' feedback matrices: the identity matrix and the matrix of ones.

It has been found that the time domain responses are quite variable between these different systems. Therefore additional optimisations have been performed which attempt to set the resultant reverberation time of the room. This can be achieved with a high degree of accuracy as long as the desired reverberation time is not too ambitious. The system cannot increase the reverberation time indefinitely without becoming unstable. It was also found that systems optimised to cause large increases in reverberation time had large variations in the frequency response.

In order to reduce this variation over frequency, the system has been optimised to a multi-term performance metric which includes terms affected by the variations over frequency and position as well as a term to adjust the reverberation time. This type of optimisation can be biased by the formulation of the performance metric. However, it has been found that a simple summation of the individual performance metrics allows reasonable performance for each of the criteria.

To verify the optimisation process used in this chapter and investigate the requirements for a practical implementation of the process, different sets of measurement systems have been tested. This included varying the number of microphones and loudspeakers used for

measuring the spatial and frequency variations as well as the positions of these transducers. It has been found that different measurement systems will generally identify similar trends. However, systems optimised to a small number of measurement positions have been found to create 'local' solutions which show reduced performance when subsequently they are measured with a larger number of measurement positions. Therefore, recommendations have been made for the minimum number of microphone and loudspeaker positions when optimising a practical system.

These investigations have shown the feasibility of improving the modal room response by optimising the processing in a reverberation enhancement system. Not only can the frequency and spatial variations be reduced but the resultant reverberation time can be set with a high degree of precision. No attempt has been made to assess the qualitative effect of this optimisation. However, it should be noted that without considering the modal frequency region, the system may have significant negative impacts such as causing large peaks in the frequency response which can be avoided using the techniques discussed here.

Alternative methods for measuring the room response above the Schroeder frequency have been considered in chapter 5. In an ideal diffuse field, the sound pressure level and reverberation time would be invariant with position, i.e. the field should be homogeneous. This is not the case in real rooms. The degree to which a room approximates a diffuse field can be estimated by measuring the spatial variation of sound pressure level and reverberation time. This is called the 'diffusion' of the sound field.

A certain amount of spatial variation is expected due to the inherent variation of the room response and also to experimental uncertainty. These kinds of variations will depend on the reverberation time of the room and can be estimated analytically. As the reverberation time is increased through the use of reverberation enhancement the spatial variations should change along with these analytically predicted values. Deviation from these values would indicate that the reverberation time has changed without the expected change in diffusion.

It has been shown that increasing the reverberation time of a room through increasing the delay time or reverberation time of processing in a system does not cause the expected changes in diffusion. Instead, larger spatial variation of both reverberation time and sound pressure are observed. This corresponds to a decrease in diffusion and relates to deviations in the linearity of the decay trace. This may limit the maximum useable reverberation time gain of these systems.

The early part of the impulse response of a room is known to be subjectively important. Reverberation enhancement systems in large concert halls often include specific components

for acting on this part of the impulse response. However, it may not be feasible to install these components in a small room. Therefore, the effects of the system on the early part of the impulse response have been examined. The early decay time and clarity have been used to assess these effects. It has been shown that, whilst the system has some effect on these quantities, increasing the delay time or reverberation time of the processing within the system has little to no effect on either the early decay time or the clarity.

As the reverberation time of the room is changed with increasing delay time and reverberation time of the processing, the consistent values of early decay time and clarity indicate that the decay trace is becoming curved. Subjectively preferred values of early decay time and clarity have been derived previously; these values can be used to set maximum values of resultant reverberation time corresponding to acceptable curvature of the decay trace. These values will depend on the unaltered response of the room, the configuration of the reverberation enhancement system and the desired application of the resultant acoustic.

The investigation into alternative measurements of the room response beyond the reverberation time has shown that the maximum performance of the system which is subjectively acceptable may be less than the absolute maximum performance seen in chapter 2. This is due to curvature of the decay trace which results in an increase in the observed reverberation time but a decrease in diffusion and subjectively poor values for early decay time and clarity. Therefore, it is important to consider these quantities when specifying a reverberation enhancement system which is especially important in a small room when the system is likely to be called upon to create larger changes in the room response.

These results show that reverberation enhancement can provide significant, useful increases in reverberation time even in small rooms. The performance of these systems can be greatly improved through judicious use of signal processing and the resulting reverberation times can be predicted using diffuse field theory. However, as the diffuse field does not wholly model the response of small rooms other parameters such as the modal resonances at low frequency and the early energy must be considered. As long as these are accounted for the desired performance of the system should be achievable. This should allow improved performance of reverberation enhancement systems in small rooms which can allow a greater range of applications for this technology.

6.2 Future work

Some suggestions for future work have been mentioned in the previous section; these will be expanded upon in this section and additional ideas will be put forward. The reverberation enhancement system using delay has been shown to allow significant increases in reverberation time. The maximum useable increases have been estimated from secondary parameters of the room response. However, it may be useful to consider the point at which the delayed signal becomes noticeable subjectively as a separate echo above the reverberant decay.

The audibility of echoes is relatively well understood for simple situations where there is a single delayed signal or, for instance, strong reflections from the ceiling of a concert hall (Cremer and Muller, 1982). The complexity of the interaction between source and receiver positions, processing delay, system gain, room volume and programme material will inevitably alter the limit of audibility. Investigation of all of these parameters would require an inordinate amount of time and effort and is not a realistic suggestion. However, a simpler investigation into some aspect of the audible limit of delay in a reverberation enhancement system would be worthwhile in order to find the maximum acceptable performance of this system configuration.

Another possible point of future investigation is the use of alternative transducers. Although it has been shown that the distributed mode loudspeaker does not offer any benefit in terms of stable feedback gain, other properties of this transducer may be useful. Namely the wide directivity may improve the diffusion of the enhanced sound field. Alternative designs for wide directivity, diffuse transducers have also been implemented in reverberation enhancement systems (Nagatomo et al., 2007; Woszczyk, 2011). In depth investigations into the spatial variations of the resultant sound field when using these transducers may show an improvement in performance over that found using traditional cone loudspeakers in this work.

It has been shown in this work that tailoring the processing of a reverberation enhancement system can improve the response of the room in the modal frequency bandwidth. This is a relatively novel piece of work and much more could be done in terms of testing its operation under ‘real world’ conditions. The work presented here was restricted to numerical simulations. Evaluation of a real-time implementation of an optimised system with a separate, parallel diffuse field enhancement scheme would be the eventual goal of work in this area.

The measured diffusion has been used here to evaluate the performance of reverberation enhancement systems. This highlighted differences in the performance of electronic reverberation and delay as processing schemes within the system. This method could be used, for example, to evaluate the performance of the different transducers mentioned above. The measures of diffusion could be used elsewhere to reveal properties of the room response which would otherwise be difficult to obtain. This could include the comparison of performance of physical and active diffusing elements.

The subjective quality of the reverberation enhancement systems could also be tested. This could include audibility of time-variant algorithms or perceived quality of electronic reverberation and delay processing. An experiment which revealed the audibility of spatial variations of reverberation time and sound pressure level would allow more precise recommendations to be made regarding the measures of diffusion. The preferred values of early decay time and clarity in small rooms could be investigated as the extrapolation from values derived from concert halls may be misrepresentative.

A Additional simulations of frequency shifting

The numerical simulation of a single channel reverberation enhancement system including frequency shifting is presented in section 3.2.2. This showed that the maximum stable feedback gain was higher for this configuration than for a time invariant system. However, it was also seen that when the feedback gain was increased the resultant reverberation time was higher than predicted. This is due to artefacts caused by the inclusion of time variant processing.

In those simulations, the difference between the simulated reverberation time and the predicted value was relatively small. This is due to the model used in that particular simulation which represents the room impulse response as exponentially decaying white noise. This model has been used throughout this thesis but for this particular simulation is useful to reproduce an alternative figure which more clearly shows the trends.

In this case an image model has been used to simulate the room impulse response, see section 1.1.3. The dimensions of the modelled room are 12 by 13 by 5 m which leads to a volume of 780 m^3 and unaltered reverberation time of 1.5 s which does not fall into the definition of 'small rooms' which has been the subject of this work. The results of this simulation can be seen in Figure A.1 clearly showing the longer reverberation time simulated for feedback gains in the range −10 to −2 dB and the sudden decrease in reverberation time for values of gain above −2 dB.

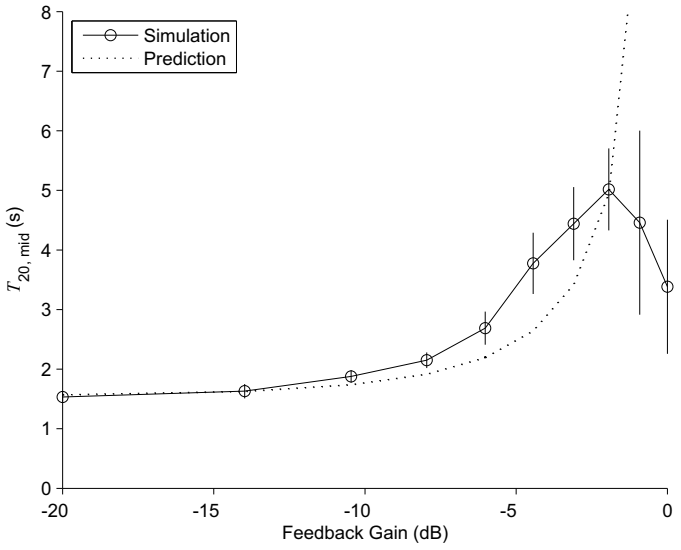

Figure A.1: Simulated reverberation times for a single channel system with frequency shifting for various values of the normalised feedback gain.

These trends have been shown to be caused by artefacts which become audible at feedback gains above −6 dB. Above this value, the artefacts, which do not dominate the impulse response, cause a slight increase in the amplitude at the end of the decay trace which causes the measured reverberation time to be higher. For gains above −2 dB, where the impulse response is dominated by the artefacts, the measured reverberation time is merely an quirk of the inverse integration method and should not be described as a true reverberation time. This simulation shows these trends much more clearly that those given in section 3.2.2 and has therefore been reproduced here even though it does not represent a 'small room'.

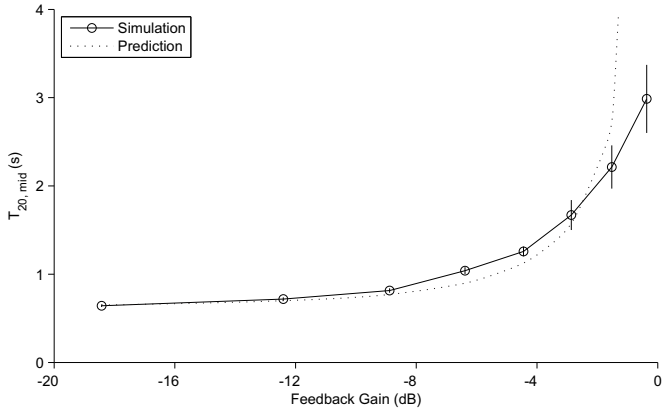

Figure A.2: Simulated reverberation times of a single channel reverberation enhancment system including frequency shifting. This simulation used an image model to create impulse responses of a room with volume 75 m^3.

The image model can also be used to simulate a small room which is close to those which have been used experimentally. A room with dimensions of 5 by 6 by 2.5 m has been simulated with a single channel reverberation enhancement system including frequency shifting. The unaltered reverberation time of this room is 0.65 s. The resulting reverberation times can be seen in Figure A.2 which shows similar trends to the previous figure. The reverberation time in the region between −10 and −2 dB is higher than the predicted value but lower than the predicted value when the feedback gain is greater than −2 dB. This is caused by the same artefacts as in the other simulations.

The noise burst model which was used for the simulations in section 3.2.2 can also be used to simulate a larger room. Figure A.3 shows the resultant reverberation times of a simulated system including frequency shifting where the room impulse response is simulated using exponentially decaying white noise. In order to simulate a large room, the unaltered reverberation time is set to 1.5 s which is similar to the room in Figure A.1. The

discrepancies between prediction and simulation are visible in Figure A.3 but are smaller than in the plots using the image model.

This implies that it is use of the image model which reveals these trends most clearly. Since these trends have also been observed experimentally, see section 3.2.3, it seems that the results of the image model are more revealing of the fine details of the acoustic response of the room, which is perhaps to be expected. These simulations confirm that the cause of the discrepancy between the simulated reverberation times and the predicted values is caused by artefacts related to the time varying processing. These artefacts have some effect on the resulting impulse response even at feedback gains where the system appears to be stable.

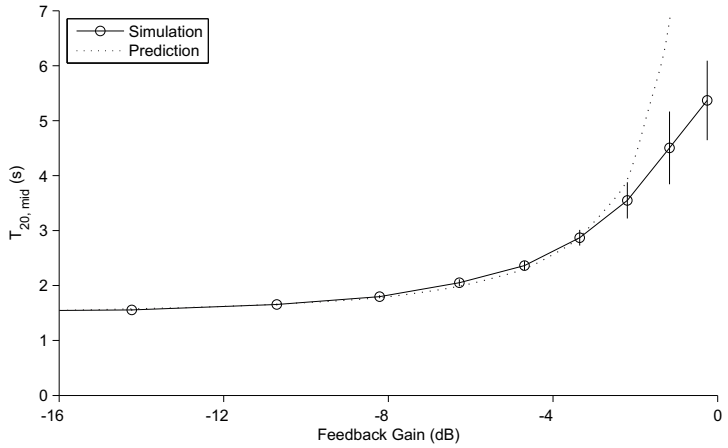

Figure A.3: Simulation of a single channel reverberation enhancement system with frequency shifting using a model of the room impulse response based on exponentially decaying white noise. The unaltered reverberation time of the room is 1.5 s.

References

Allen, J. B., and Berkley, D. A. (1979). 'Image method for efficiently simulating small-room acoustics', J. Acoust. Soc. Am. **65**(4), 943-950.

Azima, H., and Harris, N. (1997). 'Boundary interation of the diffuse field distributed-mode radiators', in *Proceedings of the 103rd Convention of the Audio Engineering Society*, New York, USA.

Azima, H., and Mapp, P. (1998). 'Diffuse field distributed-mode radiators and their associated early reflections', in *Proceedings of the 104th Convention of the AES*, Amsterdam, The Netherlands. (Audio Eng. Soc.).

Barnett, P. (1987). *Acoustic systems*. U.S. Patent: 4649564.

Barnett, P. (1988). 'A review of reverberation enhancment systems', in *Proceedings of the 6th International Conference: Sound Reinforcement*. (Audio Engineering Society).

Barron, M. (1988). 'The Royal Festival Hall acoustics revisited', Applied Acoust. **24**(4), 255-273.

Barron, M., and Lee, L.-J. (1988). 'Energy relations in concert auditoriums', J. Acoust. Soc. Am. **84**(2).

Barry, D. A., Parlange, J. Y., Li, L., Prommer, H., Cunningham, C. J., and Stagnitti, F. (2000). 'Analytical approximations for real values of the Lambert W-function', Mathematics and Computers in Simulation **53**(1-2), 95-103.

Beranek, L. (1996). *Concert Halls and Opera Houses: music, acoustics and architecture* (Springer-Verlag, New York).

Berkhout, A. J. (1988). 'A holographic approach to acoustic control', J. Aud. Eng. Soc. **36**(12).

Berkhout, A. J. (1992). *Electro-acoustical system*. U.S. Patent: 5142586.

Berndtsson, G. (1995). 'Acoustical properties of wooden loudspeakers used in an artificial reverberation system', Applied Acoust. **44**, 7-23.

Berndtsson, G., and Krokstad, A. (1994). 'A room acoustic experiment with an artificial reverberation system using wooden loudspeakers', Acta Acust. **2**(1), 37-48.

Bodlund, K. (1976). 'A new quantity for comparative measurements concerning the diffusion of stationary sound fields', Journal of Sound and Vibration **44**(2), 191-207.

Botteldooren, D. (1995). 'Finite difference time domain simulation of low frequency room acoustic problems', J. Acoust. Soc. Am. **98**(6).

Byrne, D. (2010). 'How architecture helped music evolve', in *Proceedings of the TED2010*, Long Beach, California. (TED Conferences).

Cain, G. D., Murphy, N. P., and Tarczynski, A. (1994). 'Evaluation of several variable FIR fractional-sample delay filters', in *Proceedings of the International Conference on Acoustics, Speech, and Signal Processing*, 19-22 Apr 1994, Adelaide, South Australia. (IEEE).

Chiles, S. (2004). 'Sound level distribution and scatter in proportionate spaces', J. Acoust. Soc. Am. **116**(3), 1585.

Cremer, L., and Muller, H. (1982). *Principles and Applications of Room Acoustics* (Applied Science Publishers, London).

Dahlstedt, S. (1974). 'Electronic reverberation equipment in the Stockholm concert hall', J. Aud. Eng. Soc. **22**(8).

Davy, J. L. (1979). 'The variance of decay rates in reverberation rooms', Acustica **43** (1), 12-25.

de Koning, S. H. (1983/84). 'The MCR system - multiple channel amplification of reverberation', Philips Tech. Rev. **41**(1), 12-23.

Dutton, G. F. (1966). 'Reverberation reinforcement by delayed electro-acoustic feedback - ambiphony', in *Proceedings of the 31st Convention of the Audio Engineering Society*.

Elliott, S. (2001). *Signal Processing for Active Control* (Academic Press, London).

Fahy, F., and Walker, J. (1998). *Fundamental of Noise and Vibration* (Spon Press, London).

Fazenda, B. M., Avis, M. R., and Davies, W. J. (2002). 'Low frequency room exicitation using Distributed Mode Loudspeakers', in *Proceedings of the Architectural Acoustics & Sound Reinforcement*, St. Petersburg, Russia. (Audio Eng. Soc.).

Franssen, N. V. (1968). 'Sur l'amplification des champs acoustiques', Acustica **20**(6).

Freiheit, R. R. (1996). *Acoustical virtual environment*. U.S. Patent: 5525765.

Gardner, W. (1995). 'Efficient Convolution without Input-Output Delay', J. Aud. Eng. Soc. **43**(3), 127-136.

Gontcharov, V., and Hill, N. (2000). 'Diffusivity properties of distributed mode loudspeakers', in *Proceedings of the The 108th Convention of the Audio Engineering Society*, Paris, France.

Green, E. (2011). 'Scale Model Analysis of a Rectangular Concert Hall with Variable Diffusion'. MSc Thesis. University of Southampton, U.K.

Green, E., Barron, M., and Thompson, D. (2011). 'The effect of scattering surfaces in rectangular concert halls: a scale model analysis', in *Proceedings of the 8th International Conference on Auditorium Acoustics*, Dublin, Ireland. (Institute of Acoustics).

Griesinger, D. (1991). 'Improving room acoustics through time-variant synthetic reverberation', in *Proceedings of the 90th Convention of the Audio Engineering Society*.

Griesinger, D. H. (1992). *Electroacoustic system*. U.S. Patent: 5109419.

Guicking, D., Karcher, K., and Rollwage, M. (1985). 'Coherent active methods for applications in room acoustics', J. Acoust. Soc. Am. **78**(4), 1426-1434.

Hammond, L. (1941). *Electrical musical instrument*. U.S. Patent: 2230836.

Harris, N., and Hawksford, M. O. (1997). 'The distibuted-mode loudspeaker (DML) as a broad band acoustic radiator', in *Proceedings of the The 103rd Convention of the Audio Engineering Society*.

Hepberger, A., Priebsch, H., Desmet, W., Van Hal, B., Pluymers, B., and Sas, P. (2002). 'Application of the Wave Based Method for the steady-state acoustic response prediction of a car cavity in the mid-frequency range', in *Proceedings of the ISMA2002*, Leuven, Belgium.

Hidaka, T., Nishihara, N., and Beranek, L. L. (2001). 'Relation of acoustical parameters with and without audiences in concert halls and a simple method for simulating the occupied state', J. Acoust. Soc. Am. **109**(3), 1028-1042.

Howard, D., and Angus, J. (2009). *Acoustics and Psychoacoustics* (Focal Press, Oxford, UK).

ISO3382-1 (2009). 'Acoustics - Measurement room acoustic parameters. Performance spaces.', International Standards Organisation.

ISO3382-2 (2008). 'Acoustics - Measurement of room acoustic parameters. Reverberation time in ordinary rooms.', International Standards Organisation.

ISO3741 (2010). 'Acoustics - Determination of sound power levels of noise sources using sound pressure - Precision methods for reverberation rooms', International Standards Organization.

ISO18233 (2006). 'Acoustics - Application of new measurement methods in building and room acoustics', International Standards Organisation.

ISO61260 (1996). 'Electroacoustics — Octave-band and fractional-octave-band filters', International Standards Organisation.

Jaffe, C. (1977). *Electronic sound enhancing system*. U.S. Patent: 4061876.

Jot, J. M. (1992). 'An analysis/synthesis approach to real-time artificial reverberation', in *Acoustics, Speech, and Signal Processing, 1992. ICASSP-92., 1992 IEEE International Conference on*, pp. 221-224 vol.222.

Kawakami, F., and Shimizu, T. (1990). 'Active field control in auditoria', Applied Acoust. **31**(1-3), 47-75.

Kinsler, L. E., Frey, A. R., Coppens, A. B., and Sanders, J. V. (2000). *Fundamentals of Acoustics* (John Wiley & Sons, Inc.).

Kirkegaard, L. (2011). 'Why we have changed the acoustics in the Royal Festival Hall'. Avaliable from: http://ticketing.southbankcentre.co.uk/sites/default/files/documents/rfh_acoustics.pdf [Accessed 2011].

Knuth, D. E., Corless, R. M., Gonnet, G. H., Hare, D. E. G., and Jeffrey, D. J. (1996). 'On the Lambert W function', Advances in Computational Mathematics **5**(1), 329-359.

Kobayashi, K., Furuya, K., and Kataoka, A. (2003). 'An adaptive microphone array for howling cancellation', Acoust. Sci. Technol. **24**(1), 45-47.

Krokstad, A. (1988). 'Electroacoustic means of controlling auditorium acoustics', Applied Acoust. **24**(4), 275-288.

Krokstad, A., Strom, S., and Sørsdal, S. (1967). 'Calculating the acoustical room response by the use of a ray tracing technique', J. Sound Vib. **8**(1), 118-125.

Kuhl, W. (1960). *Acoustic Reverberation Arrangements*. U.S. Patent: 2923369.

Kuttruff, H. (2000). *Room Acoustics* (Spon Press, London).

Leotwassana, W., Punchalard, R., and Silaphan, W. (2003). 'Adaptive howling canceller using adaptive IIR notch filter: simulation and implementation', in *Proceedings of the International Conference on Neural Networks and Signal Processing*, 14-17 Dec, Nanjing, China. (IEEE).

Lis, J., and Eiben, A. E. (1997). 'A multi-sexual genetic algorithm for multiobjective optimization', in *Proceedings of the IEEE International Conference on Evolutionary Computation*, Indianapolis, USA.

Lubman, D. (1968). 'Fluctuations of Sound with Position in a Reverberant Room', J. Acoust. Soc. Am. **44**(6), 1491-1502.

Mapp, P., and Ellis, C. (1999). 'Improvements in acoustic feedback margin in sound reinforcement systems', in *Proceedings of the The 106th Convention of the Audio Engineering Society*.

Martellotta, F. (2009). 'A multi-rate decay model to predict energy-based acoustic parameters in churches', J. Acoust. Soc. Am. **125**(3).

Meng, Z., Zhao, F., and He, M. (2006). 'The Just Noticeable Difference of Noise Length and Reverberation Perception', in *International Symposium on Communications and Information Technologies, 2006. ISCIT '06.*, pp. 418-421.

Miyazaki, H., Watanabe, T., Kishinaga, S., and Kawakam, F. (2003). 'Active field control (AFC) reverberation enhancement system using acoustical feedback control', in *Proceedings of the 115th Convention of the Audio Engineering Society*, New York, USA. (Audio Engineering Society).

Moorer, J. A. (1979). 'About This Reverberation Business', Computer Music Journal **3**(2), 13-28.

Nagatomo, Y., Hiramatsu, N., Yamauchi, G., and Omoto, A. (2007). 'Variable reflection acoustic wall system by active sound radiation', Acoust. Sci. Technol. **28**(2), 84-89.

Naylor, G. M. (1993). 'ODEON - Another hybrid room acoustical model', Applied Acoust. **38**(2-4), 131-143.

Nelson, P. A., and Elliott, S. J. (1992). *Active Control of Sound* (Academic Press, London).

Newell, P., and Holland, K. (2007). *Loudspeakers: for music recording and reproduction* (Focal Press, Oxford, UK).

Nielsen, J. L., and Svensson, U. P. (1999). 'Performance of some linear time-varying systems in control of acoustic feedback', J. Acoust. Soc. Am. **106**(1), 246-254.

Oppenheim, A. V., Willsky, A. S., and Young, I. T. (1983). *Signals and systems* (Prentice-Hall).

Osmanovic, N., and Clarke, V. (2010). *Acoustic feedback cancellation system*. U.S. Patent: 7664275.

Parkin, P. H., and Morgan, K. (1964). '"Warming Up" the Royal Festival Hall', in *New Scientist* (Reed Business Information Ltd, UK).

Parkin, P. H., and Morgan, K. (1965). '"Assisted resonance" in the Royal Festival Hall, London', Journal of Sound and Vibration **2**(1), 74-85.

Parkin, P. H., and Morgan, K. (1970). '"Assisted resonance" in the Royal Fesitval Hall, London: 1965-1969', The Journal of the Acoustical Society of America **48**(5), 1025-1035.

Patronis Jr, E. T. (1978). 'Electronic detection of acoustic feedback and automatic sound system gain control', J. Audio Eng. Soc. **26**(5), 323–326.

Pietrzyk, A. (1998). 'Computer modeling of the sound field in small rooms.', in *Proceedings of the 15th International Conference: Audio, Acoustics & Small Spaces*. (Audio Engineering Society).

Poletti, M. A. (1993). 'On controlling the apparent absorption and volume in assisted reverberation systems', Acustica - Acta Acustica **78**(2), 61-73.

Poletti, M. A. (1994a). 'Colouration in assisted reverberation systems', in *Proceedings of the ICASSP*, 19-22 April, Adelaide, Australia. (IEEE).

Poletti, M. A. (1994b). 'The performance of a new assisted reverberation system', Acta Acust. **2**(6), 511-524.

Poletti, M. A. (1998a). 'The analysis of a general assisted reverberation system', Acustica - Acta Acustica **84**(4), 766-775.

Poletti, M. A. (1998b). *Reverberators for use in wide band assisted reverberation systems*. U.S. Patent: 5729613.

Poletti, M. A. (1999). *Wideband assisted reverberation system*. U.S. Patent: 5862233.

Poletti, M. A. (2000). 'The stability of single and multichannel sound systems', Acustica **86**(1), 163-178.

Poletti, M. A. (2004). 'The stability of multichannel sound systems with frequency shifting', J. Acoust. Soc. Am. **114**(2), 853-871.

Poletti, M. A. (2006). 'The control of early and late energy using the variable room acoustics system', in *Proceedings of the ACOUSTICS 2006*, Christchurch, New Zealand. (Australian Acoustical Soc.).

Poletti, M. A. (2007). *In-line early reflection enhancement system for enhancing acoustics*. U.S. Patent: 7233673.

Poletti, M. A. (2010). 'Active acoustic systems for the control of room acoustics', in *Proceedings of the International Symposium on Room Acoustics*, Melbourne, Australia. (Australian Acoust. Soc.).

Prinssen, W. C. J. M. (1992). *Electro-acoustic system*. U.S. Patent: 5119428.

Prinssen, W. C. J. M. (1994). 'Technical innovations in the field of electronic modifcation of acoustic spaces', in *Proceedings of the Conference on Speech and Hearing*, Widermere, UK. (Institue of Acoustics).

Rettinger, M. (1957). 'Reverberation Chambers for Broadcasting and Recording Studios', J. Aud. Eng. Soc. **5**(1), 18-22.

Rombouts, G., van Waterschoot, T., Struyve, K., and Moonen, M. (2006). 'Acoustic feedback cancellation for long acoustic paths using a nonstationary source model', IEEE Transactions on Signal Processing **54**(9), 3426-3434.

Sabine, W. C. (1923). *Collected Papers On Acoustics* (Havard University Press, Cambridge).

Schmich, I., Rougie, C., and Butcher, H. (2011). 'The benefit of a CARMEN electroacoustic system in the Aylesbury theatre', in *Proceedings of the 8th Internation Conference on Auditorium Acoustics*, Dublin, Ireland. (Institute of Acoustics).

Schroeder, M. (1954). 'Die statistischen Parameter der Frequenzkurven von grossen Räumen', Acustica **4**(3), 594-600.

Schroeder, M. (1962). 'Frequency correlation functions of frequency responses in rooms', J. Acoust. Soc. Am. **34**(12), 1819-1823.

Schroeder, M. (1964). 'Improvement of acoustic-feedback stability by frequency shifting', J. Acoust. Soc. Am. **36**(9), 1718-1724.

Schroeder, M. (1965). 'New Method of Measuring Reverberation Time', J. Acoust. Soc. Am. **37**(3), 409-412.

Schroeder, M. (1996). 'The "Schroeder frequency" revisited', J. Acoust. Soc. Am. **99**(5), 3240-3241.

Schroeder, M., and Kuttruff, K. (1962). 'On frequency response curves in rooms. Comparison of experimental, theoretical, and Monte Carlo results for the average frequency spacing between maxima', J. Acoust. Soc. Am. **34**(1), 76.

Schroeder, M. R. (1987). 'Statistical Parameters Of The Frequency-Response Curves Of Large Rooms', J. Audio Eng. Soc. **35**(5), 299-306.

Schroeder, M. R., and Logan, B. F. (1961). '"Colorless" Artificial Reverberation', IRE Transactions on Audio **9**(6), 209-214.

Shimizu, Y., and Kawakami, F. (1991). *Reverberation imparting device*. U.S. Patent: 5025472.

Siltanen, S., Lokki, T., Kiminki, S., and Savioja, L. (2007). 'The room acoustic rendering equation', J. Acoust. Soc. Am. **122**(3), 1624-1635.

Siqueira, M. G., and Alwan, A. (2000). 'Steady-state analysis of continuous adaptation in acoustic feedback reduction systems for hearing-aids', IEEE Transactions on Speech and Audio Processing **8**(4), 443-453.

Smith, J. O. (2008). 'Physical Audio Signal Processing'. Avaliable from: http://ccrma.stanford.edu/~jos/pasp/ [Accessed 2010].

Southern, A., Siltanen, S., and Savioja, L. (2011). 'Spatial room impulse responses with a hybrid modelling method', in *Proceedings of the 130th Convention of the Audio Engineering Society*, London, UK. (Audio Engineering Society).

Valimaki, V., and Laakso, T. I. (2000). 'Principles of fractional delay filters', in *Proceedings of the International Conference on Acoustics, Speech, and Signal Processing*, 2000. (IEEE).

van Waterschoot, T., and Moonen, M. (2011). 'Fifty years of acoustic feedback control: state of the art and future challenges', Proceedings of the IEEE **99**(2), 288-327.

van Waterschoot, T., Rombouts, G., and Moonen, M. (2004). 'On the performance of decorrelation by prefiltering for adaptive feedback cancellation in Public Address systems', in *Proceedings of the IEEE Benelux Signal Processing Symposium*, Hilvarenbeek, Netherlands.

Vermeulen, R. (1956). 'Stereo reverberation', IRE Transactions on Audio **4**(4), 98-105.

Vian, J.-P., and Meynial, X. (1998). 'Virtual reflecting walls for improving the acoustics of defective halls', in *Proceedings of the 16th International Congress on Acoustics*, Seattle, USA. (Acoust. Soc. Am.).

Vuichard, O., and Meynial, X. (2000). 'On microphone positioning in electroacoustic reverberation enhancement systems', Acta Acustica united with Acustica **86**(5), 853-859.

Wardle, S. (1998). 'A Hilbert-transformer frequency shifter for audio', in *DAFX98 Workshop on Digital Audio Effects* (Barcelona, Spain), pp. 25-29.

Woszczyk, W. (2011). 'Active acoustics in concert halls - A new approach', Archives of Acoust. **36**(2), 379-393.

Yamaha (2009). 'Yamanouchi Junior High School'. Avaliable from: http://www.yamaha-afc.com/example/yamanouchi/index.html [Accessed 2011].